Iterative Learning Control with Application to Hydraulic Actuators

by

SUHA KARAM

A Thesis

Submitted to the Faculty of Graduate Studies

In Partial Fulfillment of the Requirements

for the Degree of

MASTER OF SCIENCE

Department of Mechanical & Industrial Engineering

The University of Manitoba

Winnipeg, Manitoba

THE UNIVERSITY OF MANITOBA

FACULTY OF GRADUATE STUDIES

*****

COPYRIGHT PERMISSION PAGE

ITERATIVE LEARNING CONTROL WITH APPLICATION TO HYDRAULIC ACTUATORS

BY

SUHA KARAM

A Thesis/Practicum submitted to the Faculty of Graduate Studies of The University

of Manitoba in partial fulfillment of the requirements of the degree

of

Master of Science

Abstract

The concept of Iterative Learning Control (ILC) was originated from the efforts to control systems that are required to perform repetitive tasks in the industrial field. The basic idea of ILC is that the information obtained from a previous trial is used to improve the control signal for the next trial until the desired performance level is reached. The iterative learning control has been developed and applied to many different fields, especially the robotic field. However, its application toward the hydraulic systems is rather sparse and is limited to a few articles. This thesis investigates the robust ILC of an electrohydraulic positioning system with a faulty actuator piston seal. The goal is to develop an ILC scheme that is tolerant to a faulty condition such as internal leakage. Toward this goal, three different aspects of iterative learning control are presented and compared, including the basic ILC, the ILC with proportional error feedback, and the ILC with current cycle feedback. The results prove that all ILC algorithms are tolerant to the internal leakage given same initial conditions at each trial. It is also shown that both the ILC with proportional error feedback and the ILC with current cycle feedback are tolerant to the internal leakage without the need of resetting the initial conditions. This study provided a groundwork for using an ILC-base, fault tolerant, control scheme for hydraulic actuators. Many operations that are repetitive in nature, such as injection molding or metal forming, will benefit from this approach.

Acknowledgements

First, I would like to express my deepest thanks to my thesis advisor, Dr. Nariman Sepehri, for his caring personality, hard work, and academic knowledge. I would also like to thank Dr. Sepehri for giving me the freedom to explore my thesis topic, allowing me to make mistakes so that I might learn from them, and also providing guidance and direction when it was needed.

I would like to express my appreciation to Mark Karpenco for his continuous support. I also wish to acknowledge Al Aohse for his help in running the test rig.

Finally, I would like to thank my husband for his understanding and support during the course of this work. Also, I wish to thank my parents for their support, encouragement and for instilling in me the importance of education.

Table of Contents

List of Figures and Tables

Chapter 1

Introduction

1.1 Motivation

Hydraulic actuators are known for their stiffness, compactness, and high payload carrying capacity. These features make them appropriate for high power industrial equipments such as machine tools, aircrafts, material handling devices, construction, mining, and agricultural machines. However, like any electromechanical system, electrohydraulic actuators are complex and subjected to component malfunctions, which may occur suddenly or gradually as the system wears or ages. For example, the effects of wear on the elastomer seals may cause the leakage of the fluid internally or externally. In other instances, a problem with the pump may cause a change in the supply pressure of the hydraulic actuator. These two problems are among a variety of possible faults that damage the performance of hydraulic systems. Recently, there has been an increasing interest in designing robust controllers and fault tolerant controllers that maintain the performance of the system, despite such component failures.

The design of a controller is commonly based on a model of the plant that has to be controlled. Generally, the better the knowledge about the plant, the more accurate the model that can be derived. This enables the development of a better controller and thus a better performance. However, it is not always possible to gather enough knowledge about the plant to design a good controller. When an appropriate model can not be found, learning control can be considered. An example of a learning control system is the Iterative Learning Control (ILC). The concept of ILC was originated from the efforts to control manipulators that are required to perform repetitive tasks in the industrial field (Moore, 1999). The basic idea is that the information obtained from the previous trial is used to improve the control signal for the next trial until the desired performance level is reached. The iterative learning control has been developed and applied to many different fields, especially the robotic field, which is an obvious example of a system that executes repetitive tasks (see Moore, 1998 and the references cited therein). There are also many applications in which hydraulic actuators are utilized to perform repetitive tasks. Such applications include injection molding, metal formation and industrial presses. The implementation of the ILC to improve such tasks is, however, sparse and limited to a few articles (Tsao and Tomizuka, 1994; Zheng *et al.*, 1998). Much development is needed in this area.

1.2 Objectives and Scope of this Thesis

The objectives of this thesis are: (i) to investigate the application of the ILC to the position control of a hydraulic cylinder driven by an electrohydraulic proportional valve, (ii) to apply the ILC toward establishing a control system tolerant to faulty actuator piston seals, (iii) to compare the behavior of the system under the different ILC algorithms for both the normal and the faulty operations, and (iv) to study the effect of resetting the initial conditions to the same values at the beginning of each trial on the ILC behavior.

The thesis is organized as follows. Chapter 2 describes the principles behind iterative learning control and provides an introductory example to describe the principle of the ILC algorithm and its performance. Also in Chapter 2, a discussion on the differences between iterative learning control and some other common control paradigms is provided, along with a literature review. The description of a typical servovalve controlled hydraulic positioning system is described in Chapter 3, and some common faults associated with this fluid power system are characterized. The mathematical model of the hydraulic actuation system is also developed in Chapter 3. The test rig description with the parameters of the experimental test rig is given in the same chapter. In Chapter 4, three schemes for iterative learning control algorithms are presented. Chapter 5 presents and discusses the simulation results of the three ILC algorithms (basic ILC, ILC with proportional error feedback, and ILC with current cycle feedback). Chapter 6 presents the experimental results for the two selected algorithms (the ILC with proportional error feedback, and the ILC with current cycle feedback) along with a discussion of their results. Finally, the conclusions end this thesis in Chapter 7.

Chapter 2

Iterative Learning Control

The purpose of this chapter is to describe the principles behind the iterative learning control. In Section 2.1, a detailed description of iterative learning control is given. In Section 2.2, an introductory example to describe the nature of the ILC algorithm and its performance is introduced. Section 2.3 discusses the difference between ILC and some other common control paradigms. The final section in this chapter gives a summary of the major algorithms and applications of ILC found in the literature

2.1 General Description of ILC

Iterative Learning Control (ILC) is a relatively new addition to the traditional control theory that, for a particular class of problems, can be used to overcome some of the traditional difficulties associated with the performance design of control systems. The concept of the iterative learning control was originated from the efforts to control robot manipulators that are required to perform repetitive tasks in the industrial field. The basic idea of ILC is that the information obtained from a previous trial is used to improve the control signal for the next trial until the desired performance level is reached (Choi *et al.*, 2001).

Iterative learning control contains three words. The word *Iterative* refers to a process that executes the same trajectory over and over again. The word *Learning* refers to the idea that by repeating the same thing, the system should able to perform better. The word *Control* emphasizes that the result of the learning is used to control the plant. The main idea in ILC is to utilize the situation that a plant will carry out the same trial several times, i.e., repeat the same trajectory over and over again. Then, any error in the output response will be repeated during each trial. It is possible to improve the performance of the control system by using the results from the previous trials. The idea of ILC is illustrated in Figure 2.1. The subscript k indicates a specific trial (Scholten, 2000).

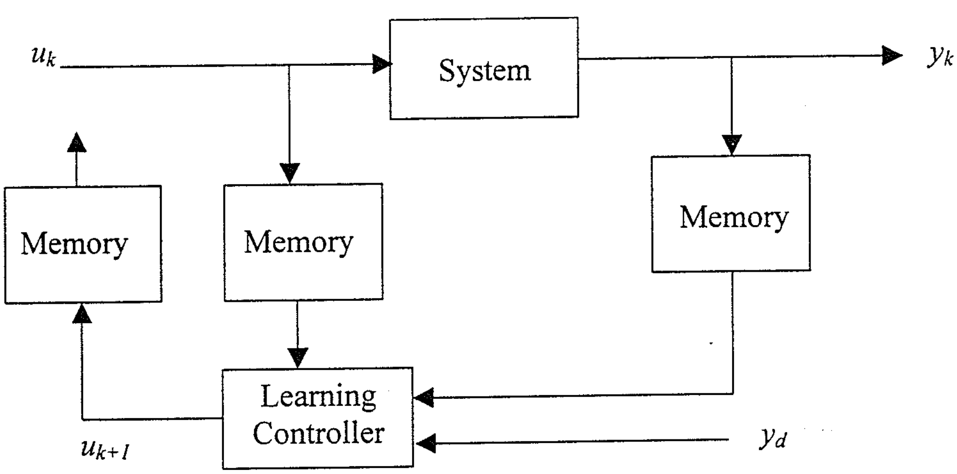

Figure 2.1: Iterative learning control configuration.

The system operates as follows: (i) during the k^{th} trial, an input signal $u_k(t)$ is applied to the plant, producing the output signal $y_k(t)$. In the meantime, these two signals are stored in a memory unit until the trial is over. (ii) At the end of the trial, a new input signal, $u_{k+1}(t)$, is computed by ILC (mainly offline) based on the error that is observed between the actual output and the desired output $e_k(t) = y_d(t) - y_k(t)$. (iii) The modified input signal, $u_{k+1}(t)$, will be stored in memory until the next time the system operates, at which this new input signal is applied to the system. This new input signal should be designed so that it will produce a smaller error than the previous input.

The principles of ILC can be described as follows (Moore, 1998): (i) in a successful ILC algorithm the next input is computed so that the error is reduced the next time the system operates. (ii) The initial conditions of the system are reset to the same values at the beginning of each trial (iteration). This has always been a key assumption in the formulation of the ILC problem. (iii) In ILC, the system repeatedly performs a specific task that ends in a fixed duration. (iv) In designing the learning control system, a little information about the system is required. (v) The convergence of ILC algorithm does not depend on the desired response $y_d(t)$; if a new desired trajectory is introduced, the learning control will simply learn and follow the new trajectory without changing any of its own algorithms.

2.2 An Introductory Example

The concepts of iterative learning control are best presented in an example. Consider the following second order, discrete-time linear system described by:

$$y(t+1) = -0.7y(t) - 0.012y(t-1) + u(t)$$

$$y(0) = 2;$$
$$y(1) = 2$$

Assume that a reference signal, y_d (t), over a finite time interval [0; t_f] is given in Figure 2.2 and that a system should track this reference trajectory repeatedly with a high accuracy. The following ILC algorithm is applied:

$$e_k(t) = y_d(t) - y_k(t)$$
$$u_{k+1}(t) = u_k(t) + 0.5e_k(t)$$

where k indicates a specific trial.

In the first trial an input signal, $u_0(t) = y_d(t)$, is applied to the system. The error, $e_0(t)$, is calculated from the difference between the actual output and the desired output. And from that, the new input signal, $u_1(t)$, is calculated from the previous input signal and the error. This new input signal is then applied to the system (which has had its initial condition reset to the same value as during the first trial) and a new output signal is recorded. A new error is determined and the next input signal, $u_2(t)$, is computed. The process is repeated until the output converges to the desired signal.

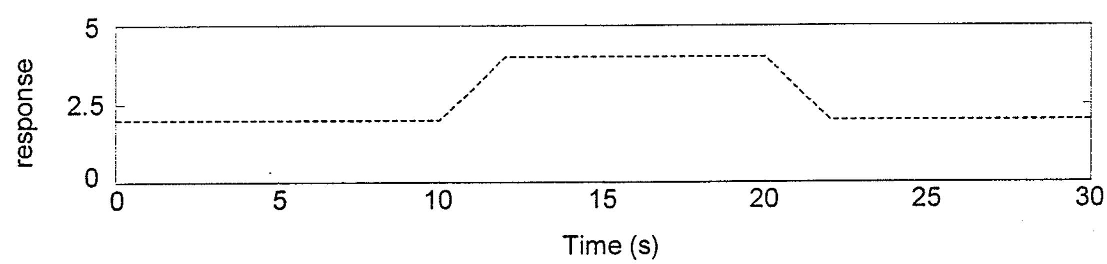

Figure 2.2: Desired system response

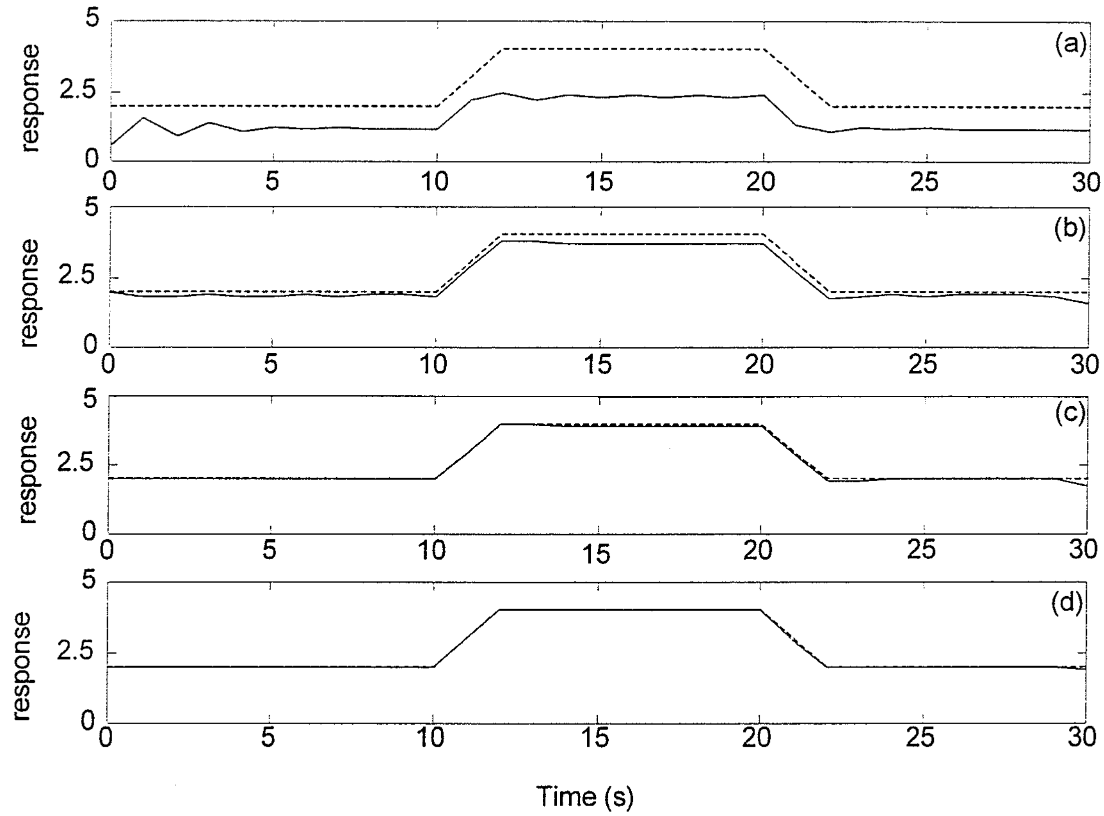

Figure 2.3: System responses (---- desired signal, — actual response): (a) 1st trial; (b) 5th trial; (c) 10th trial; (d) 15th trial.

Figure 2.3a shows the desired output and the initial output; Figures 2.3b, 2.3c and 2.3d show the output signal after at the 5th, 10th, 15th trials, respectively. These figures showed that as the number of trials increase the error decreases and the ILC algorithm has forced the output to the required value for each instant in the time interval.

2.3 Relation to Other Control Paradigms

In this section, the difference between ILC and some other common control paradigms will be discussed. The ILC sometimes seems to overlap with other approaches (Moore, 1998). Compared with feedback control technique; the main difference between the feedback controller and the ILC approach is that the ILC does not affect the system poles while the feedback controller does. The ILC can be seen as an add-on device for a feedback controller. In this case, the feedback controller is designed in such way that it guarantees robust stability and a minimum performance. By learning, the ILC improves the performance of the feedback controller. Compared with optimal control, in optimal control a controller is designed with the knowledge of a model of the system to operate in a common feedback loop. The ILC scheme does not operate in a feedback loop and uses only past behavior of the system and does not require knowledge of a model of the system. It is possible to use both techniques together (Amann *et al.,* 1996). With respect to adaptive control, most adaptive control schemes are on-line algorithms that adjust the controller's parameters until a steady-state equilibrium is reached; however, in the ILC scheme the input signal of the system is varied (off-line) at the end of each trial of the system, as opposed to the parameters of the controller.

The robust control is a set of design tools to deal with uncertainty in the plant. It is possible to incorporate the plant uncertainties in the ILC design. In this way the ILC can be seen as a robust controller. Finally, recently a number of control paradigms have been developed that can be classified as an intelligent controllers. These include artificial neural networks, fuzzy logic, and expert systems. The common thing between all of these is that they usually involve learning in some form or other. As such, ILC can be classified as a form of intelligent control. However ILC is a very specific type of intelligent control and involves a fairly standard system theoretic approach to algorithms, as opposed to the artificial intelligence approaches often found in neural nets, fuzzy logic, and expert system techniques (Moore, 1998).

2.4 Literature Review

The concept of iterative learning control was first introduced by Uchiyama (1978). Because this was a Japanese language publication it was not widely known in the west until the idea was developed by the Japanese research group led by Arimoto, from the mid to the late 1980s. The development of ILC schemes originally stemmed from the field of robotics, where repetitive motions show up naturally in many applications. The focus for the ILC research in the late 1990's and in the very beginning of the twenty-first century is not so easy to establish but it seems that it has moved from being very focused on stability to design and performance analysis. The following paragraphs give a summary for the different applications and algorithms of ILC, which has been posted in the literature.

Xu *et al.* (1995) presented the concept of a continuous ILC with current cycle feedback. This study had been used on both single input and single output (SISO) and multi-input and multi-output (MIMO) systems, and showed that this kind of controller was a robust against any unpredictable small disturbance.

Amann *et al.* (1996) proposed an ILC algorithm based on the optimization principle. This new algorithm showed three important properties. The first property was achieving a reduction of norm in the error in each step. The second one was ensuring automatic choice of step size. The third one was improving the robustness through the use of the feedback of the current trial data and feed forward of data from previous trial. The ILC algorithm achieved a geometric rate of convergence for the inevitable plant, which can be changed by design parameters.

Chen *et al.* (1996) proposed an initial state learning scheme along with the ILC algorithm to a nonlinear time varying system. It was shown that the desired initial states were identified through the learning iterations. Simulation results illustrated that the ILC in this study was effective.

Sison and Chong (1996) presented a no-reset ILC scheme. This study showed that the no-reset ILC system is an ILC system where the plant did not reset at the beginning of each iteration. This ILC algorithm had been applied to the SISO system. This study showed that using results from output feedback theory, the closed loop eigenvalues of the system could almost be placed with the selection of the appropriate finite learning gain.

Sison and Chong (1997) designed a repetitive learning control. This study was an extension to the work of the previous study for the same authors. They extended these sufficient conditions to MIMO, linear periodically time-varying plants. They were also adapted some methods to the design of a repetitive learning controller such as eigenvalue placement by basic output feedback and stabilization using a linear matrix inequality approach.

Xu (1997) developed a direct learning control scheme for some classes of non-linear system. This kind of controller was able to learn from the pre-stored control profile with different magnitude scales and to generate the desired control profile directly without any repeated learning process. This kind of controller helped to overcome the limitations of ILC and was also suitable to a non-repetitive system. A simulation result of a single link manipulator confirmed the validity of a proposed direct learning scheme.

Chen *et al.* (1998) introduced a PID-type of ILC algorithm that had been proposed for a class of delayed uncertain nonlinear systems, which perform a given task repetitively. The convergence conditions for the proposed, high-order learning control had been established. The result of this study showed that the time delay in the state variable did not affect the ILC convergence. It also showed the effectiveness of a high order ILC.

Moore and Bahl (1999) have described ideas for the use of ILC for the path tracking control of a mobile robot. It was shown that the ILC could be used to learn the nominal input commands needed to force the robot to track a prescribed path in inertial space.

Norrlöf (2000) presented a comparative study between first order and second order ILC algorithm in a frequency domain perspective. This included stability as well as performance and robustness issues. The simulation and experiment results of this study showed that the second order ILC design was not better with respect to performance or robustness than the fist order ILC design.

Choi *et al.* (2001) proposed an ILC scheme for uncertain robot manipulators that performed the same task repetitively. The proposed ILC scheme comprised a feedback controller and a feed forward learning controller using integral type parameter estimator. The results of this study showed that the entire profile of position and velocity error trajectories during the operation time converged uniformly to zero as the number of iterations approached infinity.

Gunnarsson and Norrlöf (2001) presented some new aspects of an ILC algorithm derived using optimization. This study was conducted on a linear SISO system. The result of this study showed that the error was eliminated after four iterations.

As for the application of ILC to the hydraulic system, two studies were found. Tsao and Tomizuka (1994) proposed and implemented a repetitive control to the hydraulic servo for noncircular machining. A robust adaptive feedforward tracking controller and a robust repetitive controller was developed for tracking arbitrary dynamic signals and repetitive signals, respectively. Because both algorithms for these controllers involved integration type of learning, establishing the stability was the key factor for successful implementation. This was conceived and implemented on discrete time representation of linear time invariant systems. Zheng *et al.* (1998) investigated the application of an existing adaptive learning control to the position control of a hydraulic cylinder driven by an electrohydraulic proportional valve. The system was representative of many types of manufacturing applications including injection molding, metal forming and industrial presses which perform the same operation repeatedly for many cycles. This system contained several major nonlinearities such as valve deadzones, valve flow saturation, and cylinder seal friction. The learning algorithm in this study iteratively determined an appropriate feedforward signal to be used in conjunction with simple feedback in order to track a predetermined reference signal.

From the above literature review it is evident that there are not much work done on the implementation of ILC in hydraulic systems. The two publications cited earlier studied the ILC algorithms under the same initial conditions at the beginning of each trial. Although, this is a common practice in evaluating the ILC algorithms, it is not ideal from the practical viewpoint. Furthermore, both studies were only concerned with the control of repetitive tasks under normal operations. Hydraulic systems are subjected to many faults and it is very desirable to also investigate how the ILC algorithms perform in a faulty operation.

This thesis is exploring aspects on the application of the ILC to the control of hydraulic actuators that have not been previously investigated. One of these aspects is to investigate the behavior of the ILC scheme without initializing the system at the beginning of each trial, which is more practical and desirable from the implementation viewpoint. The second aspect is to investigate the performance of the ILC scheme toward recovery from cross-port leakage fault that commonly occurs during the operation of hydraulic systems.

Chapter 3

Servovalve Controlled Hydraulic Actuators

This chapter serves to familiarize the reader with hydraulic actuation systems. A brief introduction to the hydraulic system and its components is given, followed by description of common problems with such systems. Section 3.2 develops the mathematical model for a valve controlled hydraulic positioning system. Section 3.3, gives a description of the experiment test rig and its parameters.

3.1 Hydraulic System Components

A typical servovalve controlled hydraulic actuation system consists of three main components. The first is the actuator, which consists of two cylindrical chambers separated by a piston. A rod is attached to the piston to serve as the link between the actuator and the load. The second component is the servovalve that controls the fluid flow to and from the actuator chambers to regulate the motion of the actuator. The third component is the hydraulic power supply, which delivers hydraulic fluid to the high-pressure port of the servovalve at a (nominally) constant pressure, typically 3.5 to 21 MPa (500 to 3000 psi).

Like any other system, the hydraulic system faces some common faults such as leakage, changes in power supply pressure, and a change in effective bulk modulus (EBM). Leakage is one of the most common faults that happen during the operating of the hydraulic system. There are two kinds of leakage: internal and external leakage. The internal leakage is the leakage of fluid across the actuator piston seal that closes the gap between the moveable piston and the cylinder wall. Since the seal is made of an elastomeric material, it wears as the actuator ages. As the seal wears, more fluid is allowed to flow past the piston and between the chambers of the actuator. The net effect of a faulty piston seal is an increase in the damping characteristics of the actuator as the degree of leakage increases. Another kind of internal leakage fault may also occur in the variable displacement piston (VDP) pump that supplies the high-pressure hydraulic fluid to the system. The increase in internal leakage and friction within the VDP leads to a power supply that must work harder to provide the hydraulic system with the required hydraulic pressure and flow rate.

The external leakage occurs due to a failure of the hydraulic supply line or due to a faulty connection between the system component and the line. As in the case of a leaking piston seal, rod seal leaks tend to increase the damping of the system and result in a more sluggish response. In extreme cases, it is possible that nearly the entire volume of fluid supplied to the circuit by the servovalve will be lost (Karpenco, 2002).

A change in the power supply pressure is also one of the most common faults that happen during the operating of the hydraulic system. This change in the power supply pressure may cause a serious problem for the hydraulic system. A reduction in the flow capabilities of the valve thus affects the dynamic performance of the system, which is caused from a drop in the system supply pressure. It also leads to a less efficient system. In extreme cases, a stalling of the actuator against the load is a result of a drop in the supply pressure. On the other, hand an increase in the supply pressure due to a faulty pressure relief valve tends to increase the flow gain of the servovalve and in some cases may lead to an unstable closed-loop system.

Another common problem with hydraulic systems is the change in the effective bulk modulus (EBM) of the hydraulic fluid. The EBM is associated with the hydraulic stiffness or compliance of the system, which affects the ability of the actuator to work against a load. As the magnitude of the EBM increases, the system is less compliant and better able to attenuate the effects of disturbances. On the other, hand as the magnitude of the EBM decreases, the hydraulic stiffness decreases and the system becomes more compliant (less able to attenuate disturbances) and more sluggish (Karpenco, 2002).

3.2 Derivation of the Mathematical Model

The schematic of a typical hydraulic positioning system with the appropriate nomenclature for mathematical modeling is shown in Figure 3.1.

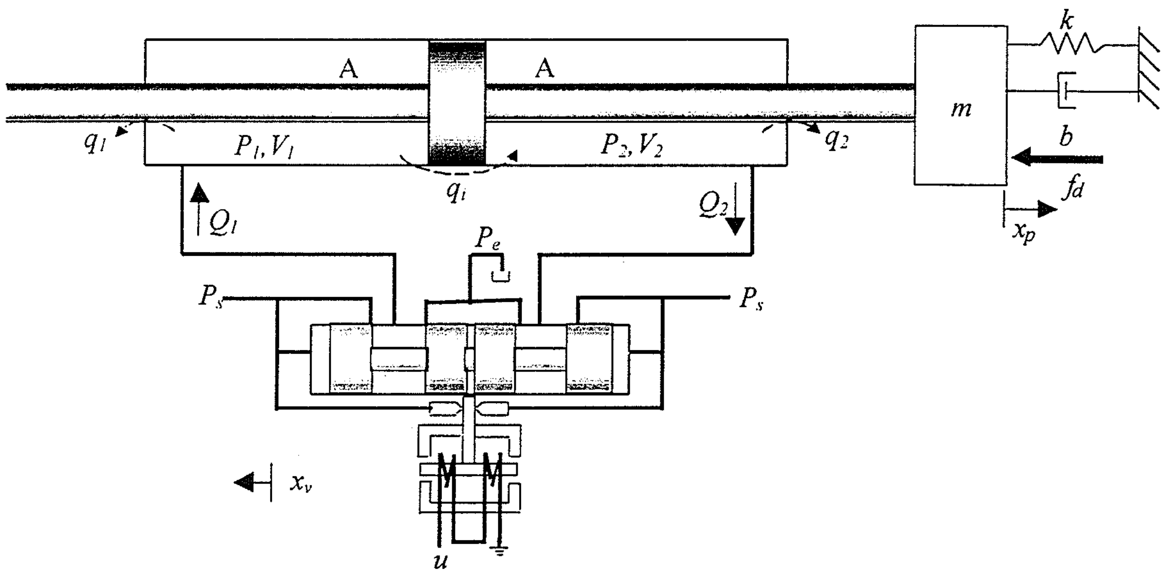

Figure 3.1: Schematic of a hydraulic positioning system

3.2.1 Actuator Dynamic Equations

With the reference of figure 3.1, the dynamic equation that describe the dynamics of this system is:

$$m\ddot{x}_p + b\dot{x}_p + kx_p = A(P_1 - P_2) - f_d \tag{3.1}$$

where x_p is the position of the actuator and m is the combined mass of the piston, rod, and load. P_1 and P_2 denote the pressures in the actuator chambers, f_d is an unknown disturbing force, b is the equivalent viscous damping resulting from friction between the piston and the cylinder walls, k is the spring constant of the load, and A is the annulus area of the piston.

The first derivatives of the time dependencies of the chamber pressures may be written as:

$$\dot{P}_1 = \frac{\beta}{V_1(x_p)}\left[Q_1 - q_1 - q_i - A\dot{x}_p\right] \tag{3.2}$$

and

$$\dot{P}_2 = \frac{\beta}{V_2(x_p)}\left[-Q_2 - q_2 + q_i + A\dot{x}_p\right] \tag{3.3}$$

where β is the effective bulk modulus of the system, V_1 is the volume of chamber 1, and V_2 is the volume of chamber 2, q_1, q_2 represent the external leakage flow rate in chamber 1 and 2 , respectively, and q_i is the internal leakage flow rate. The chamber volumes vary with the actuator position according to:

$$V_1(x_p) = V_{line} + V_o + Ax_p \tag{3.4}$$

and

$$V_2(x_p) = V_{line} + V_o - Ax_p \tag{3.5}$$

where V_o is the equivalent to the volume of either chamber when the piston is centered in the cylinder, and V_{line} is the volume of oil contained in the line connecting the actuator to the servovalve.

3.2.2 Servovalve Flow and Dynamic Equations

The nonlinear equations that describe the fluid flow distribution in the valve can be written as (Merritt, 1967):

$$\left.\begin{aligned} Q_1 &= C_v w x_v \sqrt{\frac{2(P_s - P_1)}{\rho}} \\ Q_2 &= C_v w x_v \sqrt{\frac{2(P_2 - P_e)}{\rho}} \end{aligned}\right\} \qquad x_v \geq 0 \tag{3.6}$$

and

$$\left.\begin{aligned} Q_1 &= C_v w x_v \sqrt{\frac{2(P_1 - P_e)}{\rho}} \\ Q_2 &= C_v w x_v \sqrt{\frac{2(P_s - P_2)}{\rho}} \end{aligned}\right\} \qquad x_v < 0 \tag{3.7}$$

In equations (3.6) and (3.7), Q_1 and Q_2 represent fluid flows into and out of the valve, respectively, ρ is the mass density of the hydraulic fluid, C is the valve coefficient of discharge, and w is the slot width of the port through which the fluid flows, *and* x_v is the valve spool position. Note that equations (3.6) and (3.7) assume the valve ports are match and symmetrical. Furthermore, it is assumed that the supply pressure, P_s, as well as the pressure in the line connecting the exhaust port of the servovalve to the tank, P_e, are constant. Similarly, the leakage flows can be approximated as turbulent orifices (Thompson *et al.*, 1999b) by:

$$q_1 = C_{l1} a_{l1} \sqrt{\frac{2P_1}{\rho}} \tag{3.8}$$

$$q_2 = C_{l2} a_{l2} \sqrt{\frac{2P_2}{\rho}} \tag{3.9}$$

and

$$q_i = C_i a_i \sqrt{\frac{2|P_1 - P_2|}{\rho}} \operatorname{sgn}(P_1 - P_2) \tag{3.10}$$

where C_{l1}, C_{l2} and C_i are the effective discharge coefficients of the leakage orifices and a_{l1}, a_{l2} and a_i are the effective areas of the leakage orifices, q_1, q_2 represent the external leakage flow rate in chamber 1 and 2 , respectively, and q_i is the internal leakage flow rate. The signum function is utilized in equation (3.10) to accommodate the directionality of the leakage across the piston seal.

In this work, the dynamics of the servovalve are modeled as a second-order lag, because the second-order lag model is generally more suited to the design of both position and force control loops since it yields more realistic servovalve phase information. The relationship between the torque motor current and the spool position is modeled as:

$$u = \frac{1}{k_v}\left(\frac{1}{\omega_v^2}\ddot{x}_v + \frac{2\zeta_v}{\omega_v}\dot{x}_v + x_v\right) \tag{3.11}$$

where u is the torque motor current, x_v is the valve spool position, k_v is the valve spool position gain, and ω_v and ζ_v are the equivalent second-order natural frequency and damping ratio, respectively.

By assembling equations (3.1) through (3.11) the nonlinear state equations of the hydraulic system may be written as:

for $x_v \geq 0$

$$\begin{aligned}
\dot{x}_p &= v_p \\
\dot{v}_p &= \frac{1}{m}\left(-kx_p - bv_p + AP_1 - AP_2\right) - \frac{1}{m}f_d \\
\dot{P}_1 &= \frac{\beta}{V_1(x_p)}\left(C_v w x_v\sqrt{\frac{2(P_s - P_1)}{\rho}} - C_{l1}A_{l1}\sqrt{\frac{2P_1}{\rho}} - C_i A_i\sqrt{\frac{2|P_1 - P_2|}{\rho}}\operatorname{sgn}(P_1 - P_2) - Av_p\right) \\
\dot{P}_2 &= \frac{\beta}{V_2(x_p)}\left(-C_v w x_v\sqrt{\frac{2(P_2 - P_e)}{\rho}} - C_{l2}A_{l2}\sqrt{\frac{2P_2}{\rho}} + C_i A_i\sqrt{\frac{2|P_1 - P_2|}{\rho}}\operatorname{sgn}(P_1 - P_2) + Av_p\right) \\
\dot{x}_v &= v_v \\
\dot{v}_v &= -\omega_v^2 x_v - 2\zeta_v\omega_v v_v + k_v\omega_v^2 u
\end{aligned} \tag{3.12}$$

and for $x_v < 0$

$$
\begin{aligned}
\dot{x}_p &= v_p \\
\dot{v}_p &= \frac{1}{m}\left(-kx_p - bv_p + AP_1 - AP_2\right) - \frac{1}{m} f_d \\
\dot{P}_1 &= \frac{\beta}{V_1(x_p)}\left(C_v w x_v \sqrt{\frac{2(P_1 - P_e)}{\rho}} - C_{l1} A_{l1}\sqrt{\frac{2P_1}{\rho}} - C_i A_i \sqrt{\frac{2|P_1 - P_2|}{\rho}} \operatorname{sgn}(P_1 - P_2) - A v_p\right) \\
\dot{P}_2 &= \frac{\beta}{V_2(x_p)}\left(-C_v w x_v \sqrt{\frac{2(P_s - P_2)}{\rho}} - C_{l2} A_{l2}\sqrt{\frac{2P_2}{\rho}} + C_i A_i \sqrt{\frac{2|P_1 - P_2|}{\rho}} \operatorname{sgn}(P_1 - P_2) + A v_p\right) \\
\dot{x}_v &= v_v \\
\dot{v}_v &= -\omega_v^2 x_v - 2\zeta_v \omega_v v_v + k_v \omega_v^2 u
\end{aligned}
\tag{3.13}
$$

In equations (3.12) and (3.13), the output is the actuator position x_p and the inputs are the torque motor current u and the disturbing force, f_d.

3.3 Description of the Test Station

Figure 3.2 shows a simplified schematic of the hydraulic test station developed in this work to allow the experimental simulation of faults in the hydraulic system. The system consists of a simulation circuit (Figure 3.3) that can be made to interact with an environment. This system is mounted to a reinforced steel table and is supplied with filtered hydraulic fluid from a common hydraulic power supply. The power supply is capable of delivering fluid at a maximum pressure of approximately 21 MPa (see Figure 3.4).

The system consists of an electrohydraulic servovalve, one main actuator, two slave actuators, a needle valve, and a power supply unit. The computer system used for monitoring and controlling proposes is a personal computer with a Pentium III CPU running under the Windows 98 operating system. Two I/O boards are used to perform the communication between the computer and the test station. To convert the digital control signals to analog control signals, a CIO-DAS16F board is used.

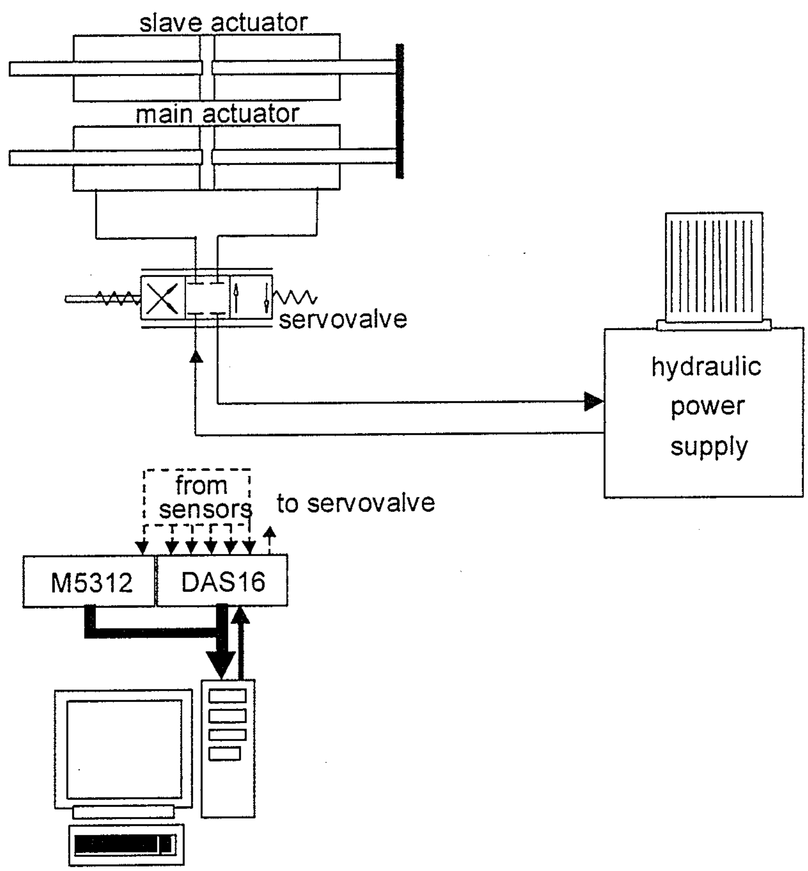

Figure 3.2: Schematic of the experimental test station.

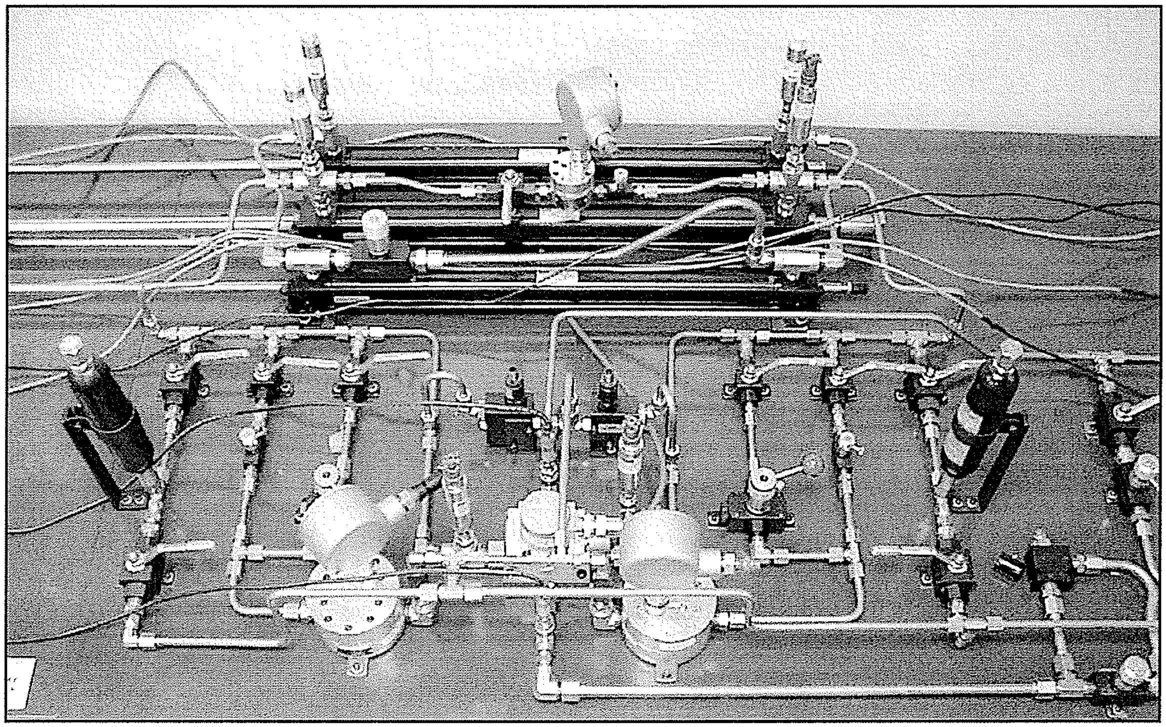

Figure 3.3: Fault simulation circuit.

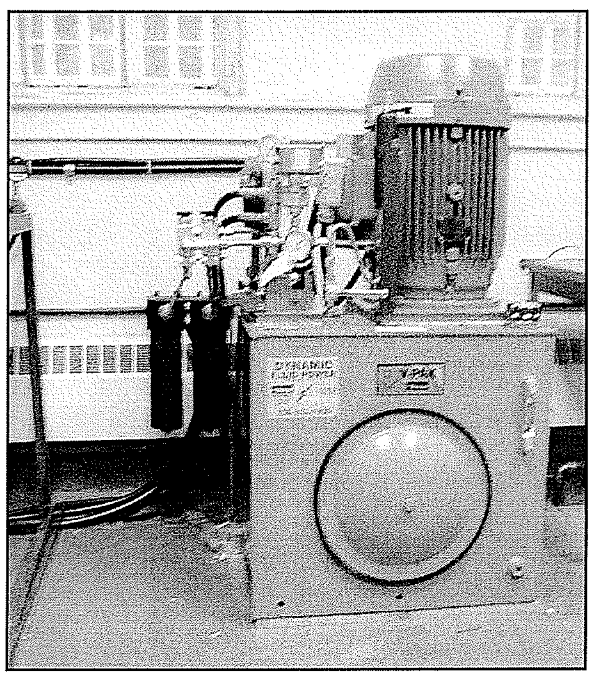

Figure 3.4: Hydraulic power supply.

The system parameters were either obtained directly, or estimated from the available manufacturer's catalogues. Table 3.1 lists the system parameters.

Table 3.1: System parameters.

Parameter	*Symbol*	*value*	*Unit*
Actuator			
- *mass*	m	*10.0*	*kg*
- *bore*	d_a	*38.1*	*mm*
- *effective piston area*	A	*633.0*	mm^2
- *stroke length*	l	*609.6*	*mm*
- *viscous damping*	d	*1000.0*	*N.s/m*
- *chamber volume*	V_o	*192.1*	cm^3
- *line volume*	V_{line}	*41.8*	cm^3
Servovalve			
- *min input voltage , max input voltage*	u_{min}, u_{max}	*-10 to +10*	*V*
- *min and Max spool displacement*	$x_{v\ min/max}$	*-0.406 to +0.406*	*mm*
- *spool position gain*	k_v	*0.0406*	*mm/V*
- *discharge coefficient*	C_v	*0.6*	
- *flow rate slot width*	w	*20.75*	*mm*
- *2nd order natural frequency*	w_v	*150*	*Hz*
- *2nd order damping rate*	ξ_v	*0.5*	
Pump			
- *supply pressure*	P_s	*0 to 21*	*MPa*
-*return pressure*	P_e	*Variable*	*MPa*
Hydraulic fluid			
- *density*	ρ	*847*	Kg/m^3
- *effective bulk modulus*	β	*689*	*MPa*

Chapter 4

Development of the Controllers

In this chapter three design schemes for iterative learning control methods are presented. Section 4.1 describes the basic algorithm of ILC. In Section 4.2, the iterative learning control with proportional error feedback algorithm is presented. In Section 4.3, a description of the iterative learning control with current cycle feedback is given.

4.1 Basic ILC

The algorithm of the basic ILC is:

$$u_{k+1}(t) = T_u u_k(t) + T_e e_k(t) \qquad t \in \left[t_{o(k)}, t_{o(k)} + T\right] \tag{4.1}$$

where T is the time required to perform the trajectory, $t_{o(k)}$ is the time for the kth trial, and T_e and T_u are the weights of the error and the previous control signal, respectively.

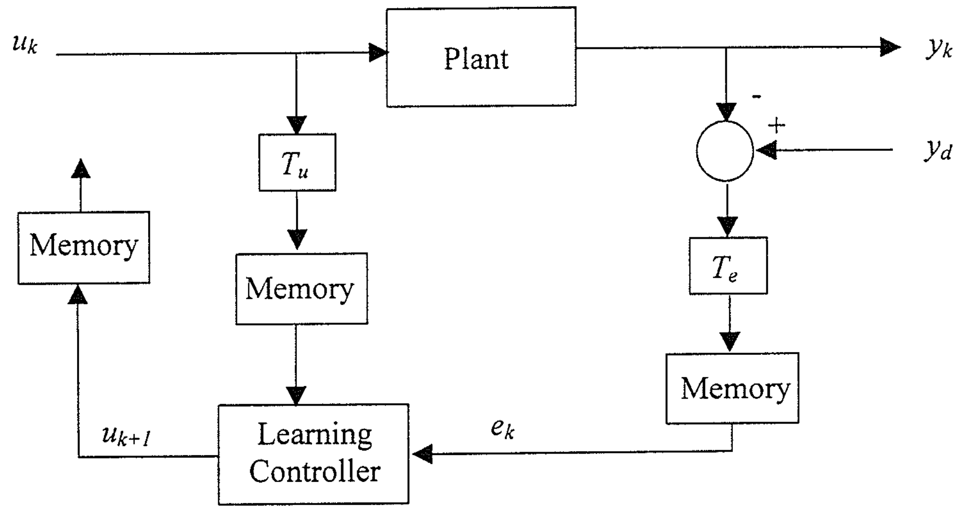

Figure 4.1: Block diagram of the basic ILC

The system operates as follows: (i) during the k^{th} trial input $u_k(t)$ is applied to the hydraulic system producing an output $y_k(t)$; the error between the actual output and the desired output is calculated $e_k(t) = y_d(t) - y_k(t)$; (ii) both the error signal and the input signal are stored in the memory until the trial is over; and (iii) the ILC computes a new input signal, $u_{k+1}(t)$, that will be stored in the memory until the next time the system operates. This new input signal is designed according to the ILC algorithm to produce a smaller error than the previous trial. Note that the basic ILC is acting off-line and the new input signal is fed in a point-to-point fashion each time the system operates. Also, the initial conditions of the system are reset to the same value at the beginning of each trial. Finally in the basic ILC, the system repeatedly performs a specific motion that ends in a fixed duration which means that the trial length is fixed.

4.2 ILC with Proportional Error Feedback

This design scheme is based on the work of Zheng *et al.* (1998), where the ILC with a feedback controller has been applied to the system. The following equations represent the controller algorithm:

$$\underbrace{u_k(t)}_{\substack{present\\iteration\\input}} = \overbrace{\underbrace{k_p e_k(t)}_{\substack{present\\iteration\\error}}}^{\substack{feedback\\term}} + \underbrace{\lambda u_k^{ILC}(t)}_{\substack{present\\iteration\\feedforward\\term}} \tag{4.2}$$

where λ and k_p are the feedforward and the feedback gains respectively. u_k^{ILC} is the present signal from feedforward ILC,

$$u_k^{ILC}(t) = T_u u_{k-1}^{ILC}(t) + T_e e_{k-1}(t) \tag{4.3}$$

and where T_e and T_u are the weights of the error and the previous control signal respectively.

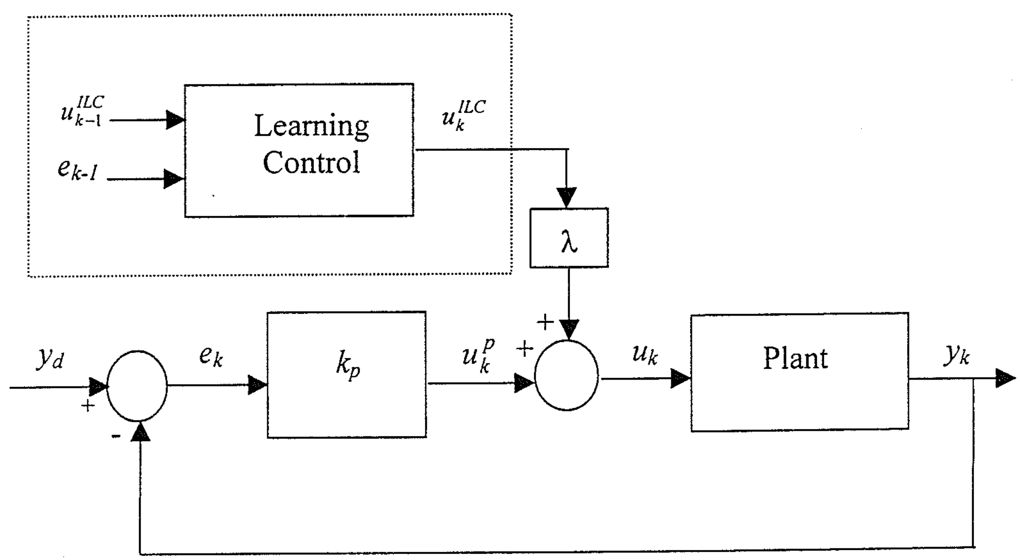

Figure 4.2: Block diagram of the ILC with proportional error feedback

In this design scheme, the ILC is a feedforward controller and it is similar to basic ILC, which is acting as an off-line controller. The overall control signal is the sum of the ILC new input signal and the proportional current error. Adding the ILC as a feedforward controller enhances the system performance where the controller learns from the previous trial and reduces the error as the number of trials increase.

4.3 ILC with Current Cycle Feedback

Xu *et al.* (1995) classified the iterative learning control algorithms into two major categories, according to the different feedback patterns. The first type is a PCF type, which refers to the previous cycle feedback(PCF). Both the basic ILC and the ILC with proportional error feedback are fallen into this category. The second type is a CCF type, which refers to the current cycle feedback (CCF). This includes the ILC with current cycle feedback. The ILC with current cycle feedback algorithm is:

$$u_k^{ILC}(t) = \lambda u_{k-1}^{ILC}(t) + k_p e_k(t) \tag{4.4}$$

where λ and k_p are the feedforward and the feedback gains, respectively..

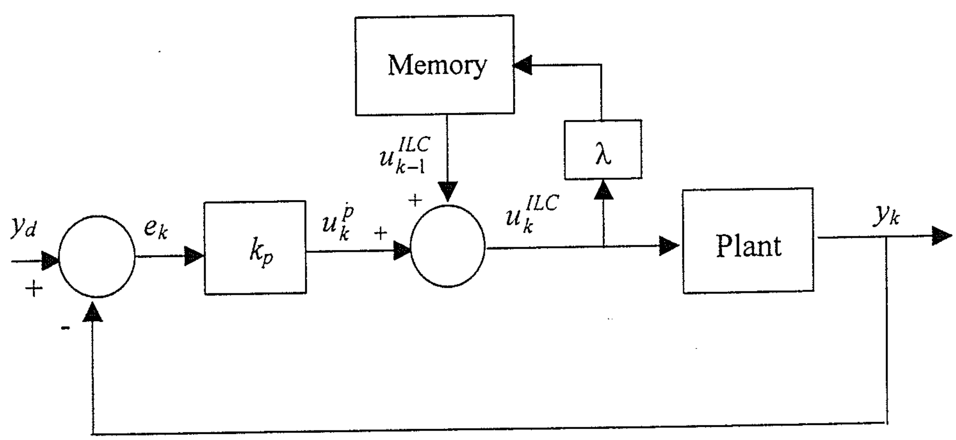

Figure 4.3: Block diagram of the ILC with current cycle feedback

The ILC with current cycle feedback scheme is essentially a closed-loop control method with respect to the current cycle feedback. The learning law scheme corrects the feedforward input directly by adding a fraction of current feedback error which means the current cycle tracking information is involved in the closed loop. The ILC with a current cycle feedback scheme uses the information from both of the previous and the current trials, which makes it robust against external input disturbances.

Chapter 5

Simulation Results

In this chapter, the ILC schemes presented in Chapter 4 are implemented in simulation for the control of a nonlinear hydraulic positioning system. To carry out the simulations, each ILC algorithm was first transformed into its equivalent state-space representations and was coupled with the nonlinear state equations (3.12) and (3.13). The system parameters of Table 3.1 were used. The integration of the resulting assemblage was accomplished by the fourth-order Runge-Kutta scheme with a fixed integration time step of 0.001 second. The initial physical states of the hydraulic system were set as y_0=0.30 m (initial position), and v_0=0 m/sec (initial velocity); the supply and the return pressures were set to 17.2 MPa and 0 MPa, respectively. The initial pressures in each of the actuator chambers were set to half of the supply pressure (i.e., 8.6 MPa). Friction was considered in the simulation, as well as a 5% dead-band. The simulation program is written in C^{++} language. Table 5.1 gives the controller's gains used in the simulations.

Table 5.1: Controller gains used in the simulations

Controllers	T_u	T_e **(V/m)**	λ	k_p**(V/m)**
Basic ILC	0.95	25	-	-
ILC with proportional error feedback	0.95	25	1.0	50
ILC with current cycle feedback	-	-	0.93	50

Two case studies were conducted. In the first case study, two tests were carried out under normal operations. First, a step signal was repetitively performed and the initial conditions of the system were reset to the same values at the beginning of each trial. Second, a step signal was repetitively performed without resetting the initial conditions of the system to the same values at the beginning of each trial. In the second case study, the same two tests as in the first case study were carried out under the presence of internal leakage fault. In Section 5.1, the simulations with the basic ILC are discussed. The simulations with the ILC with proportional error feedback are given in Section 5.2. In Section 5.3, the simulations with the ILC with current cycle feedback are discussed.

5.1 Basic ILC

The basic ILC algorithm, which is described in equation 4.1, is introduced to the simulation program, and a several tests have been done on the system.

Case study 1 (normal operation): In the first set of simulations, a step signal was repeatedly performed and the initial conditions of the system were reset to the same values at the beginning of each trial. The results are shown in Figures 5.1 and 5.2. Figures 5.1a, b, c, d, and e show the system responses at the 1^{st}, 10^{th}, 20^{th}, 40^{th}, and the 80^{th} trials, respectively. It is clear that as the number of trials increase, the ILC algorithm has driven the system to follow the desired trajectory. Figures 5.1 a, b, c, d, and e show the learning control signal at the 1^{st}, 10^{th}, 20^{th}, 40^{th}, and the 80^{th} trials, respectively. By the time of the 80^{th} trial, the basic ILC has learned the feedforward command necessary for the position to track the desire trajectory. In the second set of simulations where a step signal was repetitively performed without resetting the initial conditions of the system to the same values at the beginning of each trial, the basic ILC gave an unstable performance.

Case study 2 (faulty operation): In this set of simulations, the initial conditions of the system were reset to the same values at the beginning of each trial and an internal leakage was introduced to the system after the 80th trial. The results are shown in Figures 5.3 through 5.5. Figure 5.3a shows the system response using the basic ILC when the fault occurs. Figure 5.3b shows the system response after one trial from applying the internal leakage. It is clear that a little improvement in the system response as well as less error can be noticed. Figures 5.3c and 5.3d show the output signal after the 6th and 12th trials, respectively. It is clear that after 12 trials, the basic ILC has forced the output to the desired value and has overcome the internal leakage fault. In another wards, the internal leakage fault caused an error on the position. Due to this error, the control signal changed its value to eliminate this error and tracks the desired trajectory.

Figures 5.4 a, b, c, and d show the learning control signals at the 81st, 82nd, 87th, and 93rd trials, respectively. It is seen that after only 12 trials from the internal leakage occurrence, the basic ILC has learned the feedforward command necessary to overcome the fault and the position to track the desire trajectory. Figures 5.5a, b, c, and d show the internal leakage flow rates at the 81st, 82nd, 87th, and 93rd trials, respectively.

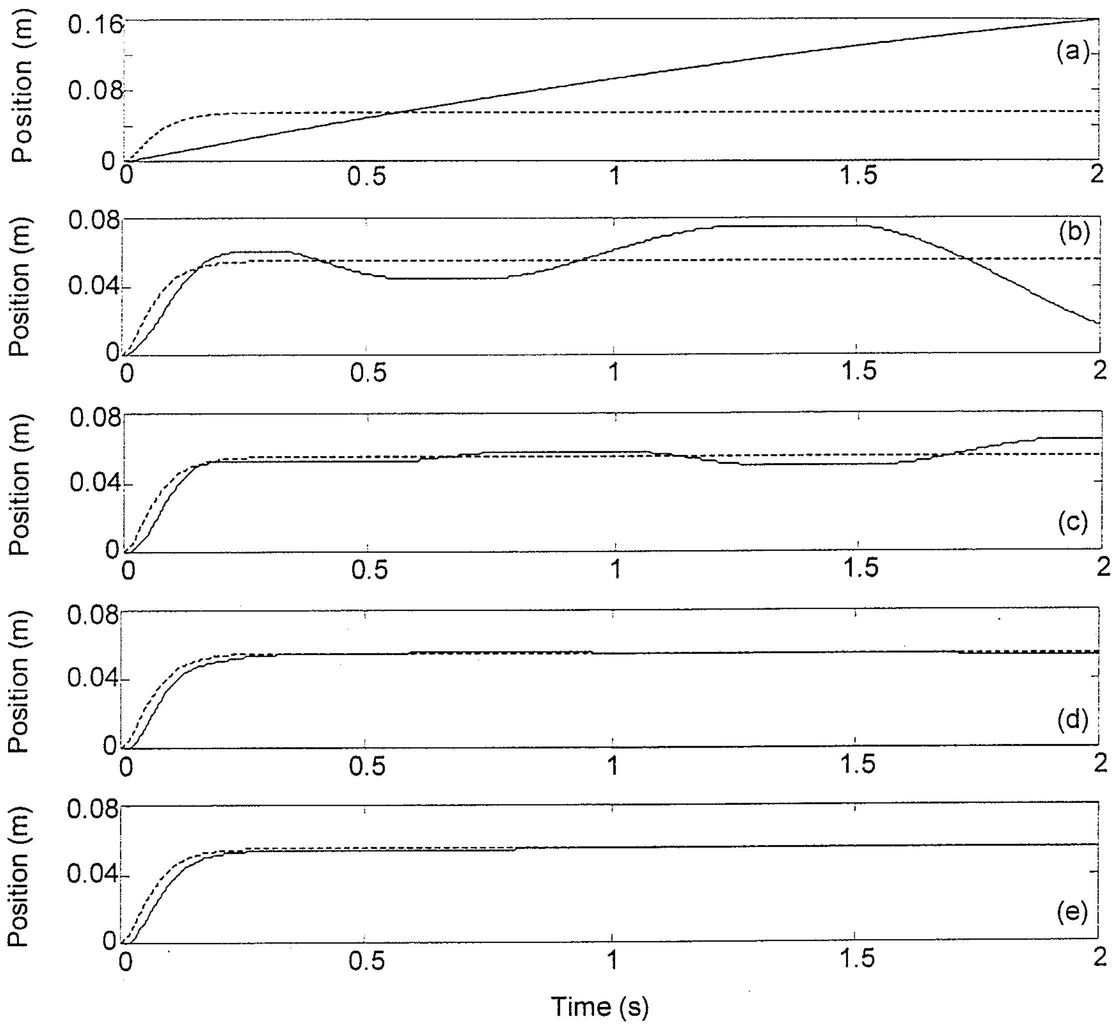

Figure 5.1: System responses of the basic ILC (---- desired output, — actual output): (a) at 1st trial; (b) 10th trial; (c) 20th trial; (d) 40th trial; (e) 80th trial (simulations).

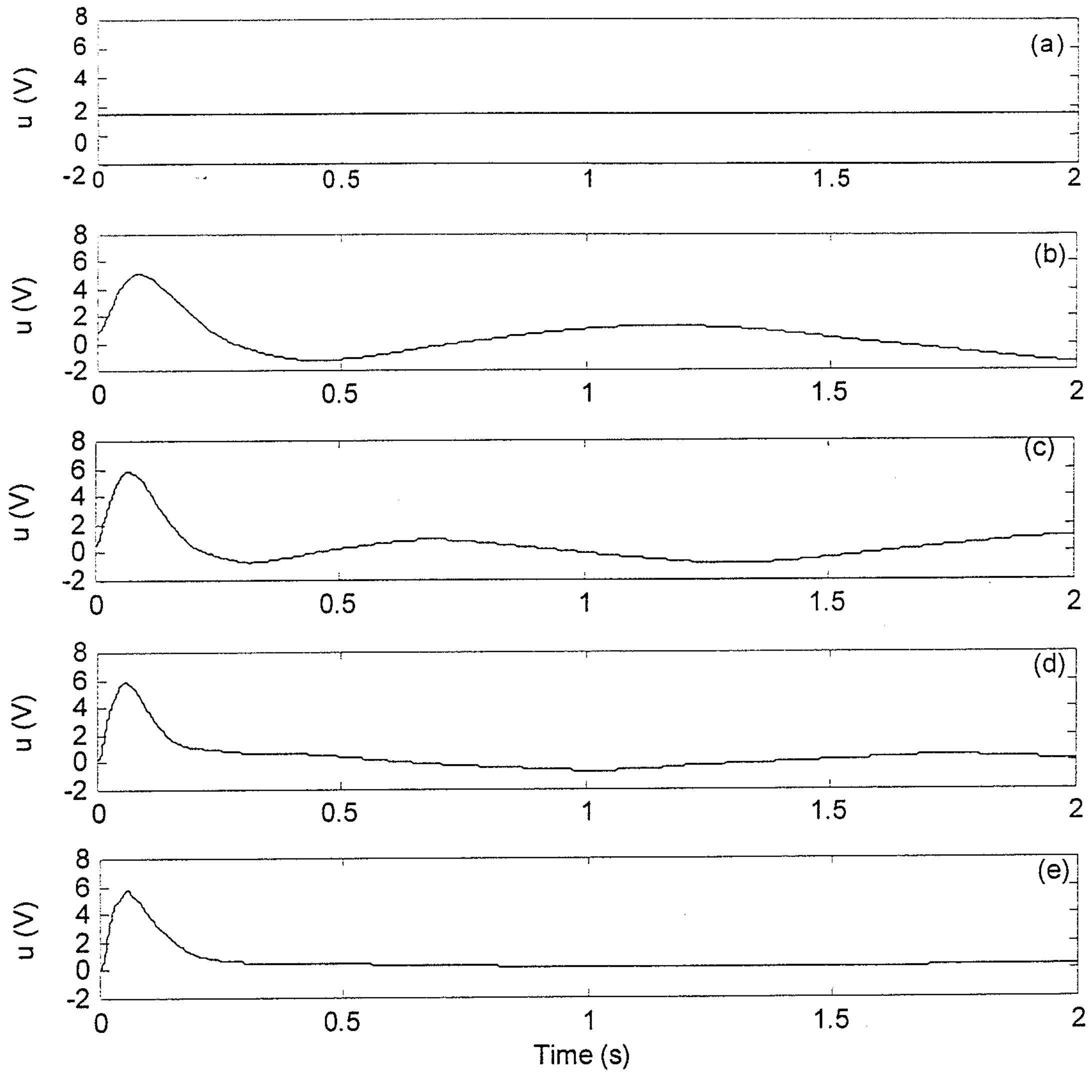

Figure 5.2: Control signals of the basic ILC: (a) at 1st trial; (b) 10th trial; (c) 20th trial; (d) 40th trial; (e) 80th trial (simulations).

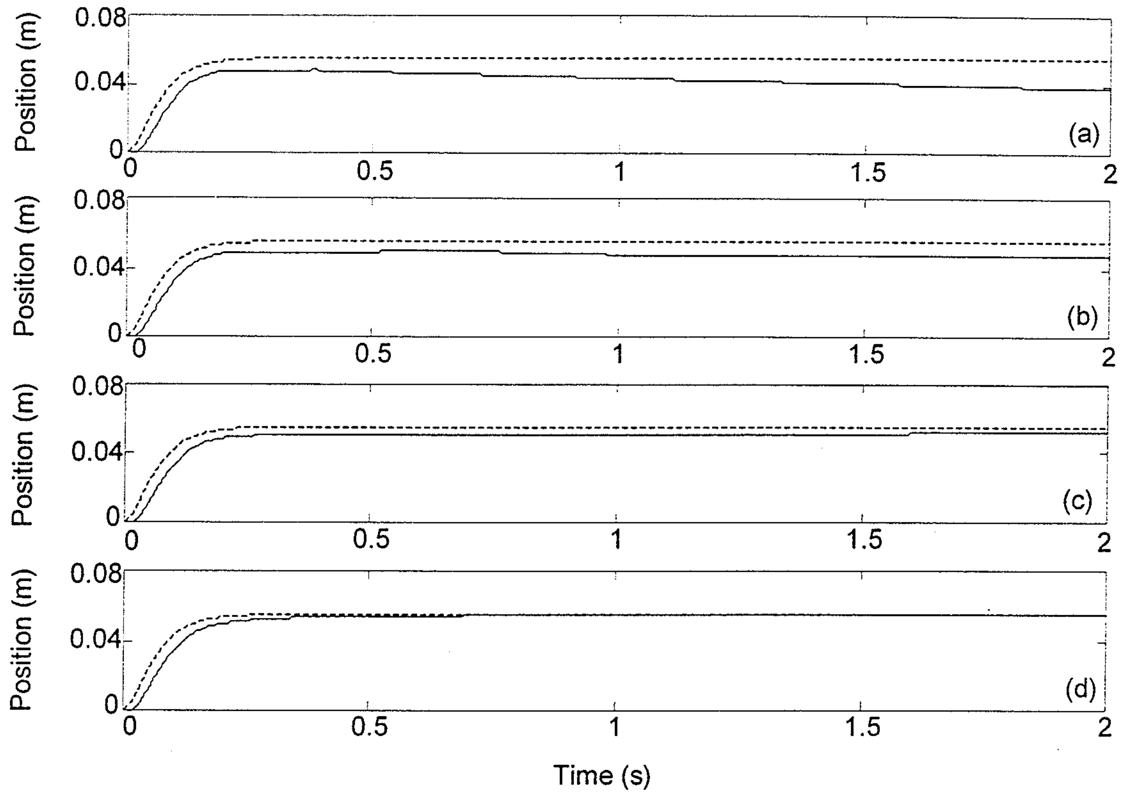

Figure 5.3: System responses of the basic ILC: (---- desired output, — actual output) (a) at 81^{st} trial; (b) 82^{nd} trial; (c) 87^{th} trial; (d) 93^{rd} trial (simulations).

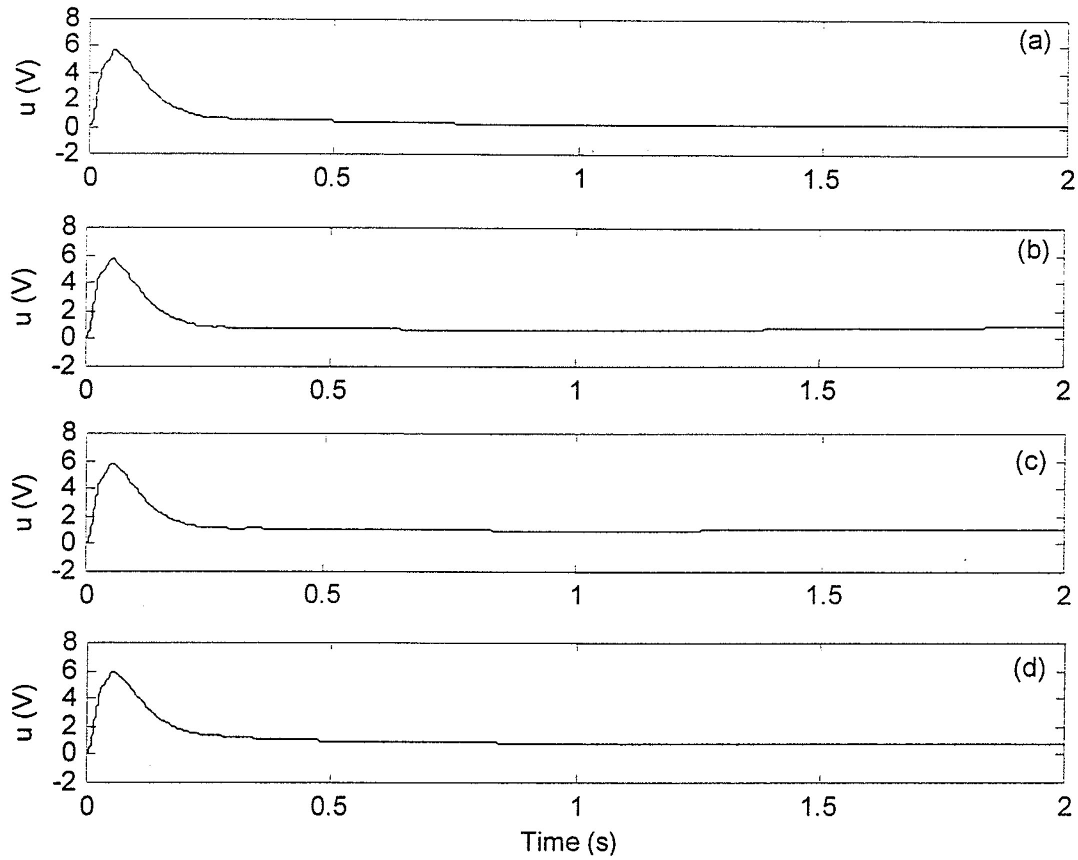

Figure 5.4: Control signals of the basic ILC: (a) at 81st trial; (b) 82nd trial; (c) 87th trial; (d) 93rd trial (simulations).

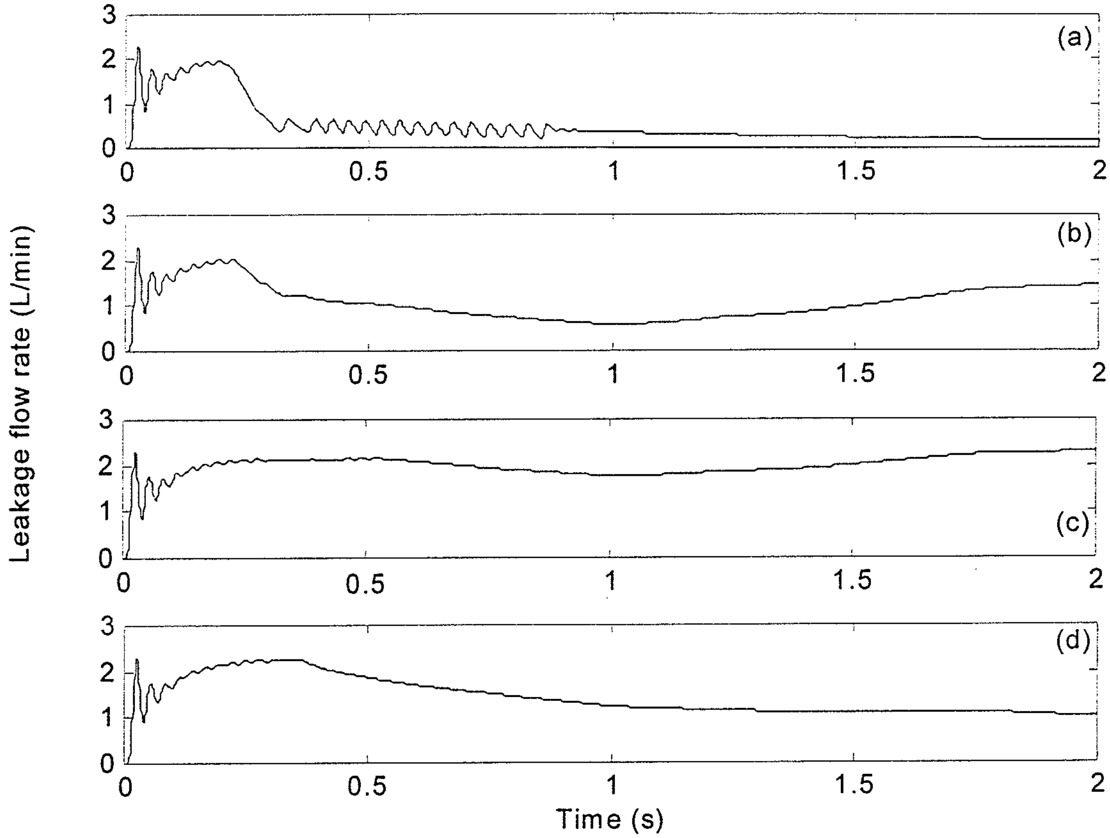

Figure 5.5: Internal leakage flow rates: (a) at 81st trial; (b) 82nd trial; (c) 87th trial; (d) 93rd trial (simulations).

5.2 ILC with Proportional Error Feedback.

Case study 1 (normal operation): In the first set of simulations, a step signal was repeatedly performed and the initial conditions of the system were reset to the same values at the beginning of each trial. The results are shown in Figures 5.6 and 5.7. Figure 5.6a shows the system response at the 1st trial; this trial uses strictly the feedback term and there is no feedforward term. Figures 5.6b, c, and d show the system responses at the 10th, 20th, and 40th trials, respectively. It is seen that the ILC with proportional error feedback is able to accommodate the nonlinearities and adapt the feedforward function to reduce the error. It is also clear that the algorithm has forced the output to reach the desired value as the number of trials increase.

Figure 5.7a1 shows the feedforward, Figure 5.7a2 shows the feedback term and Figure 5.7a3 shows the total control signal of the ILC for the 1st trial. At this trial, there is no feedforward term u^{ILC}=0 and the total control signal will be equal to the feedback term. Figures 5.7d1, d2 and d3 show the feedforward term, the feedback term, and the total control signal at the 40th trial. It is seen that the effect of the feedforward term is increasing as the number of trial increase and the effect of the feedback term is decreasing.

In the second set of simulations, a step signal was repetitively performed without resetting the initial conditions of the system to the same values at the beginning of each trial. The results are shown in Figures 5.8 through 5.10. Figure 5.8 shows that the ILC with proportional error feedback can track the desired trajectory without the need for resetting the initial conditions to the same values at the beginning of each trial. Figure 5.9 shows the total control signal of the ILC and Figures 5.10a and 5.10b show the feedforward term and the feedback term of the control signal respectively. It is seen that the effect of the feedforward term on the total control signal is bigger than the feedback term under the normal operation.

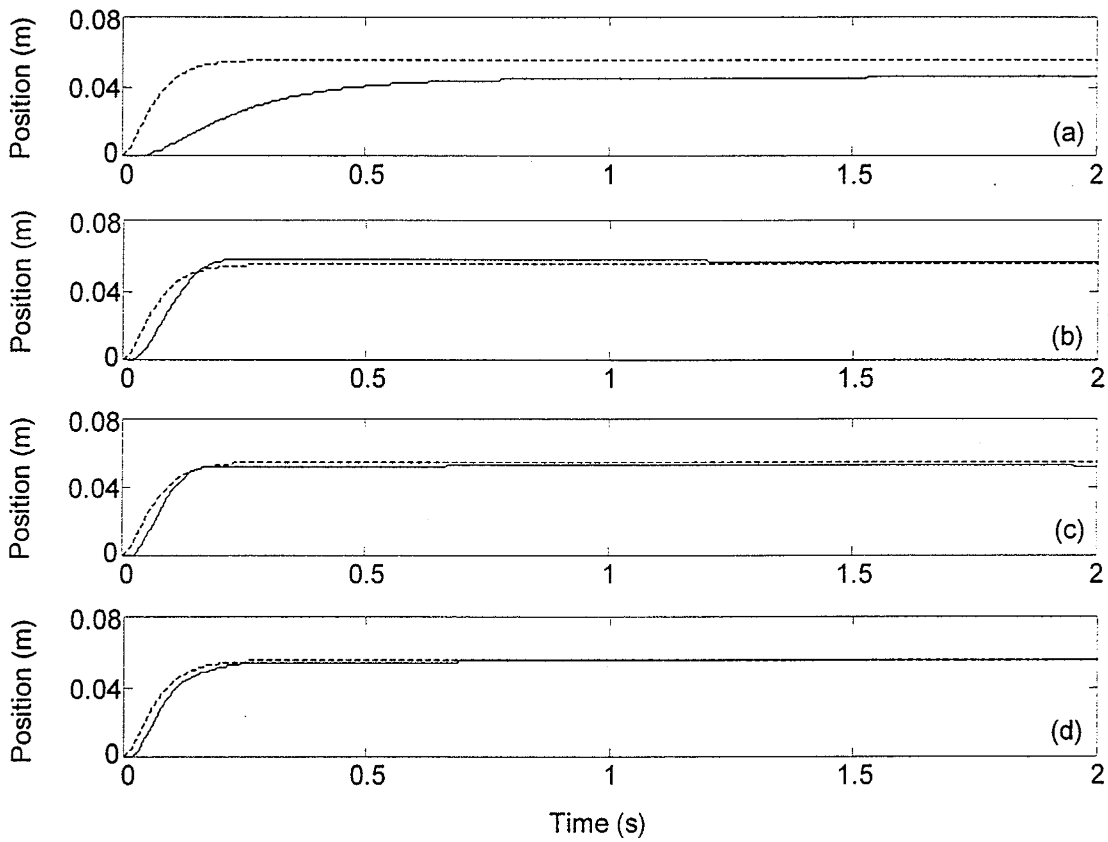

Figure 5.6: System responses of the ILC with proportional error feedback: (--- desired, — actual), (a) at 1st trial; (b) 10th trial; (c) 20th trial; (d) 40th trial (simulations).

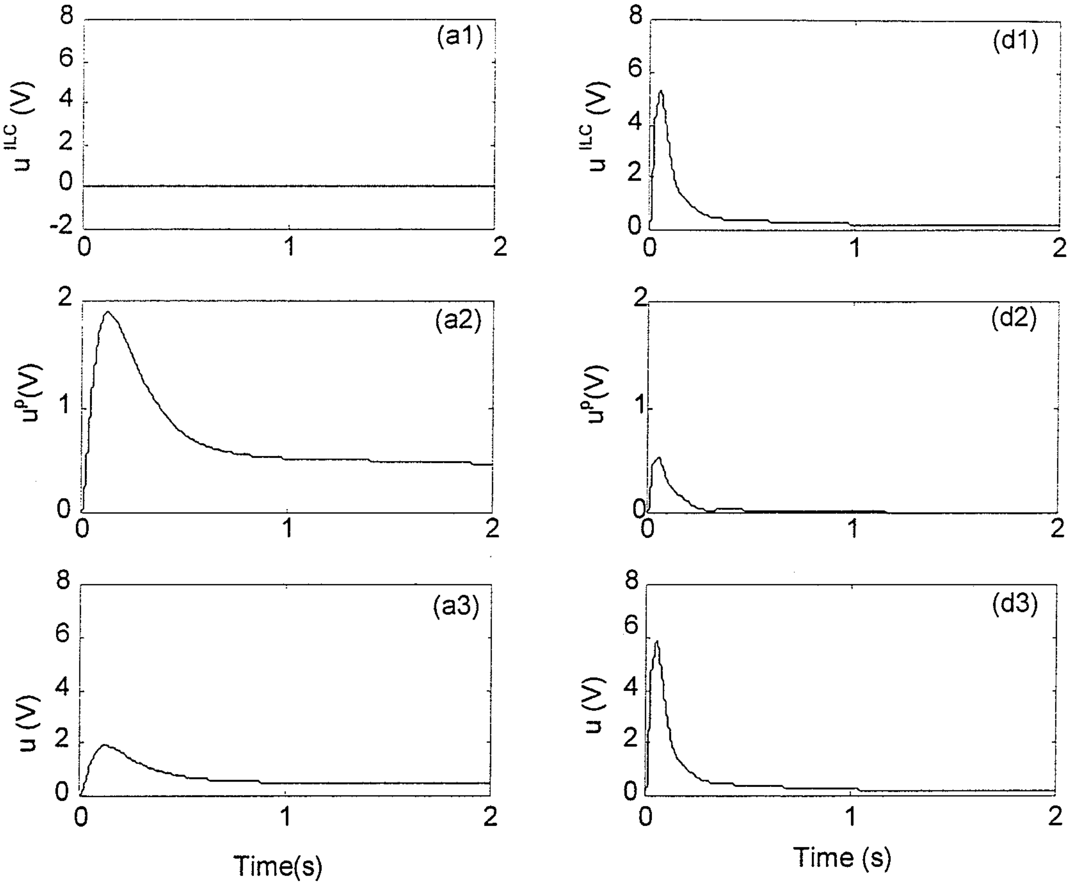

Figure 5.7: Control signal contributions of the ILC with proportional error feedback: (a1), (a2), and (a3) at the 1st trial; (d1), (d2), and (d3) at the 40th trial (simulations).

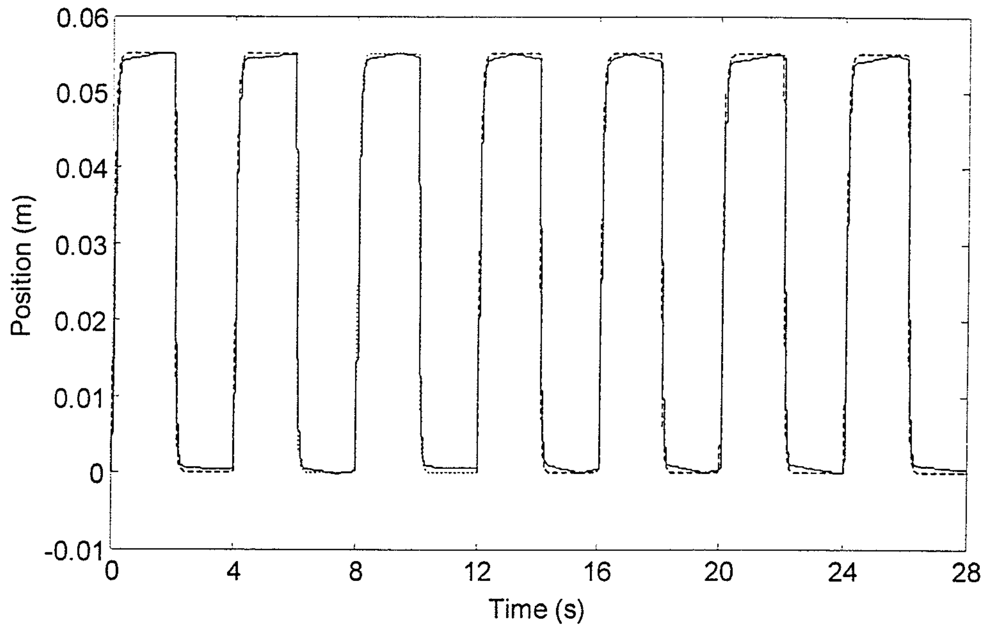

Figure 5.8: System response using ILC with proportional error feedback: (----- desired, —— actual) under normal operation (simulations).

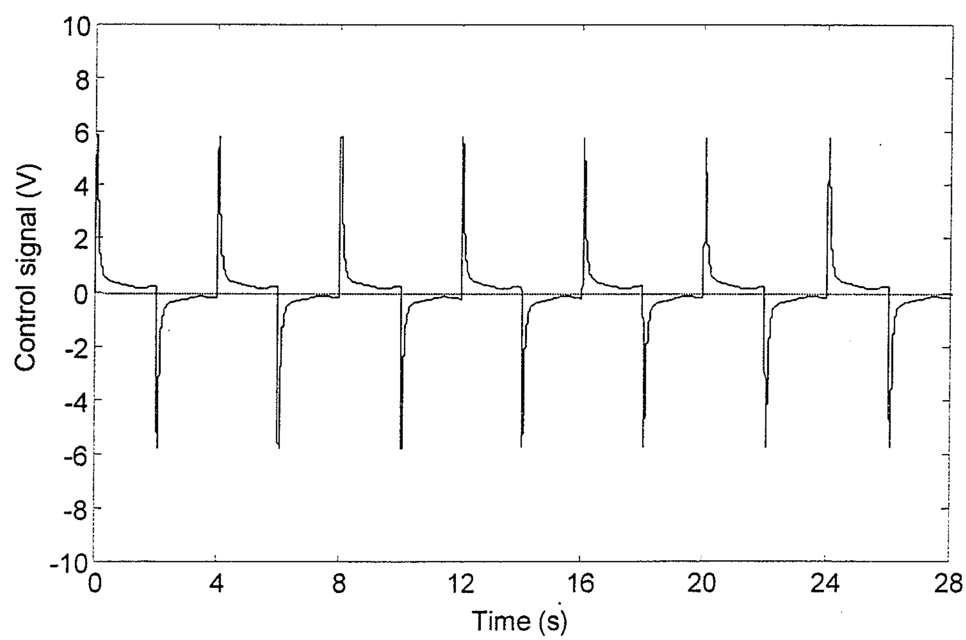

Figure 5.9: Control signal of the ILC with proportional error feedback under normal operation (simulations).

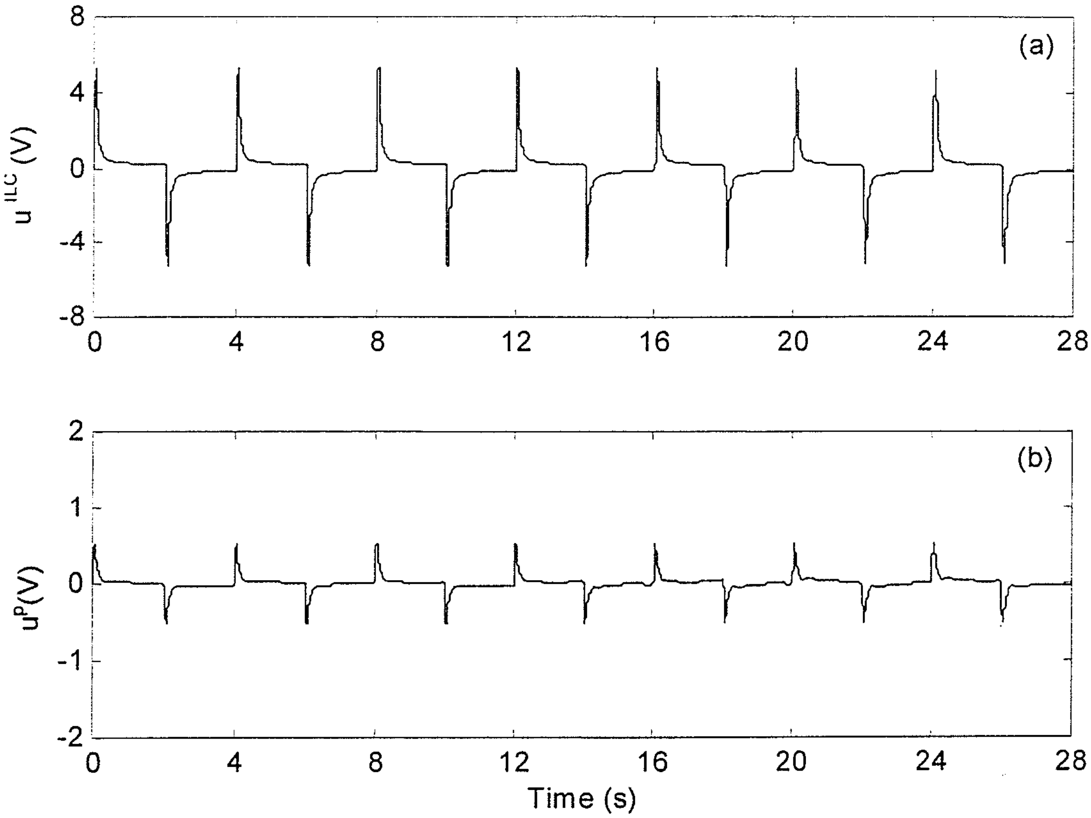

Figure 5.10: Control signal contribution of the ILC with proportional error feedback under a normal operation: (a) feedforward term; (b) feedback term (simulations).

Case study 2 (faulty operation): in this set of simulations, the initial conditions of the system were reset to the same values at the beginning of each trial, and an internal leakage was introduced to the system after the 40th trial. The results are shown in Figures 5.11 through 5.13. Figure 5.11a shows the system response using the ILC with proportional error feedback when the internal leakage fault occurred. Figures 5.11b, c, and d show the system responses at the 43rd, 45th, and 49th trials, respectively. It is seen that the within only 8 trials the system was able to overcome the leakage fault and to track the desired trajectory. Figures 5.12a1, a2, and a3 show the controller responses when an internal leakage occurred in the system. Figures 5.12d1, d2, and d3 show the control signals after 8 trials from applying the leakage. When these results are compared, it is clear that after 8 trials of applying the leakage the feedforward signal is very close to the total control signal and the feedback is nearly zero. Figures 5.13a, b, c, and d show the internal leakage flow rates at the 41^{st}, 43^{rd}, 45^{th}, and the 49^{th} trials, respectively.

In the next set of simulations, a step signal was repeatedly performed without resetting the initial conditions of the system to the same values at the beginning of each trial. An internal leakage was introduced to the system after 4 seconds. The results are shown in Figures 5.14 through 5.17. Figure 5.14 shows the system response of the ILC with proportional error feedback with the occurrence of the internal leakage. It is shown that the controller is able to reduce the position error due to the leakage.

Figure 5.15 shows the total control signal of the ILC with proportional error feedback. Figures 5.16a and 5.16b show the feedforward term and the feedback term of the control signal respectively. When these results are compared, it is clear that after about 4 trials of applying the leakage the feedforward signal is close to the total control signal and the value of the feedback term is nearly zero. Figure 5.17 shows the internal leakage flow rate.

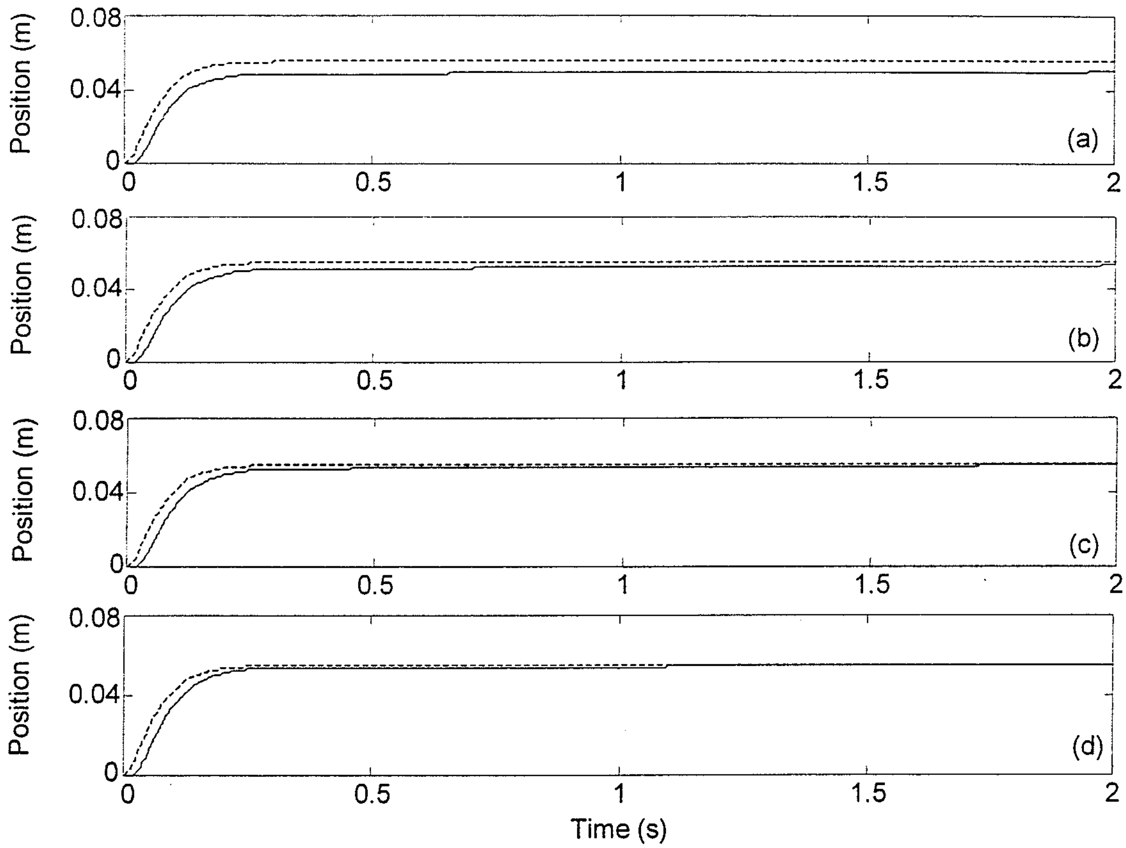

Figure 5.11: System responses of the ILC with proportional error feedback: (---- desired, —— actual), (a) at 41st trial; (b) 43rd trial; (c) 45th trial; (d) 49th trial (simulations).

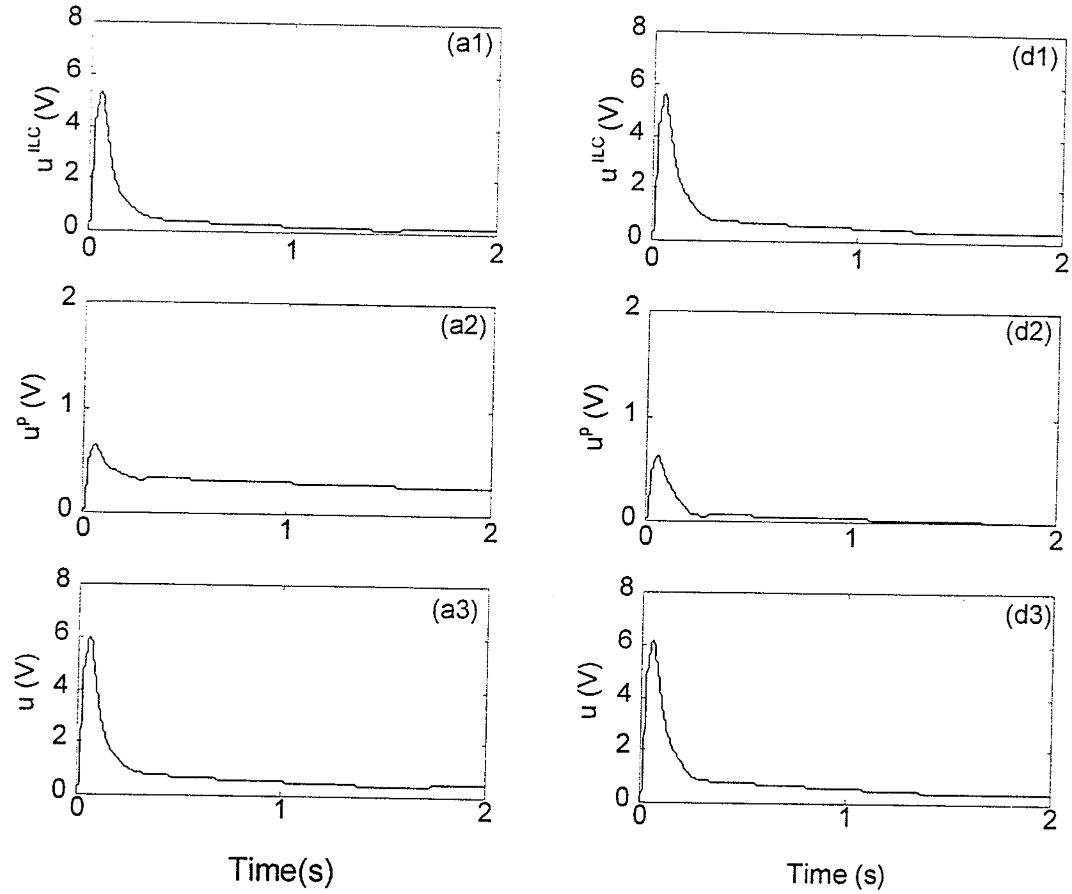

Figure 5.12: Control signal contributions of the ILC with proportional error feedback: (a1), (a2), and (a3) at the 41st trial; (d1), (d2), and (d3) at the 49th trial (simulations).

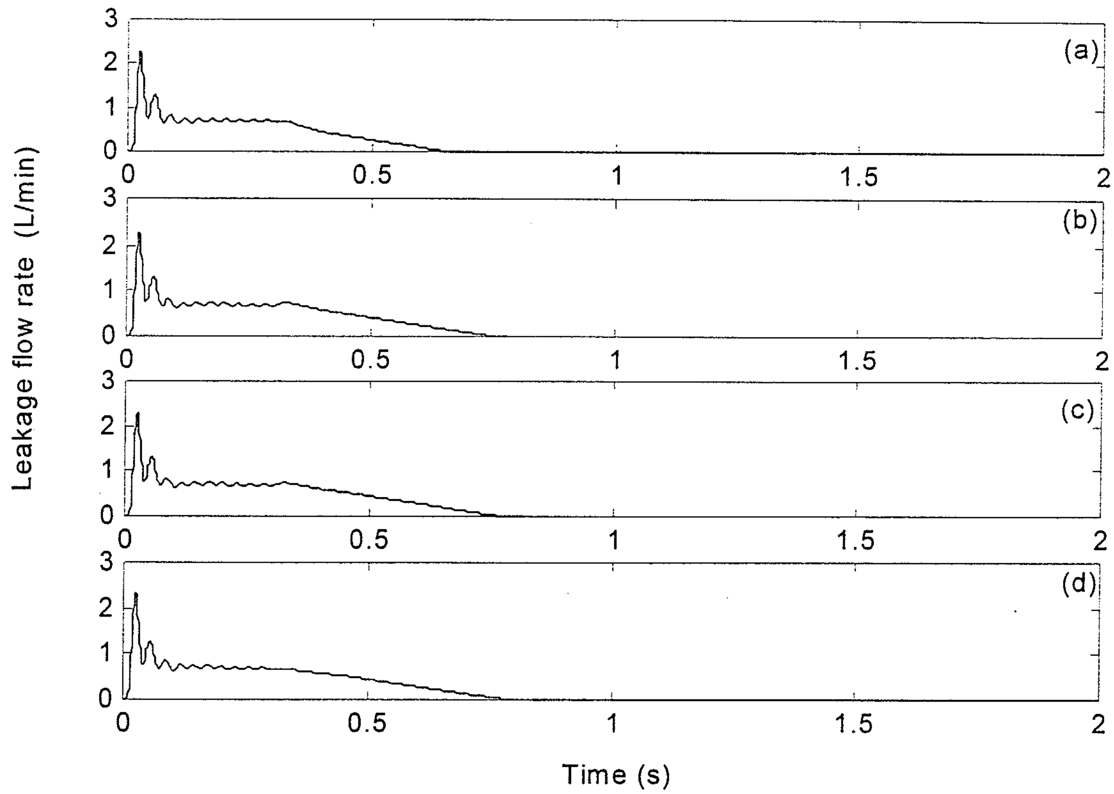

Figure 5.13: Internal leakage flow rates: (a) at 41st trial, (b) 43rd trial, (c) 45th trial, (d) 49th trial (simulations).

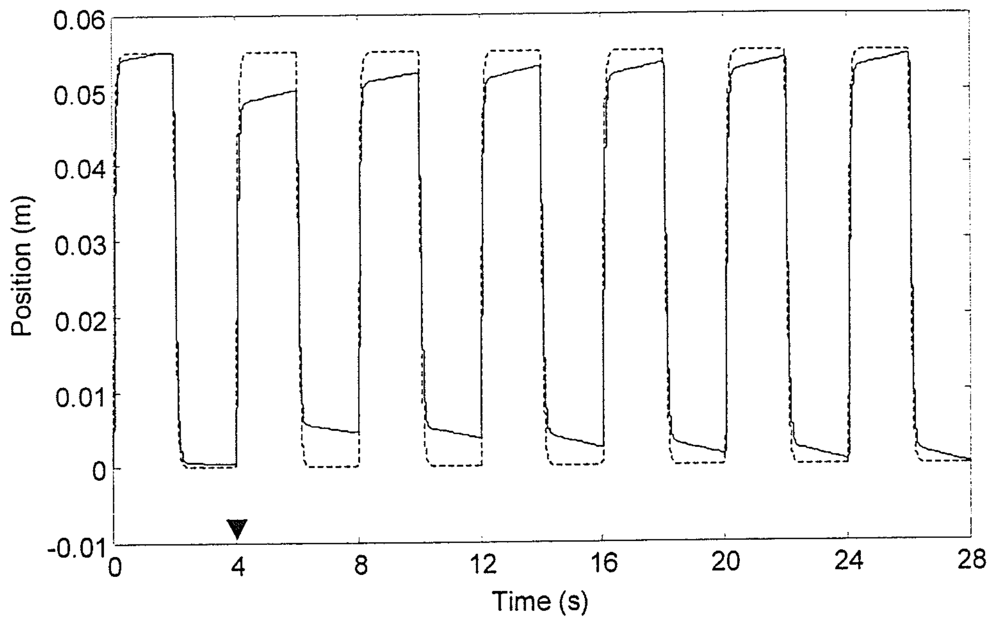

Figure 5.14: System response of the ILC with proportional error feedback (---- desired, —— actual) under faulty operation (simulations).

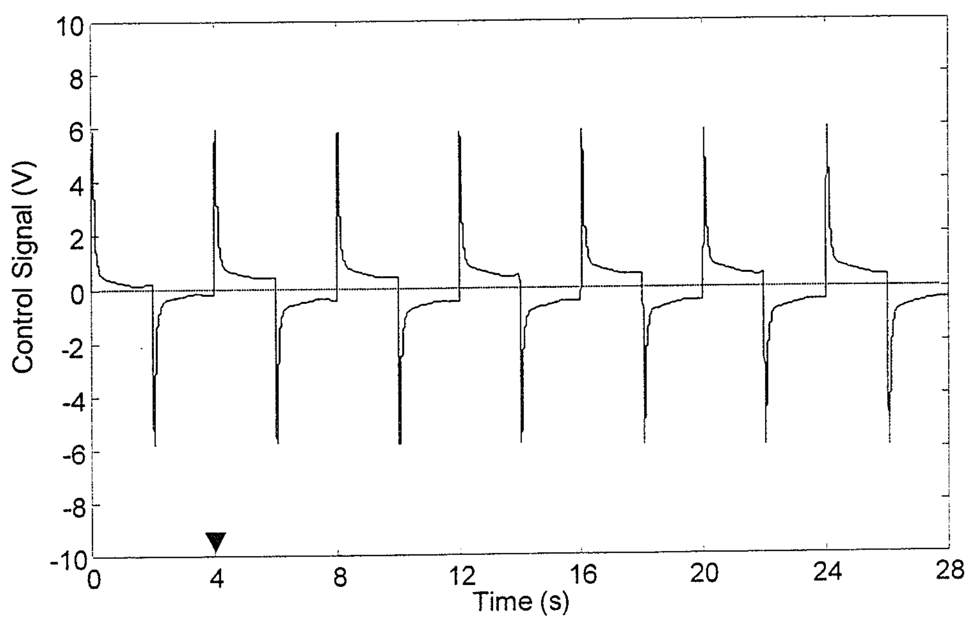

Figure 5.15: Control signal of the ILC with proportional error feedback under faulty operation (simulations).

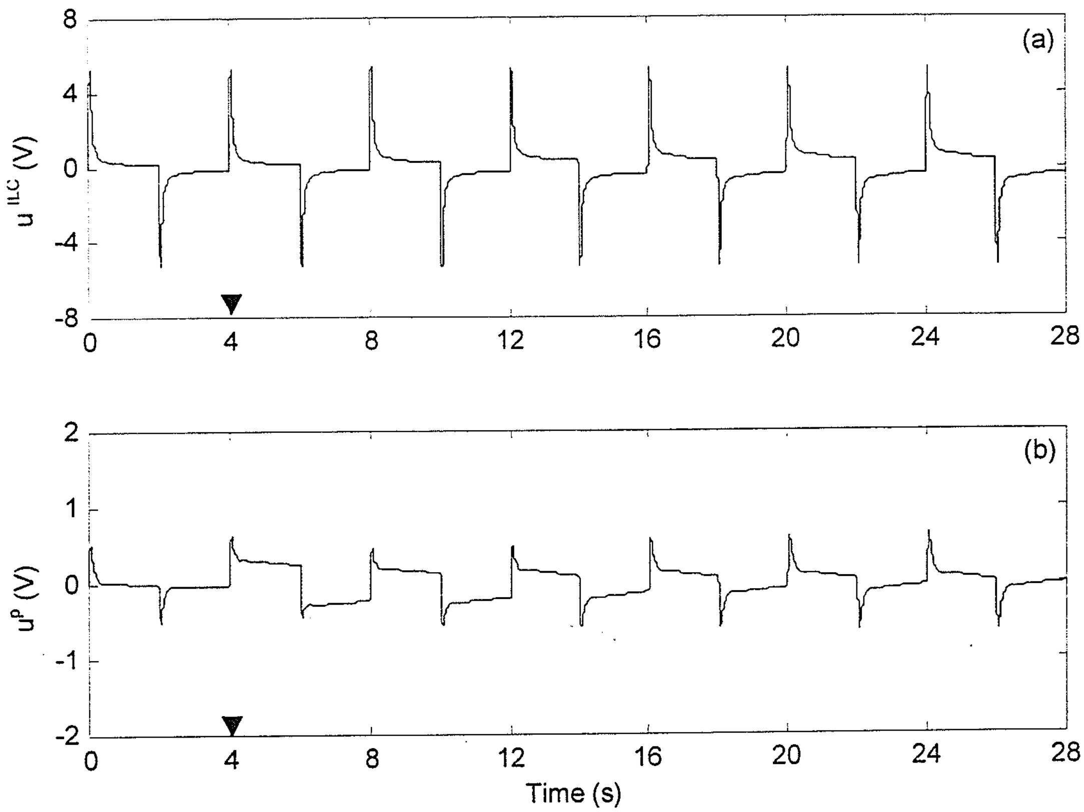

Figure 5.16: Control signal contribution of the ILC with proportional error feedback under faulty operation: (a) feedforward term; (b) feedback term (simulations).

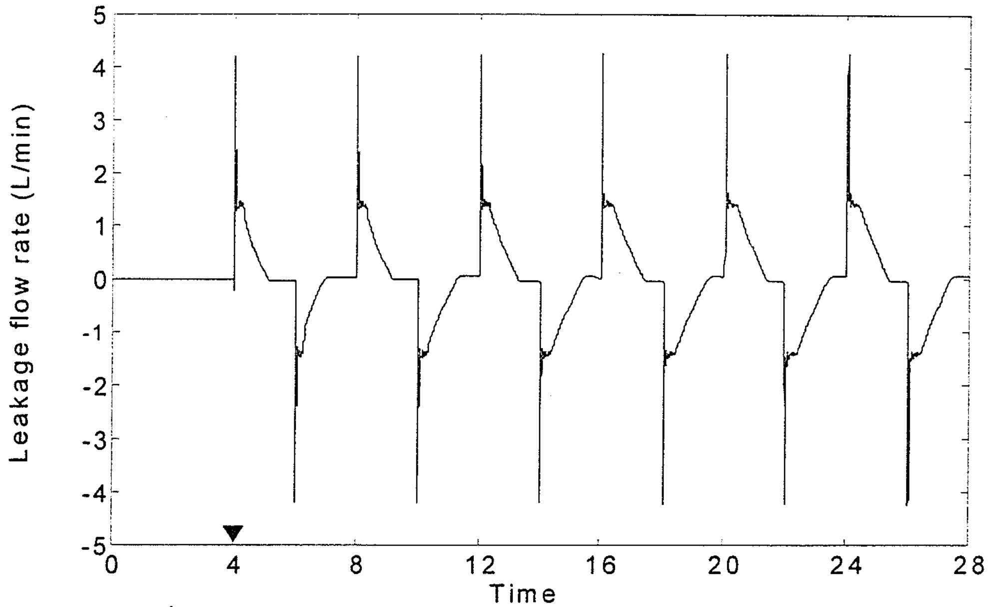

Figure 5.17: Internal Leakage flow rate (simulations).

5.3 ILC with Current Cycle Feedback

Case study 1 (normal operation): In the first set of simulations, a step signal was repeatedly performed and the initial conditions of the system were reset to the same values at the beginning of each trial. The results are shown in Figures 5.18 through 5.20. Figures 5.18a, b, c, and d show the system responses at the 1^{st}, 10^{th}, 20^{th}, and 40^{th} trials, respectively. The position response for the first trial is the same as the response using an ordinary proportional (P) controller. This is because there is no prior information available and the signal from the feedforward part is zero. The only input the system can respond to is the P feedback control. In each of the trials after that, there is a feedforward signal, which increases the tracking ability of the controller. Figures 5.19a, b, c, and d show the controller response at the 1^{st}, 10^{th}, 20^{th}, and 40^{th} trials, respectively. It is seen that by the 40^{th} trial, the controller was able to derive the correct input signal needed to force the system to follow the desired trajectory.

Figures 5.20a1, a2, and a3 show the feedforward term, feedback term, and the total control signal of the ILC with current cycle feedback all at the 1^{st} trial. At this trial there is no prior information available and the feedforward signal is zero. The only input to which the system can respond is the P feedback control. Figures 5.20d1, d2, and d3 show the feedforward term, the feedback term and the total control signal of the ILC with current cycle feedback at the 40^{th} trial. It is seen from this figure that the effect of the feedforward term is increasing as the number of trials increase, while the effect of the feedback is nearly zero.

In the second set of simulations, a step signal was repeatedly performed without resetting the initial conditions of the system to the same values at the beginning of each trial, The results are shown in Figures 5.21 through 5.23. Figure 5.21 shows that the ILC with current cycle feedback can track the desired trajectory without the need of resetting the initial conditions to the same values at the beginning of each trial. Figure 5.22 shows the total control signal of ILC with current cycle feedback and Figures 5.23a and 5.23b show the feedforward term and the feedback term of the control signal, respectively. It is seen that the effect of the feedforward term on the total control signal is bigger than the feedback term under the normal operation.

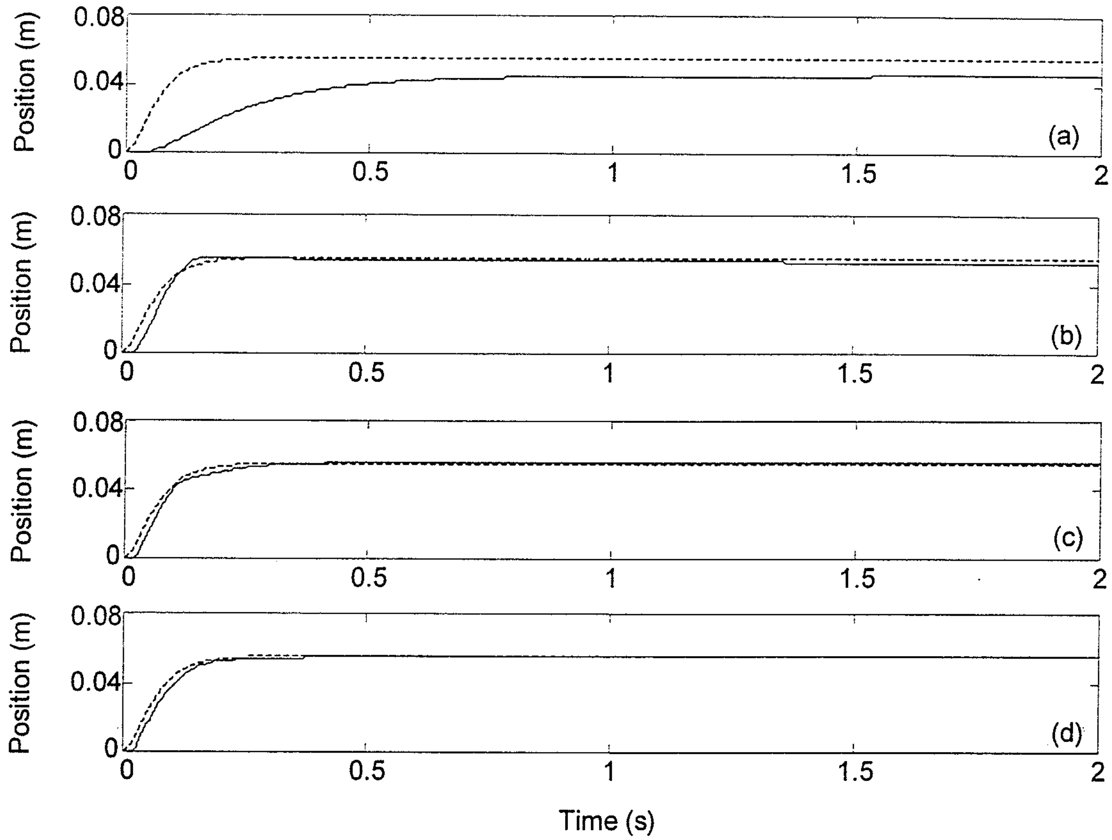

Figure 5.18: System responses using ILC with current cycle feedback: (----- desired, —— actual) (a) at 1st trial; (b) 10th trial; (c) 20th trial; (d) 40th trial (simulations).

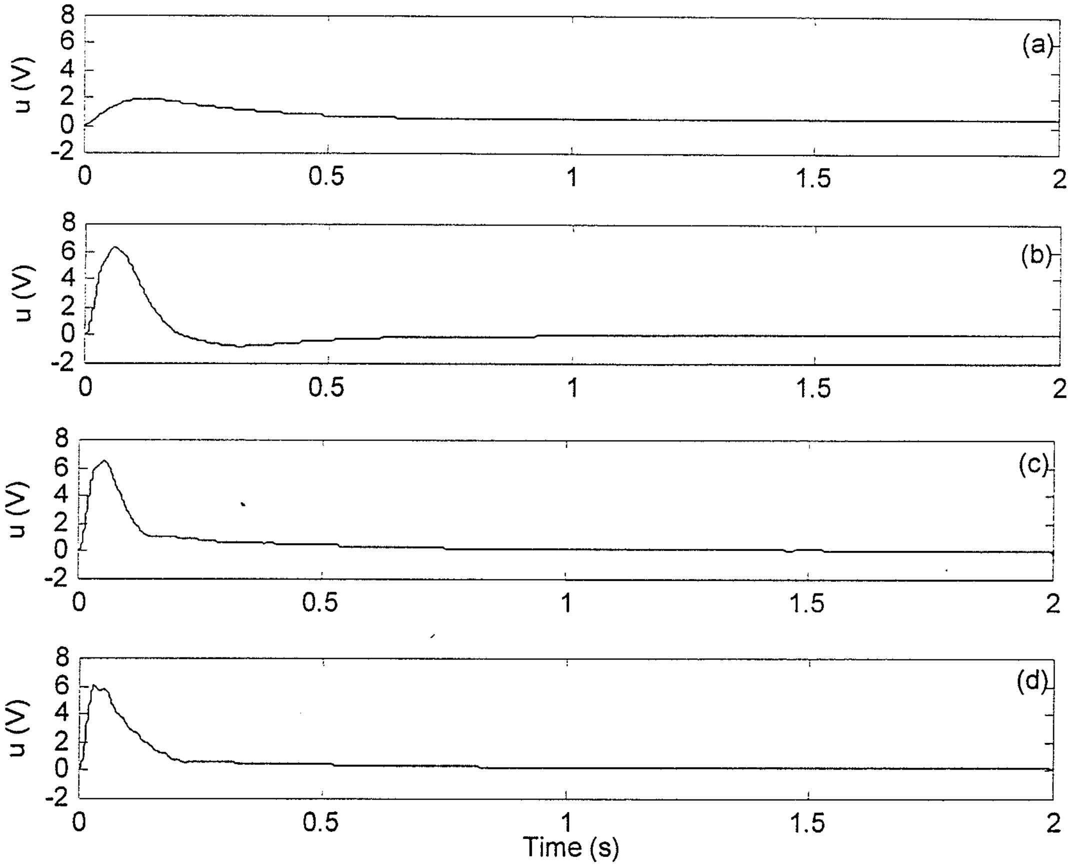

Figure 5.19: Control signals of ILC with current cycle feedback: (a) at 1^{st} trial; (b) 10^{th} trial; (c) 20^{th} trial; (d) 40^{th} trial (simulations).

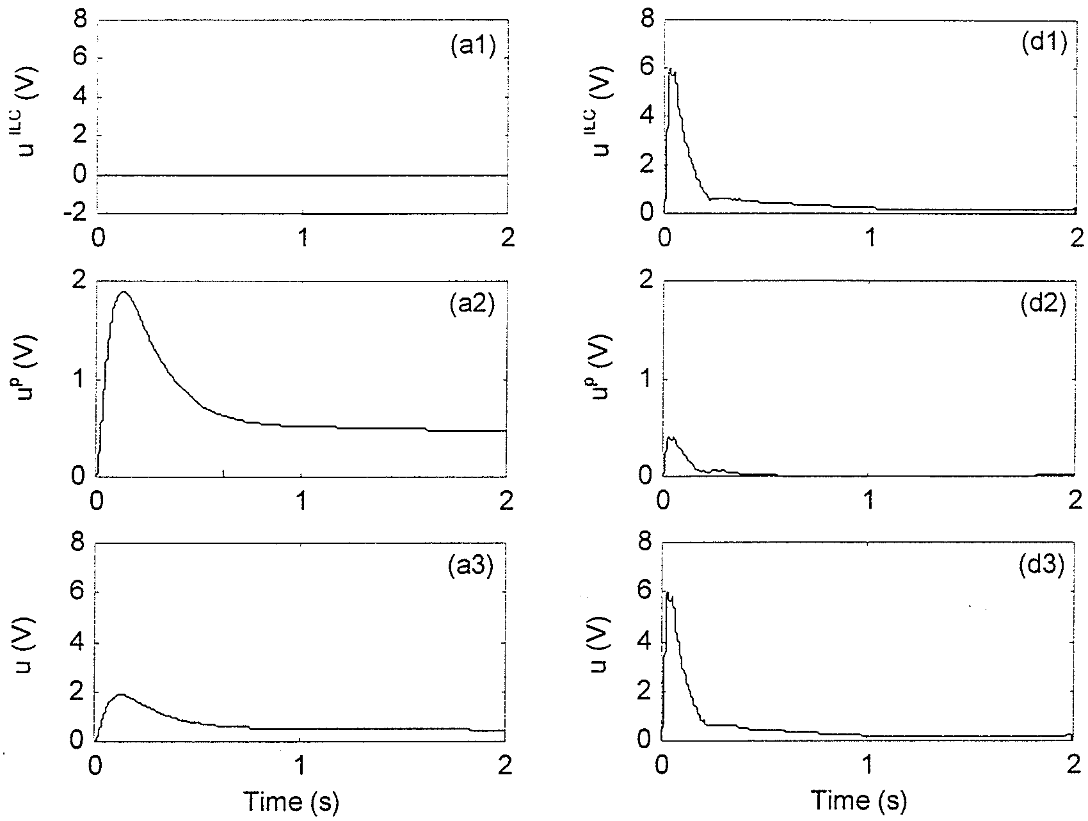

Figure 5.20: Control signal contributions of the ILC with current cycle feedback: (a1), (a2), (a3) at the 1st trial; (d1), (d2), (d3) at the 40th trial (simulations).

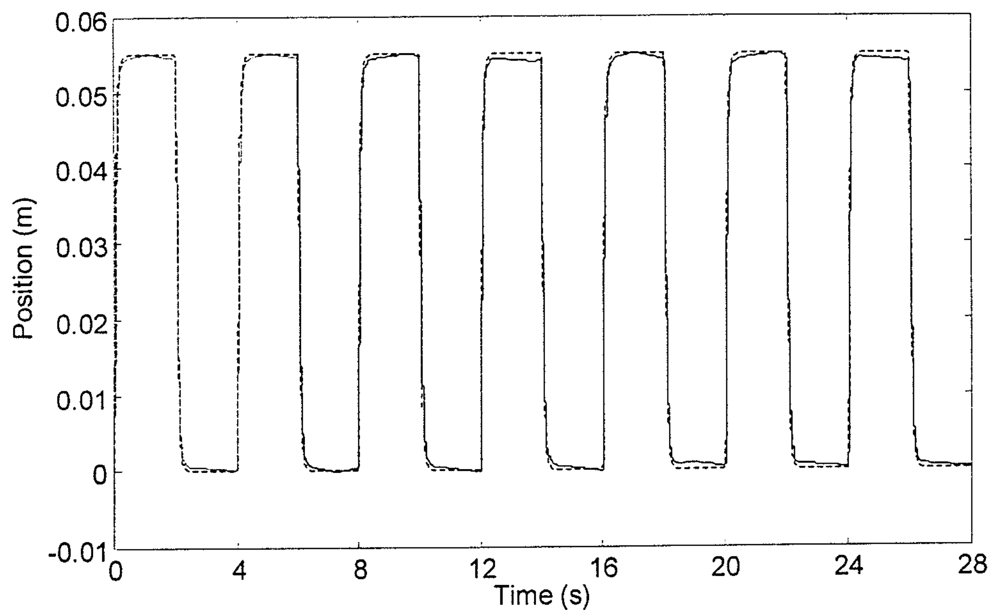

Figure 5.21: System response using ILC with current cycle feedback (----- desired, —— actual) under normal operation (simulations).

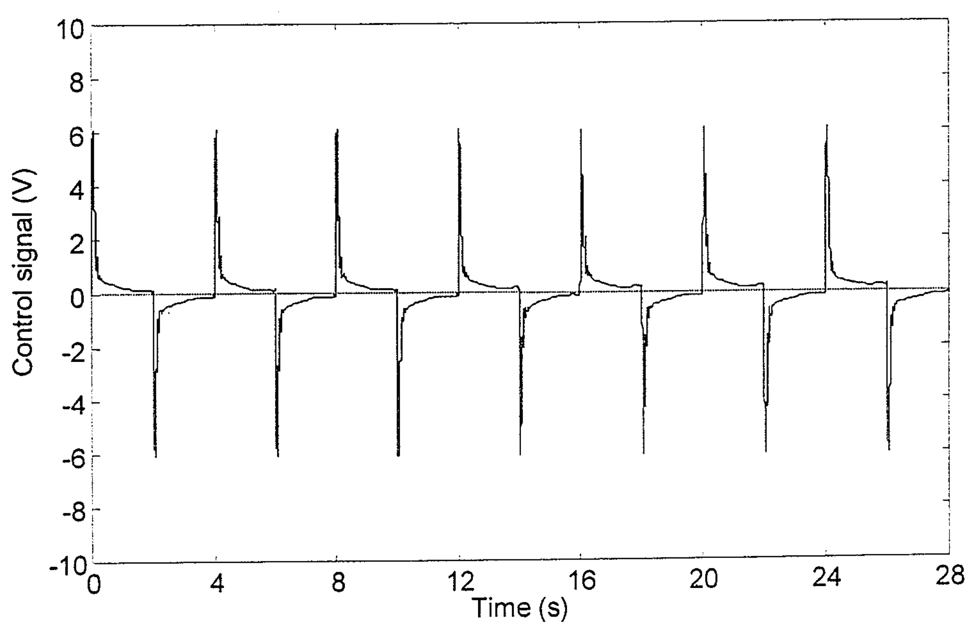

Figure 5.22: Control signal of the ILC with current cycle feedback under normal operation (simulations).

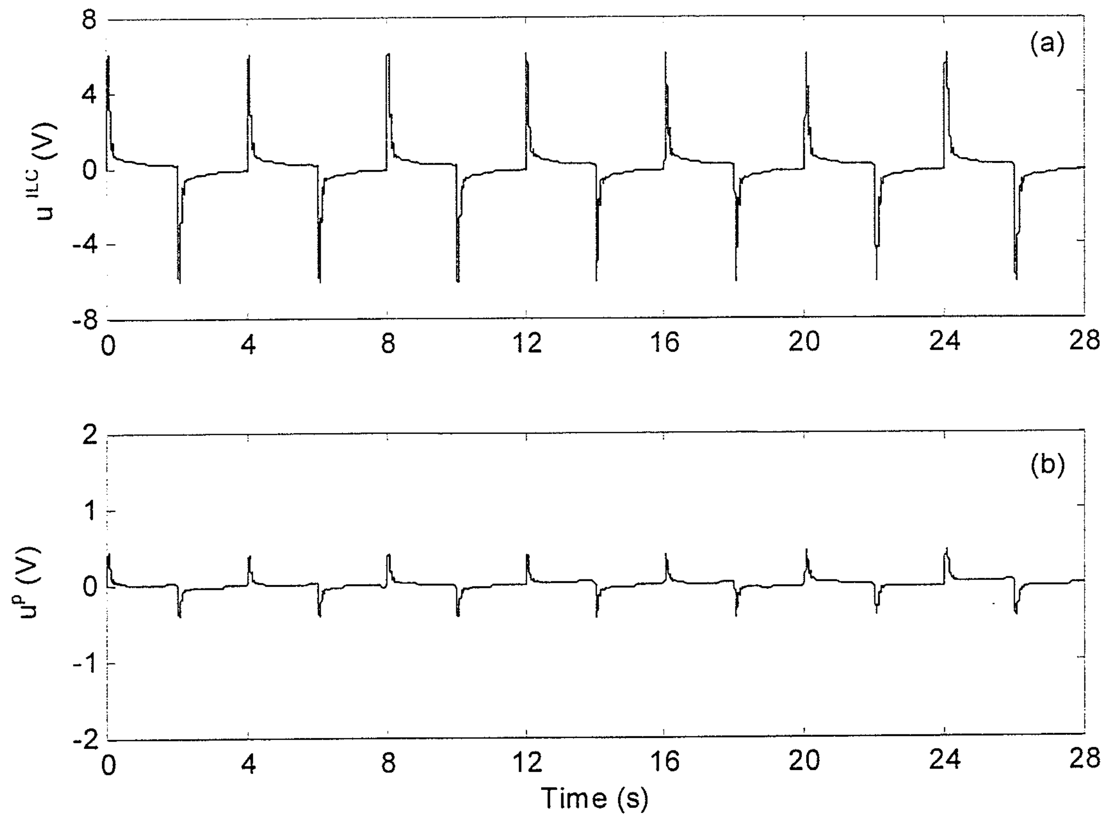

Figure 5.23: Control signal contribution of the ILC with current cycle feedback under normal condition: (a) feedforward term; (b) feedback term (simulations).

Case study 2 (faulty operation): In this set of simulations, the initial conditions of the system were reset to the same values at the beginning of each trial and an internal leakage was introduced to the system after the 40th trial. The results are shown in Figures 5.24 through 5.27. Figure 5.24a shows the system response of the ILC with current cycle feedback when the internal leakage fault occurred. Figures 5.24b, c, and d show the system responses after the 43rd, 45th, and 47th trials, respectively. It is seen that the within only 6 trials the system was able to overcome the leakage fault and to track the desired trajectory. Figures 5.25a, b, c and d show the controller responses at the 41^{st}, 43^{rd}, 45^{th}, and 47^{th} trials, respectively. It is clear that within only 6 trials, the controller was able to derive the correct input signal needed to force the system to follow the desired trajectory and to overcome the internal leakage fault.

Figures 5.26a1, a2 and a3 show the controller responses when an internal leakage occurs in the system. Figures 5.26d1, d2, and d3 show the control signals after the 6^{th} trial from applying the leakage. When these results are compared, it is clear that the feedforward signal is close to the total control signal and the value of the feedback term is nearly zero. Figures 5.27a, b, c and d show the internal leakage flow rates at the 41^{st}, 43^{rd}, 45^{th}, and the 47^{th} trials, respectively.

In this set of simulations, a step signal was repeatedly performed without resetting the initial conditions of the system to the same values at the beginning of each trial. An internal leakage was introduced to the system after 4 seconds. The results are shown in Figures 5.28 through 5.31. Figure 5.28 shows the system response of the ILC with current cycle feedback when the internal leakage fault occurred. It is shown that the controller is able to reduce the position error due to the leakage and tracks the desired trajectory.

Figure 5.29 shows the total control signal of the ILC with current cycle feedback; Figures 5.30a and 5.30b show the feedforward term and the feedback term of the control signal respectively. When these results are compared, it is clear that within 3 trials from applying the leakage, the feedforward signal is close to the total control signal and the feedback term is nearly zero. Figure 5.31 shows the internal leakage flow rate.

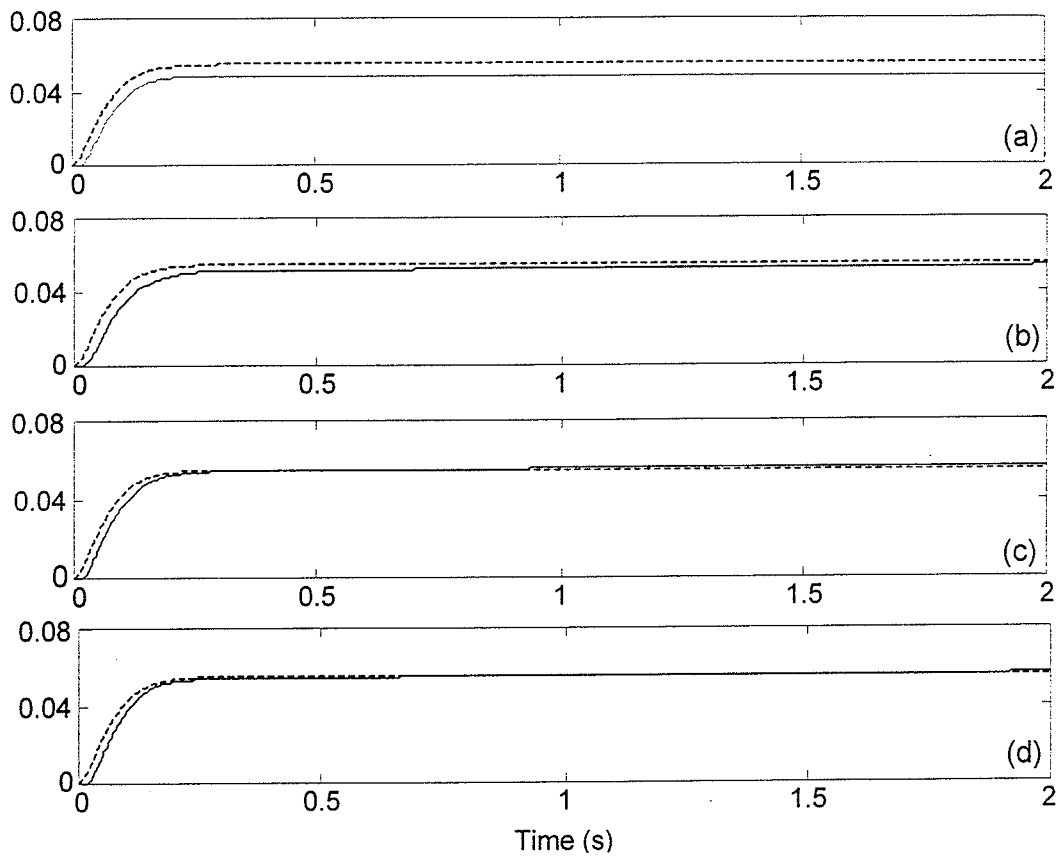

Figure 5.24: System responses of the ILC with current cycle feedback (----- desired, — actual): (a) at 41st trial; (b) 43rd trial; (c) 45th trial; (d) 47th trial (simulations)

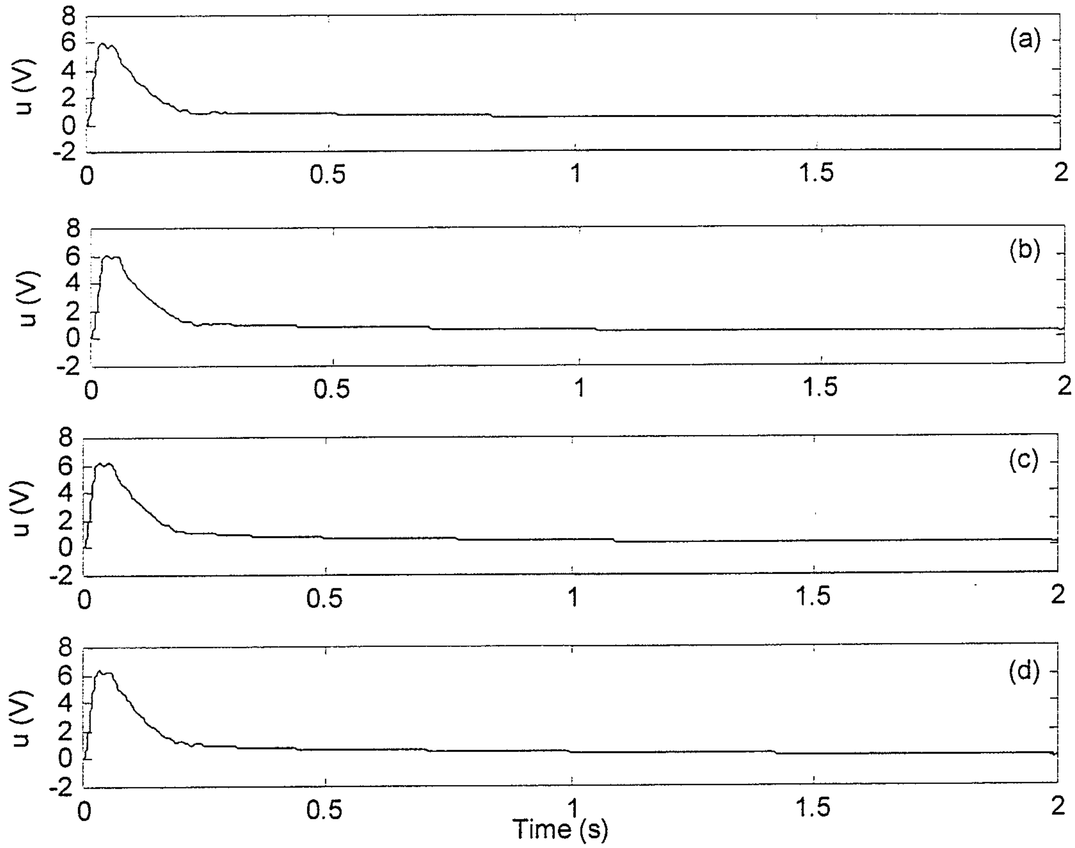

Figure 5.25: Control signals of the ILC with current cycle feedback: (a) at 41st trial; (b) 43rd trial; (c) 45th trial; (d) 47th trial (simulations).

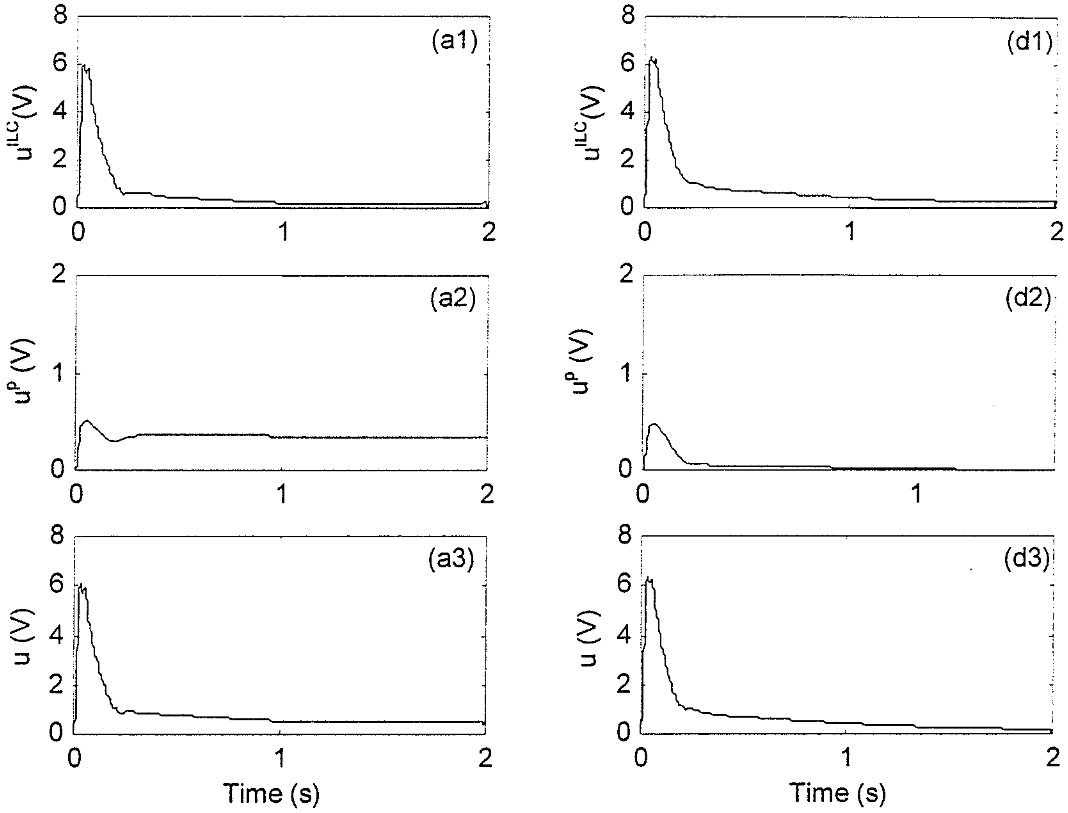

Figure 5.26: Control signal contributions of the ILC with current cycle feedback: (a1), (a2), (a3) at the 41st trial; (d1), (d2), (d3) at the 47th trial (simulations).

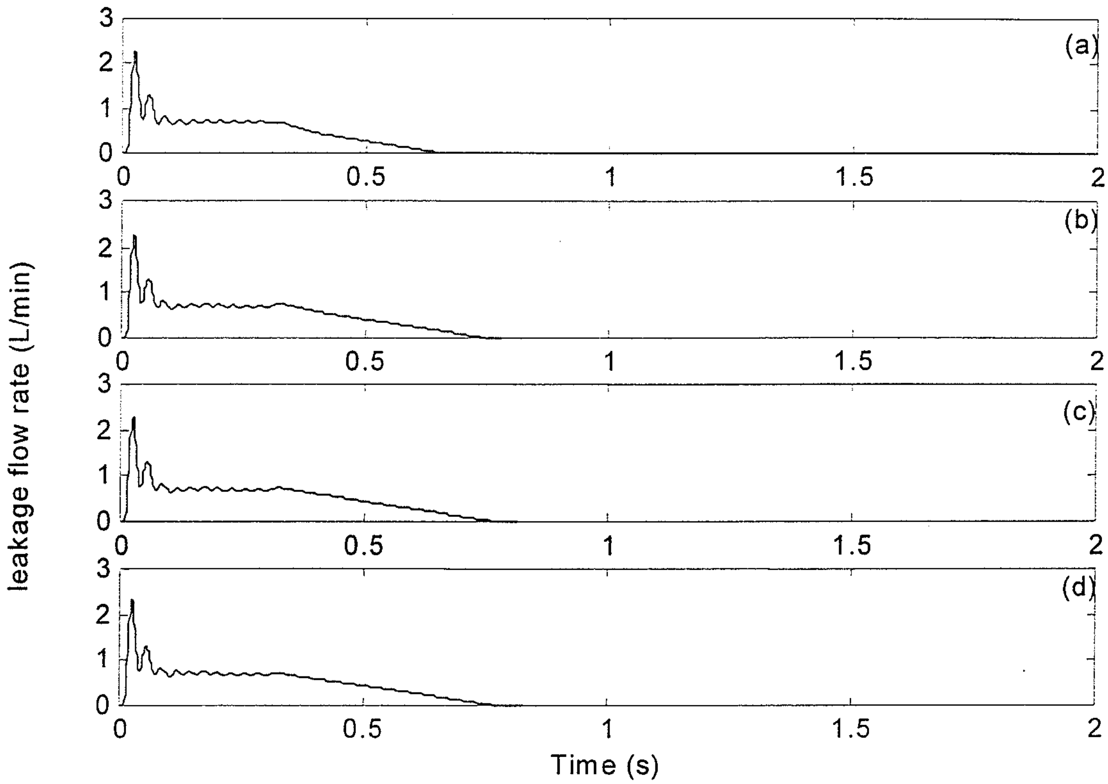

Figure 5.27: Internal leakage flow rates (a) at 41st trial; (b) 43rd trial; (c) 45th trial; (d) 47th trial (simulations).

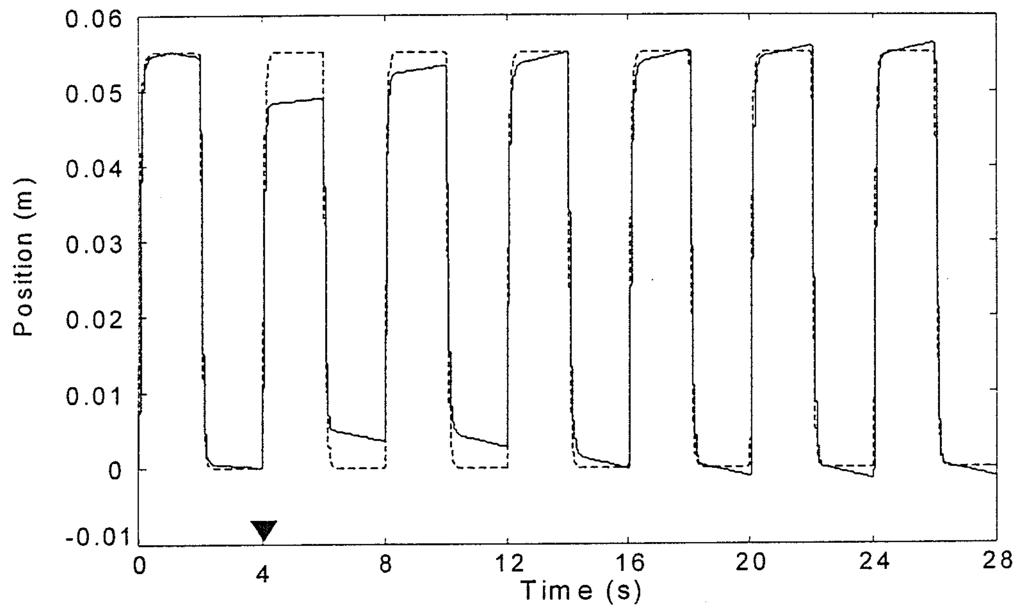

Figure 5.28: System response of the ILC with current cycle feedback: (----- desired, —— actual) under faulty operation (simulations).

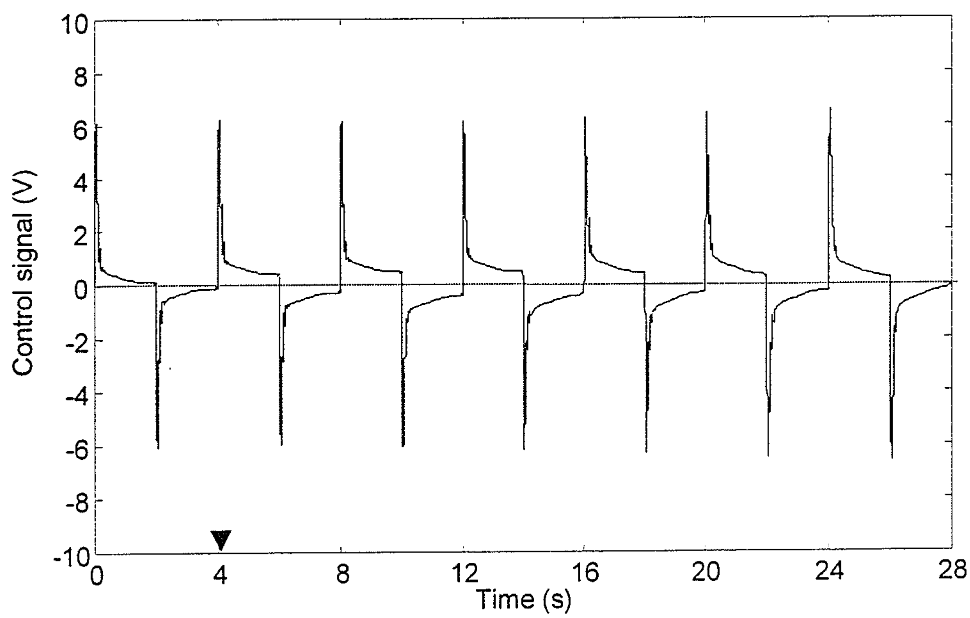

Figure 5.29: Control signal of the ILC with current cycle feedback under faulty operation (simulations).

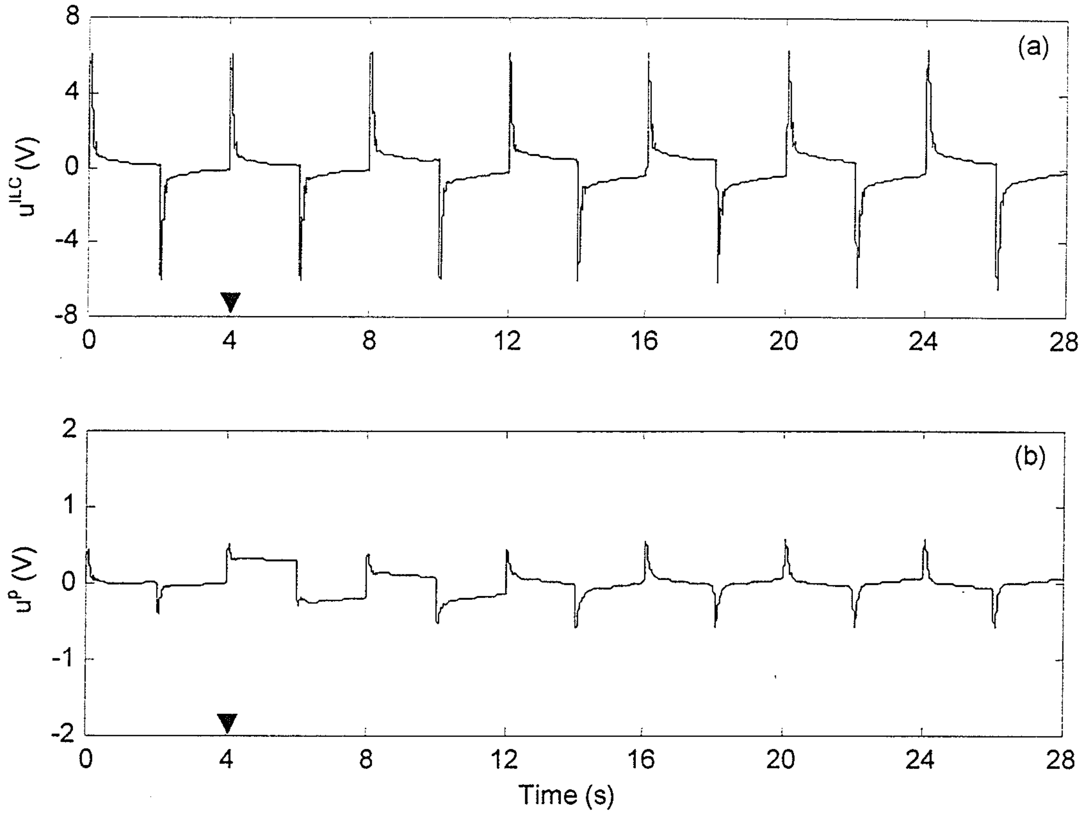

Figure 5.30: Control signal contribution of the ILC with current cycle feedback under faulty operation: (a) feedforward term; (b) feedback term (simulations).

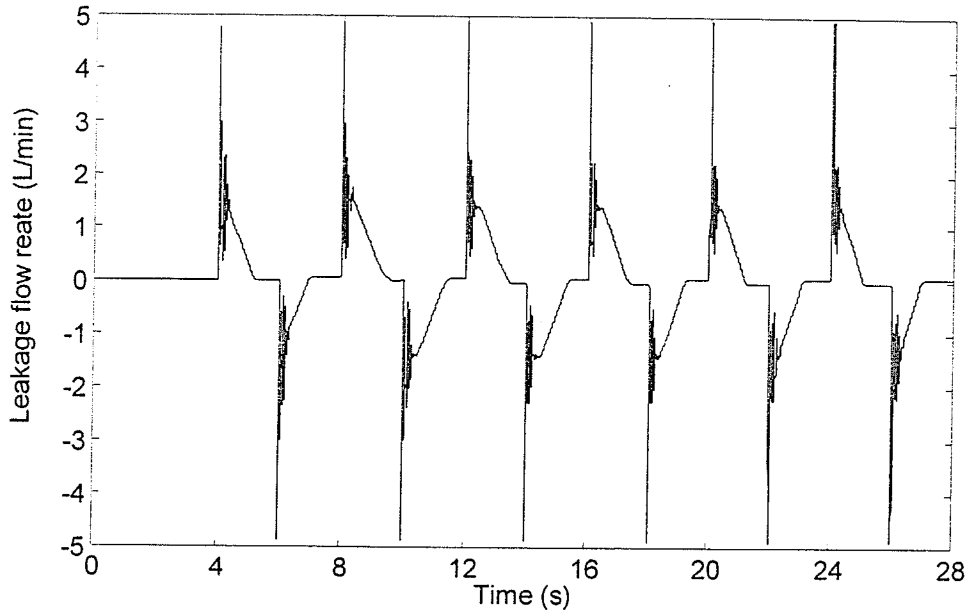

Figure 5.31: Internal leakage flow rate (simulations).

5.4 Summary and Discussions

In the simulations the friction was considered as well as a 5% dead-band in the servovalve. The values for the controller gains (T_u, T_e, λ and k_p) were chosen by trial and error in order to provide an acceptable rise time, no overshoot and zero steady-state error for the responses under normal operation. Comparing the values of the controller gains as shown in Table 5.1, it is seen that T_u and T_e have the same values in both the 'basic ILC' and the 'ILC with proportional error feedback'. The value of k_p is the same in both the 'ILC with proportional error feedback' and 'ILC with current cycle feedback'. The only difference is in the value of λ. λ=1.0 in 'ILC with proportional error feedback' and λ=0.93 in 'ILC with current cycle feedback'.

Extensive simulations were also done to study the sensitivity of each controller to the change in the corresponding gains. The results show that for the basic ILC an increase of 30% on the value of T_e caused a slight increase in the rise time; while a 30% decrease in its value caused a slower response. On the other hand, an increase of 3% in the value of T_u resulted in a faster response with a noticeable overshoot. However, this overshoot was reduced as the number of trials increased.

The ILC with proportional error feedback scheme has the same sensitivity toward T_u and T_e as the basic ILC. An increase by 10% in the value of λ was needed to produce a noticeable faster response than the original one. With respect to k_p, a ±50% change in its value produced proportionally a very small change in the system's response rise-time.

The ILC with current cycle feedback scheme has the same sensitivity toward k_p as the ILC with proportional error feedback scheme. However, a change of ±5% in the value of λ changed the system response in the same manner that ±10% change in its value did in the ILC with proportional error feedback scheme.

In the simulations a similar leakage fault was used in order to compare the speed of convergence rates between the three controllers. Some additional simulations were done on the basic ILC to study the limitation of the ILC in the recovery from increased leakage faults. The results obtained show that the basic ILC was able to overcome an internal leakage of 2.25 L/min within 12 trials. By doubling the leakage amount to 5 L/min the basic ILC was still able to reach a 100% convergence (i.e., zero steady-state error) within

20 trials. When the leakage fault was increased to 10 L/min, the system was not able to reduce the error caused by the leakage, completely. There was a 4% steady-state error after 40 trials. This error did not diminish as the number of trials increased because the control signal reached the saturation level. As was discussed earlier in Section 5.1, the internal leakage fault caused an error on the position. Due to this error, the control signal changed its value to eliminate this error. Although the control signal of the basic ILC was increasing because of the error, reaching to the saturation level limited the ability of the system to overcome the high amount of leakage.

Under the condition of resetting the initial conditions of the system to the same values at the beginning of each trial, all three control algorithms had good responses under normal operation, but with different speed of convergence. Both the ILC with proportional error feedback and the ILC with current cycle feedback were two times faster than the basic ILC to track the desired trajectory. For the faulty operation, the ILC with current cycle feedback was the fastest controller to overcome the leakage fault. It was 2 times and 1.33 times faster than the basic ILC and the ILC with proportional error feedback, respectively. When a step signal was repetitively performed without resetting the initial conditions of the system to the same values at the beginning of each trial, the results showed that both the ILC with proportional error feedback and the ILC with current cycle feedback gave similar results under normal and faulty operations. Therefore, these two controllers were chosen to be applied on the experimental test rig.

Chapter 6

Experimental Results

This chapter presents the experiments that have been done on the test rig with different ILC configurations. Section 6.1 gives a brief introduction of the experimental setup. The second section presents the experimental results for the ILC with proportional error feedback. In Section 6.3 the experimental results for the ILC with current cycle feedback is discussed.

6.1 Experimental Setup

The experiments were carried out using the experimental test rig described in Chapter 3. The two learning controllers were first implemented by writing them in their equivalent state space presentations. The internal leakage fault was experimentally created by adjusting the needle valve that controls the flow rate through the fluid line that connects the actuator chambers (see Figure 6.1). Table 6.1 gives the controller's gains used in the experiments.

Table 6.1: Controller gains used in the experiments

Controllers	T_u	T_e **(V/m)**	λ	k_p **(V/m)**
ILC with proportional error feedback	0.9	25	1.0	50
ILC with current cycle feedback	-	-	0.85	50

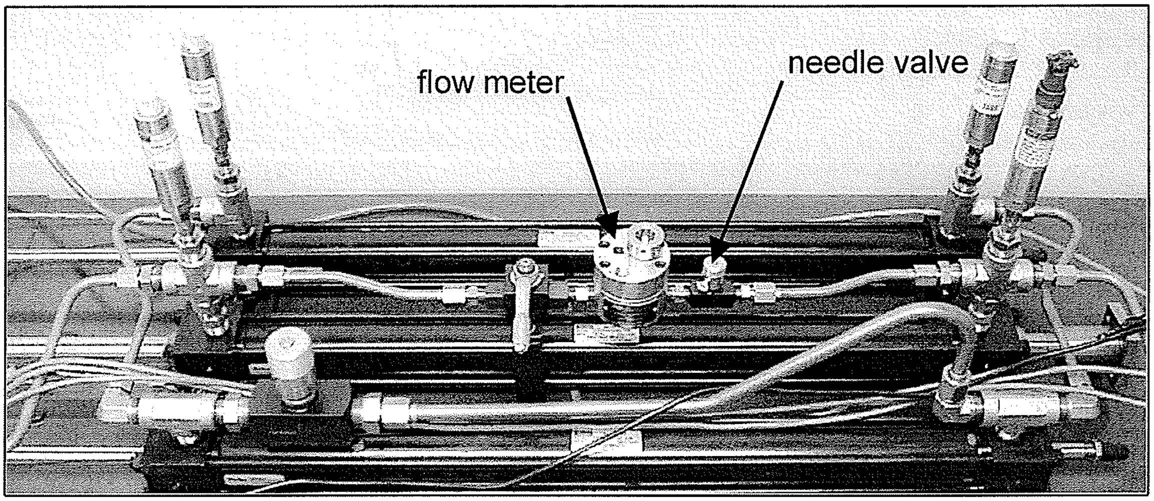

Figure 6.1: Photograph of the needle valve and flow meter used to set and measure the piston seal leakages in the experiments.

6.2 ILC with Proportional Error Feedback.

Case study 1 (normal operation): In this experiment, a step signal was repeatedly performed and the initial conditions of the system were reset to the same values at the beginning of each trial. Figures 6.2a, b, c, and d show the responses at the 1^{st}, 10^{th}, 20^{th}, and 40^{th} trials, respectively. The position for the first trial is the same as the response using a Proportional (P) controller. This is because there is no prior information available and the signal from the feedforward part is zero. The only input the system can respond to, is the P feedback control. In each of the trials after that, there is a feedforward signal which increases the tracking ability of the controller. These results are similar to the results obtained from the simulations

Figures 6.3a, b, c, and d show the controller responses at the 1^{st}, 10^{th}, 20^{th}, and 40^{th} trials, respectively. It is seen that by the 40^{th} trial, the controller was able to derive the correct input signal needed to force the system to follow the desired trajectory. Figures 6.4a1, a2, and a3 show the feedforward term, feedback term, and the total control signal of the ILC with proportional error feedback for the 1st trial. At this trial, there is no prior information available and the feedforward signal is zero. The only input the system can respond to is the P feedback control. Figures 6.34d1, d2, and d3 show feedforward term, the feedback term, and the total control signal of the ILC with proportional error feedback at the 40th trial. It is seen that the effect of the feedforward term is increasing as the number of trials increase while the effect of the feedback becomes relatively small.

In the next experiment, a step signal of a period of 4 seconds was performed without resetting the initial conditions of the system to the same values at the beginning of each trial, the actuator was monitored for 28 seconds which is equal to 7 trials. The results are shown in Figures 6.5 through 6.7. Figure 6.5 shows that by the 7th trial, the actual response has converged with very small error. There remains a small area around 25 milliseconds where the error is not zero. This does not seem to diminish much with additional trials and seems to be a product of the actual dead zone in the valve (see Appendix, Figures A1 and A2).

Figure 6.6 shows the total control signal of the ILC with proportional error feedback, and Figures 6.7a and 6.7b show the feedforward term and the feedback term of the control signal, respectively. It is seen that the effect of the feedforward term on the total control signal is bigger than the feedback term under the normal operation.

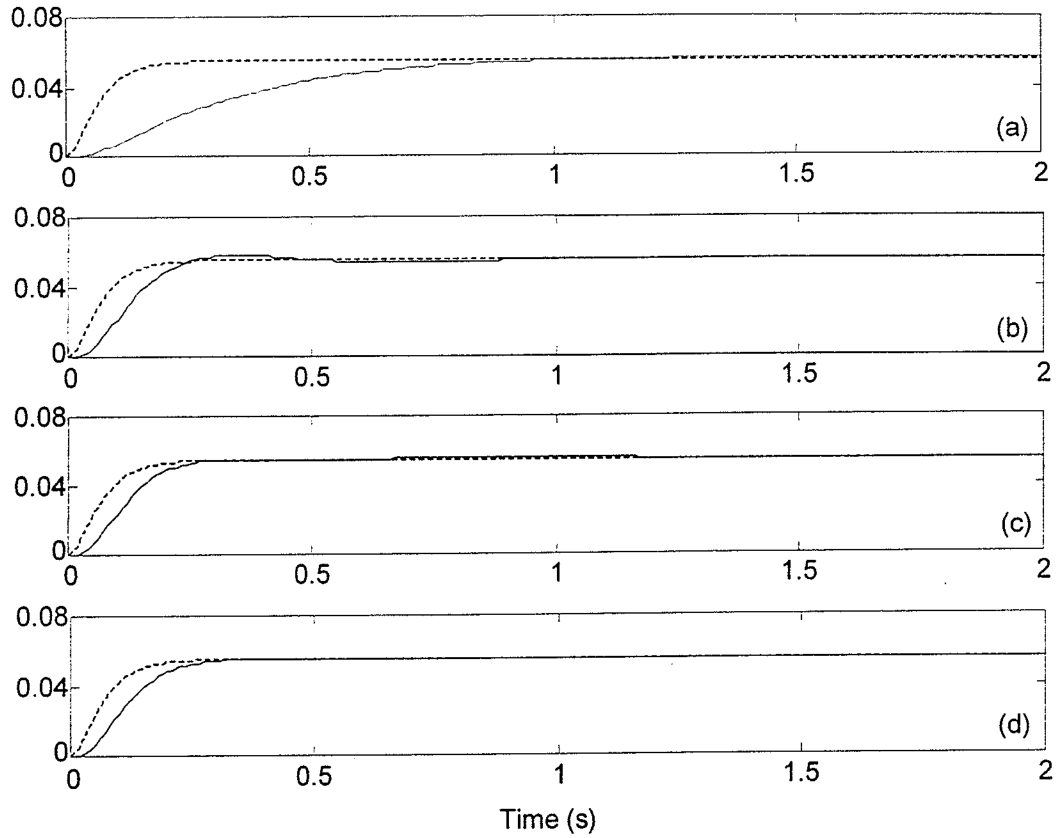

Figure 6.2: System responses of the ILC with proportional error feedback under normal operation (---- desired position, — actual position): (a) at 1st trial; (b) 10th trial; (c) 20th trial; (d) 40th trial (experiments).

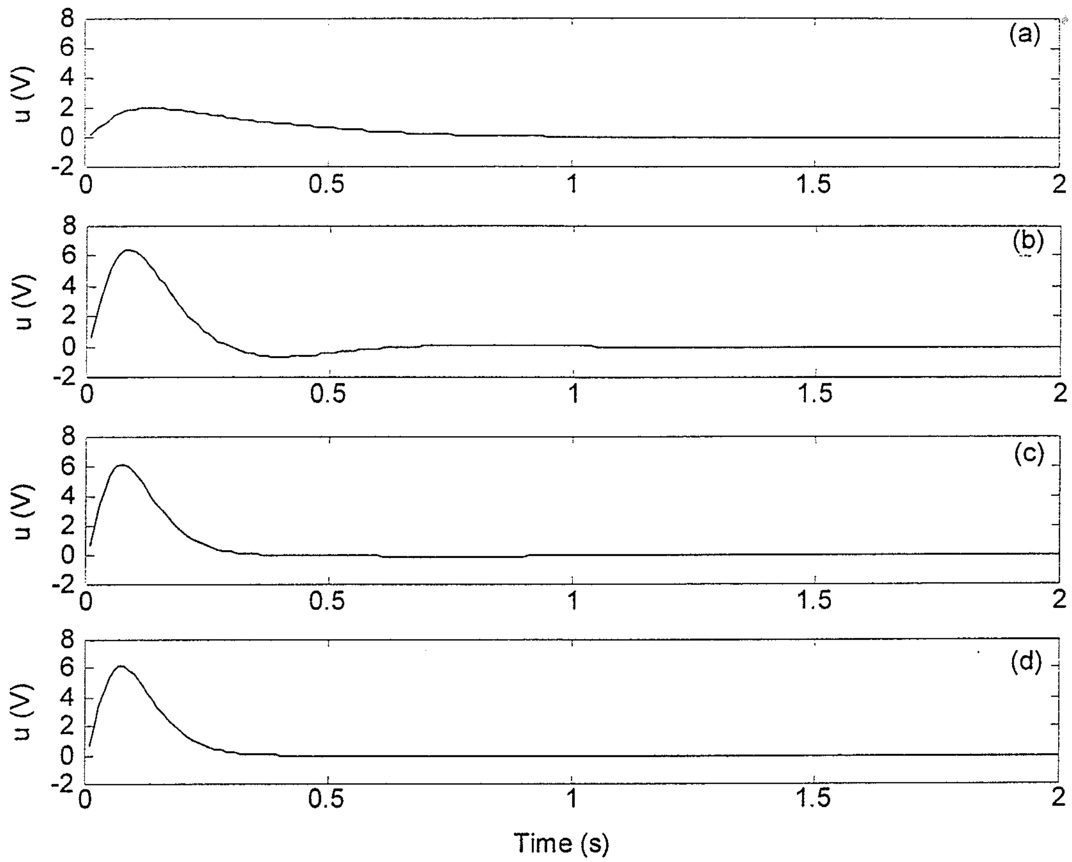

Figure 6.3: Control signals of the ILC with proportional error feedback (a) at 1st trial; (b) 10th trial; (c) 20th trial; (d) 40th trial (experiments).

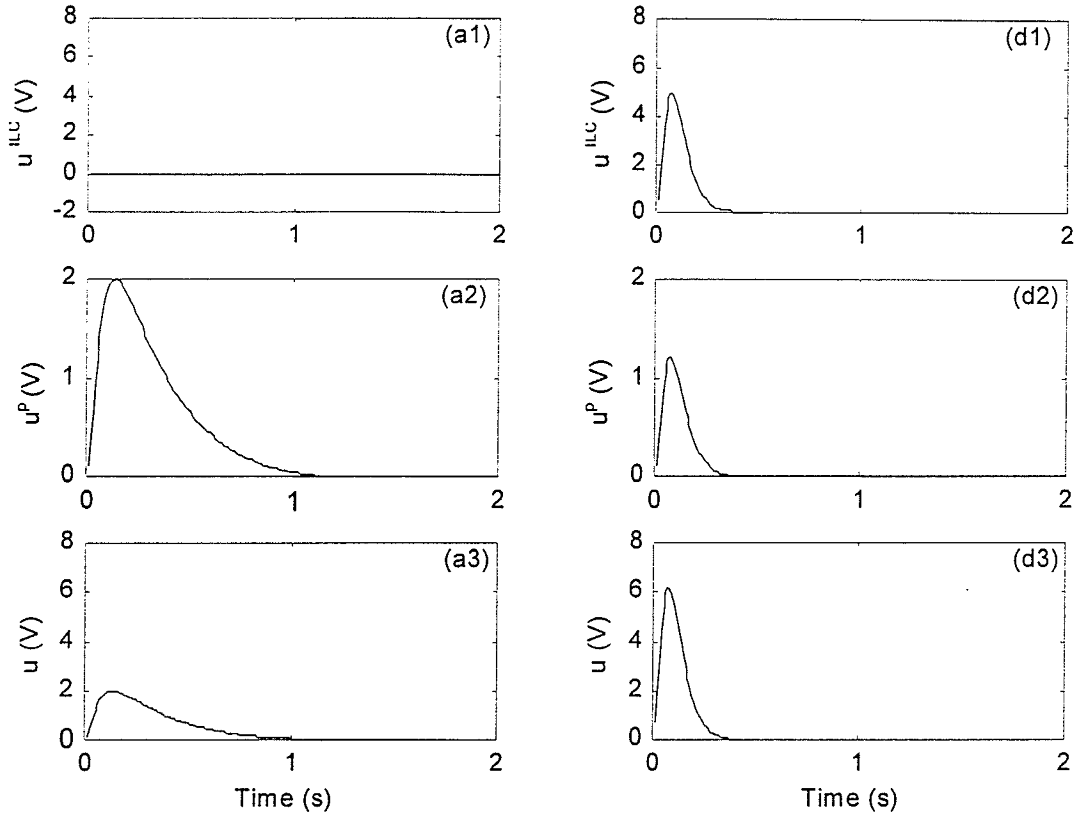

Figure 6.4: Control signal contributions of the ILC with proportional error feedback: (a1), (a2) and (a3) at the 1st trial; (d1), (d2) and (d3) at the 40th trial (experiments).

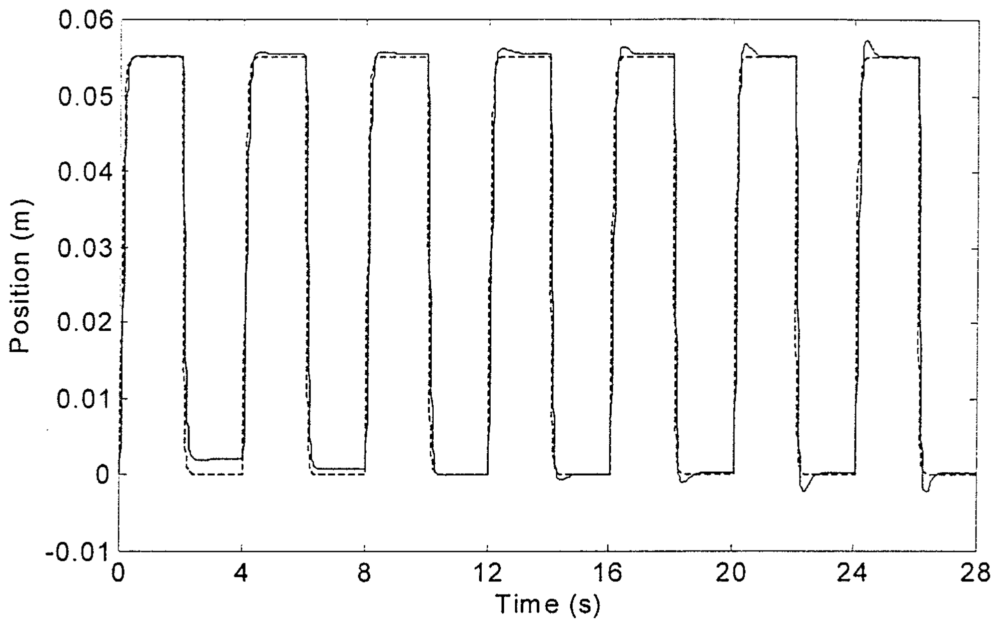

Figure 6.5: System response of the ILC with proportional error feedback (----- desired, —— actual) under normal operation (experiments).

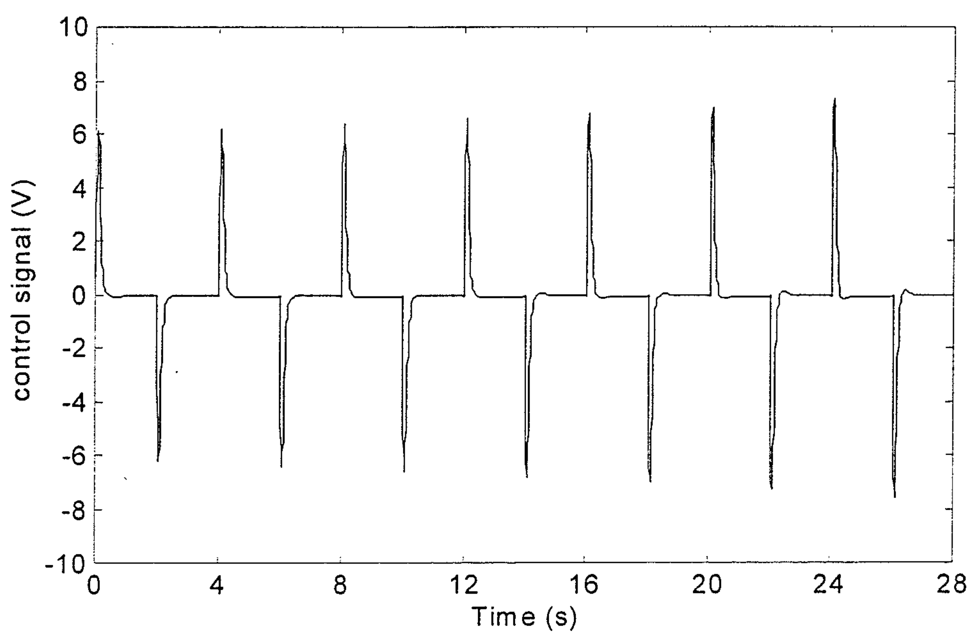

Figure 6.6: Control signal of the ILC with proportional error feedback under normal operation (experiments).

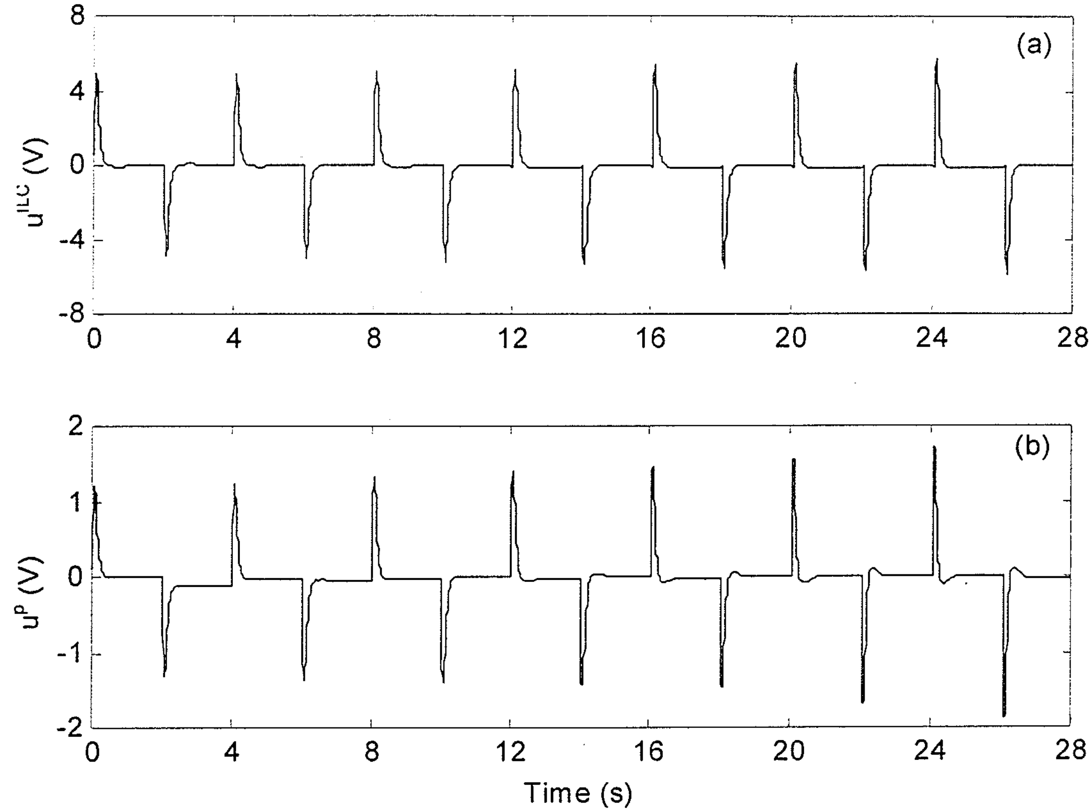

Figure 6.7: Control signal contribution of the ILC with proportional error feedback under normal operation: (a) feedforward term; (b) feedback term (experiments).

Case study 2 (faulty operation): In this experiment, the initial conditions of the system were reset to the same values at the beginning of each trial and an internal leakage was introduced to the system after the 40th trial. The results are shown in Figures 6.8 through 6.10. Figure 6.8a shows the system response of the ILC with proportional error feedback when the internal leakage fault occurred. Figures 6.8b, c, and d show the system responses at the 43rd, 45th, and 49th trials, respectively. It is seen that the within only 8 trials the system was able to overcome the leakage fault and tracks the desired trajectory and this is similar to the simulation results.

Figures 6.9a1, a2, and a3 show the controller response when an internal leakage occurred in the system. Figures 6.9d1, d2, and d3 show the control signals after the 8^{th} trial from applying the leakage. When these results are compared, it is clear that the feedforward signal is very close to the total control signal and the feedback nearly to zero. Figures 6.10a, b, c, and d show the internal leakage flow rates at the 41^{st}, 43^{rd}, 45^{th}, and 49^{th} trials, respectively.

In the next experiment, a step signal was repetitively performed without resetting the initial conditions of the system to the same values at the beginning of each trial. An internal leakage was introduced to the system after 2 seconds. The results are shown in Figures 6.11 through 6.14. Figure 6.11 shows the system response of the ILC with proportional error feedback with the occurrence of the internal leakage. It is shown that the controller is able to reduce the position error due to the leakage.

Figure 6.12 shows the total control signal of the ILC with proportional error feedback and Figures 6.13a and 6.13b show the feedforward term and the feedback term of the control signal respectively. When these results are compared, it is clear that after about 4 trials from applying the leakage, the feedforward signal is very close to the total control signal that the feedback has gone nearly to zero. Figure 6.14 shows the internal leakage flow rate.

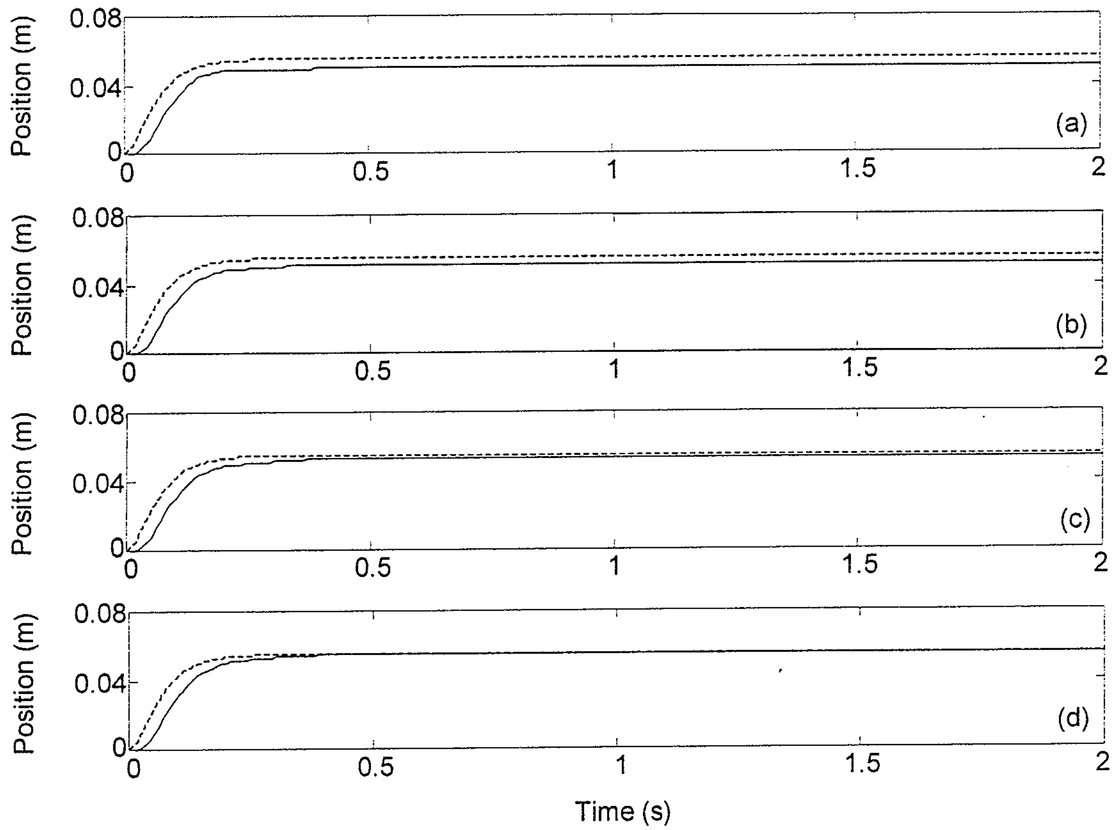

Figure 6.8: System responses of the ILC with proportional error feedback under faulty operation: (---- desired position, — actual position); (a) at 41^{st} trial; (b) 43^{rd} trial; (c) 45^{th} trial; (d) 49^{th} trial (experiments).

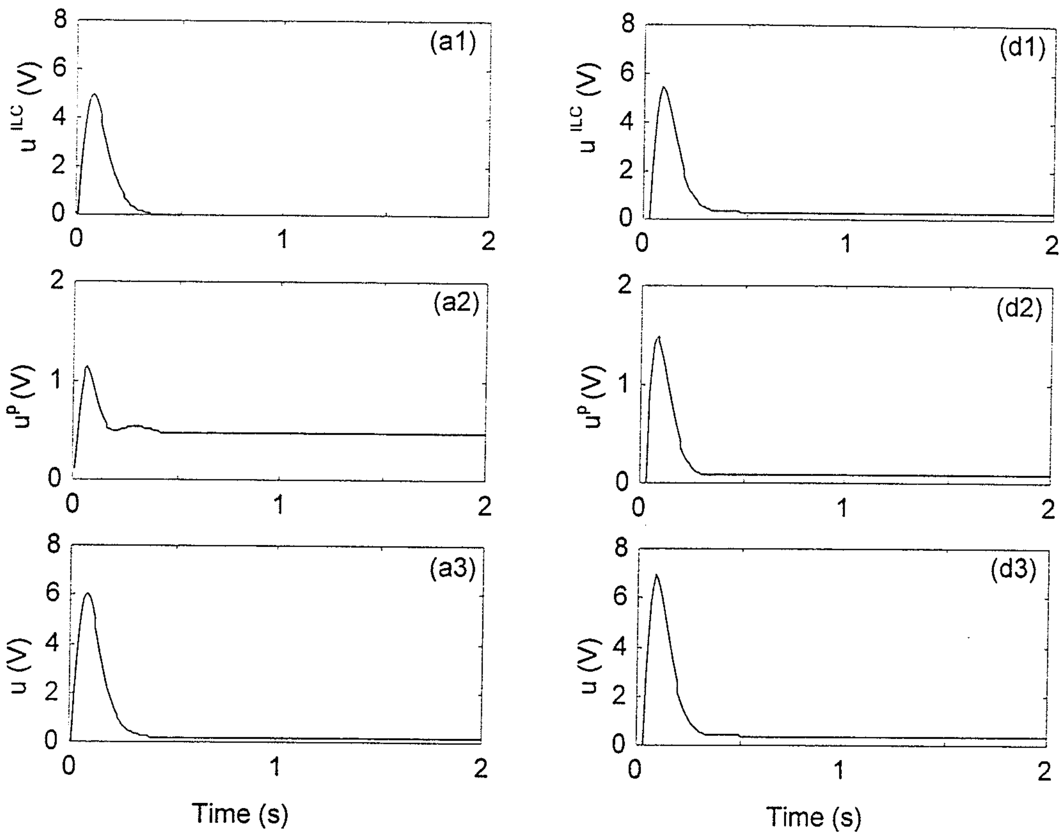

Figure 6.9: Control signal contributions of the ILC with proportional error feedback: (a1), (a2) and (a3) at the 41st trial; (d1), (d2) and (d3) at the 49th trial (experiments)

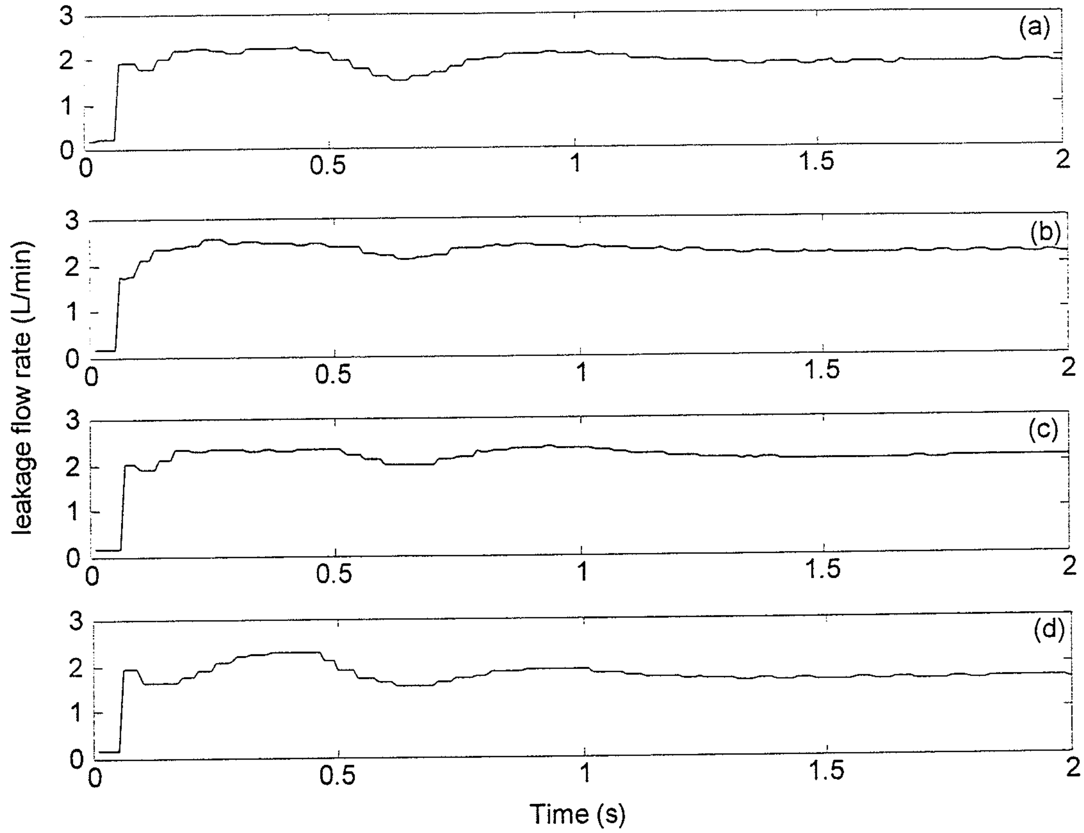

Figure 6.10: Internal leakage flow rates: (a) at 41st trial, (b) 43rd trial, (c) 45th trial, (d) 49th trial (experiments).

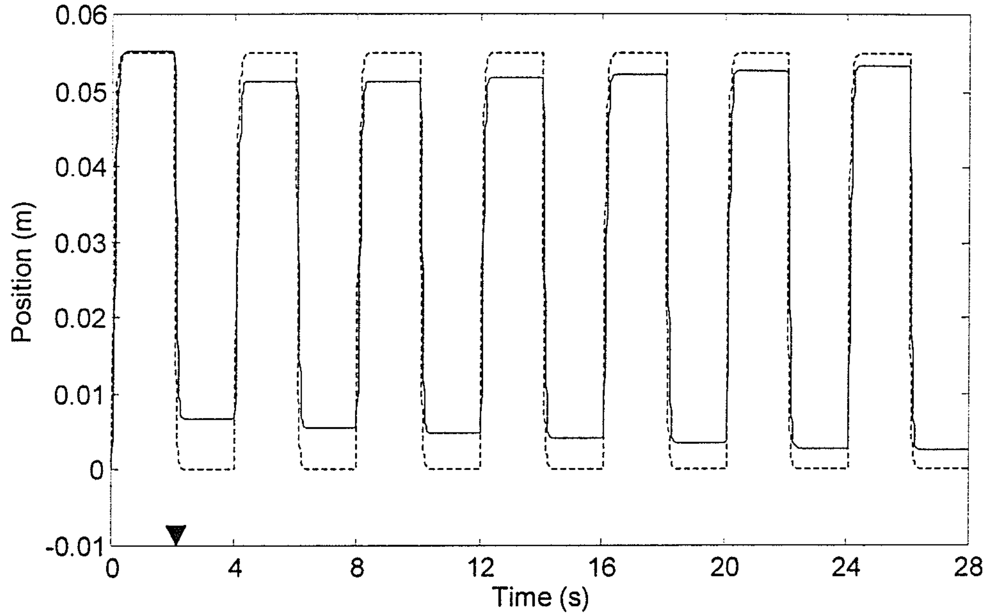

Figure 6.11: System response of the ILC with proportional error feedback: (-·-·- desired, —— actual) under faulty operation (experiments).

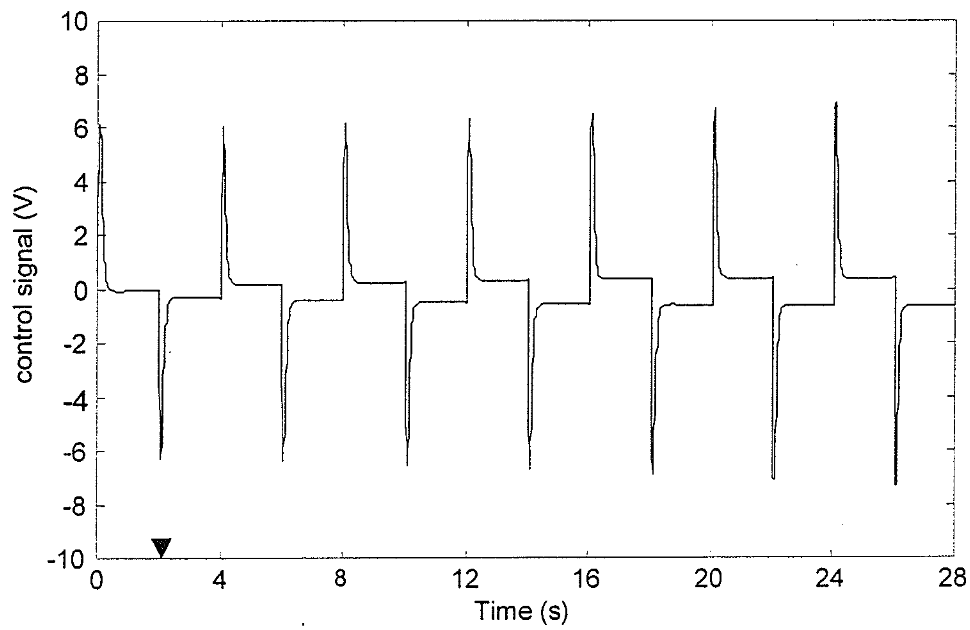

Figure 6.12: Control signal of the ILC with proportional error feedback under faulty operation (experiments).

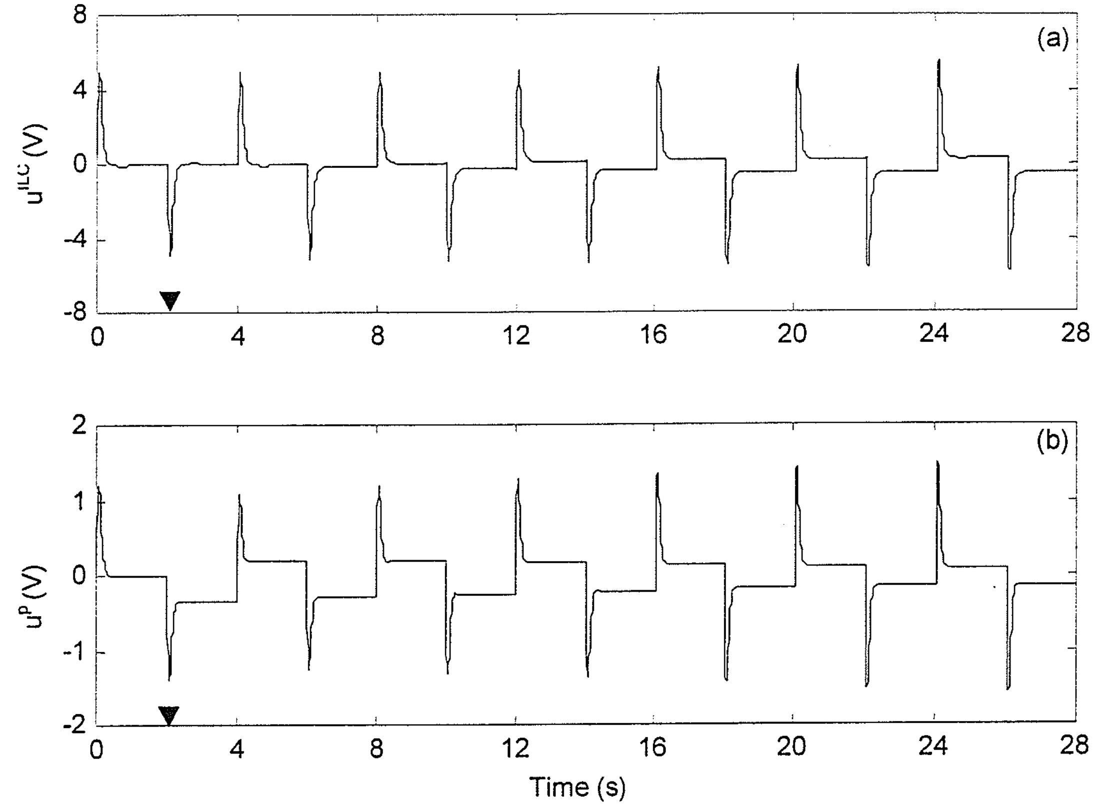

Figure 6.13: Control signal contribution of the ILC with proportional error feedback under faulty operation: (a) feedforward term; (b) feedback term (experiments).

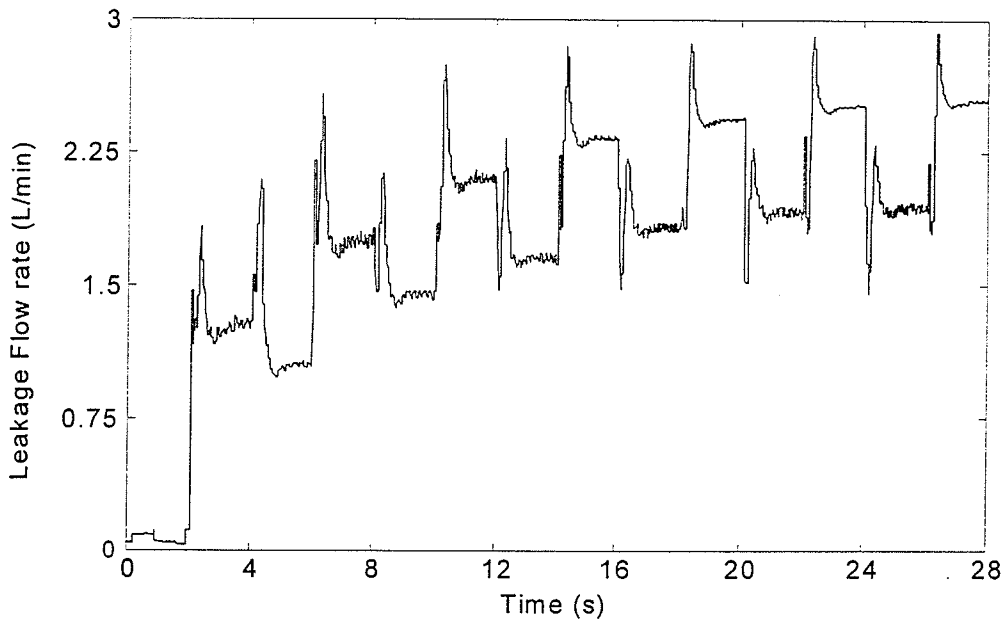

Figure 6.14: Internal leakage flow rate (experiments).

6.3 ILC with Current Cycle Feedback

Case study 1 (normal operation): In the first experiment, a step signal was repeatedly performed and the initial conditions of the system were reset to the same values at the beginning of each trial. The results are shown in Figures 6.15 through 6.17. Figures 6.15a, b, c, and d show the system responses at the 1^{st}, 10^{th}, 20^{th}, and 40^{th} trials, respectively. In the first trial, the system response was the same as the response using a proportional feedback controller. This is because there is no prior information available in the memory and the feedforward signal is zero. The only input the system can respond to is the P feedback control. In each of the trials after that, there is a feedforward signal, which increases the tracking ability of the controller. Figures 6.16a, b, c, and d show the controller responses at the 1st, 10th, 20th, and 40th trials, respectively. It is seen that by the 40th trial, the learning control was able to derive the correct input signal needed to force the system to follow the desired trajectory.

Figures 6.17a1, a2, and a3 show the feedforward term, feedback term, and the total control signal of the ILC with current cycle feedback at the 1st trial. At this trial, there is no prior information available in the memory, and the signal from the feedforward part is zero. The total control signal is equal to the control signal from the P feedback control. Figures 6.17d1, d2, and d3 show the feedforward term, the feedback term, and the total control signal of the ILC with current cycle feedback at the 40th trial. It is seen that the effect of the feedforward term is increasing, as the number of trials increase while the effect of the feedback is relatively small.

In the second experiment, a step signal was repeatedly performed without resetting the initial conditions of the system to the same values at the beginning of each trial, The results are shown in Figures 6.18 through 6.20. Figure 6.18 shows that the actual response was converged with very small error. This does not seem to diminish much with additional trials and seems to be a product of the actual dead zone in the valve (see Appendix, Figures A3 and A4).

Figure 6.19 shows the total control signal of ILC with current cycle feedback and Figures 6.20a and 6.20b show the feedforward term and the feedback term of the control signal, respectively. It is seen that the effect of the feedforward term on the total control signal is bigger than the feedback term under the normal operation.

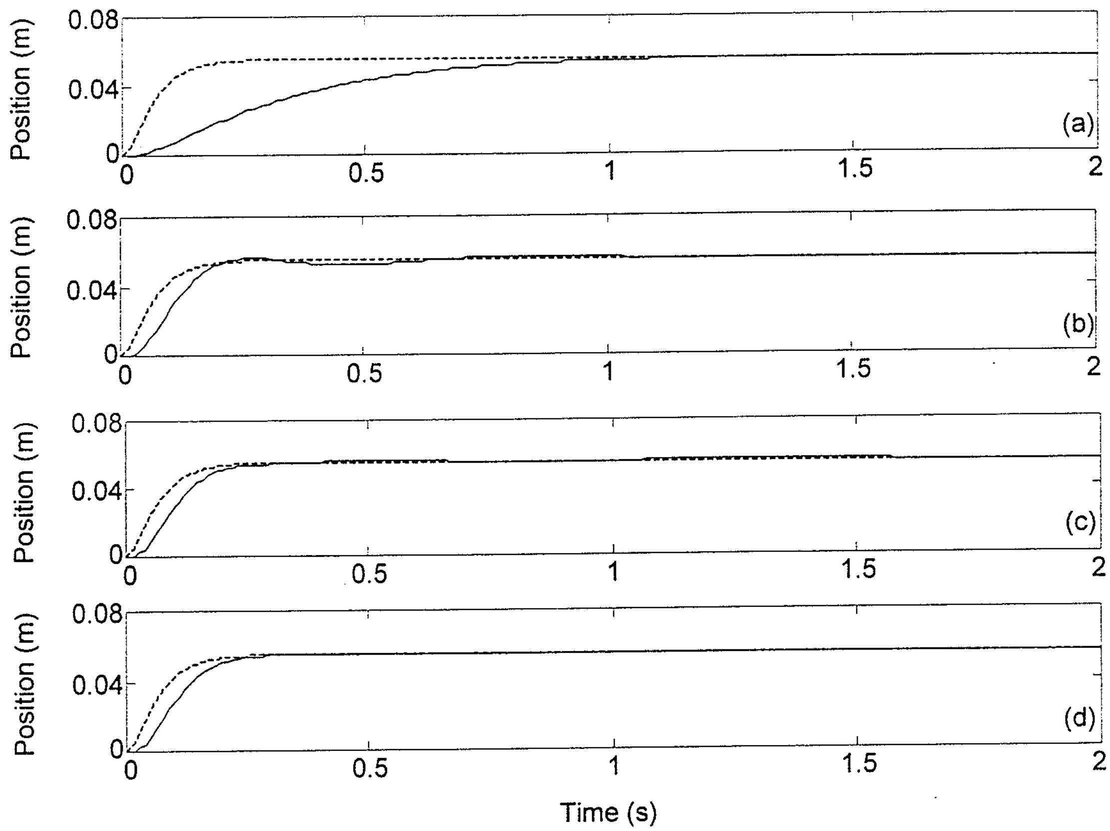

Figure 6.15: System responses of the ILC with current cycle feedback: (----- desired output,— actual output) under normal operation: (a) at 1st trial; (b) 10th trial; (c) 20th trial; (d) 40th trial (experiments).

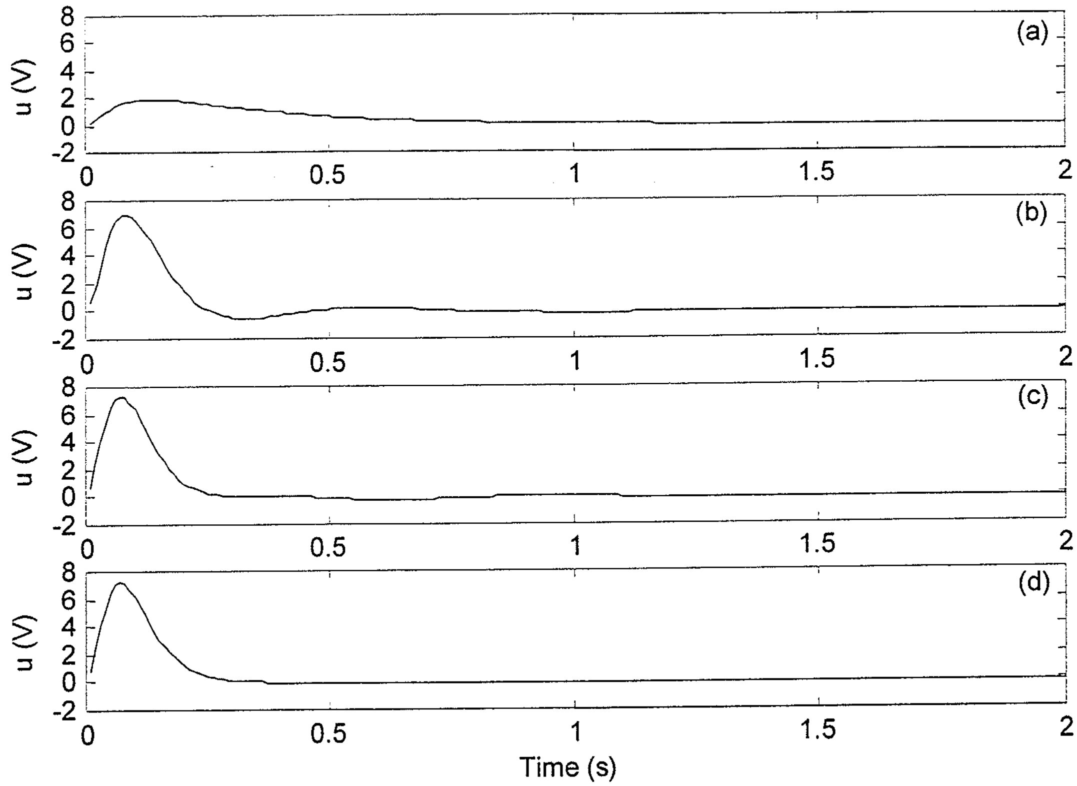

Figure 6.16: Control signals of the ILC with current cycle feedback: (a) at 1st trial; (b) 10th trial; (c) 20th trial; (d) 40th trial (experiments).

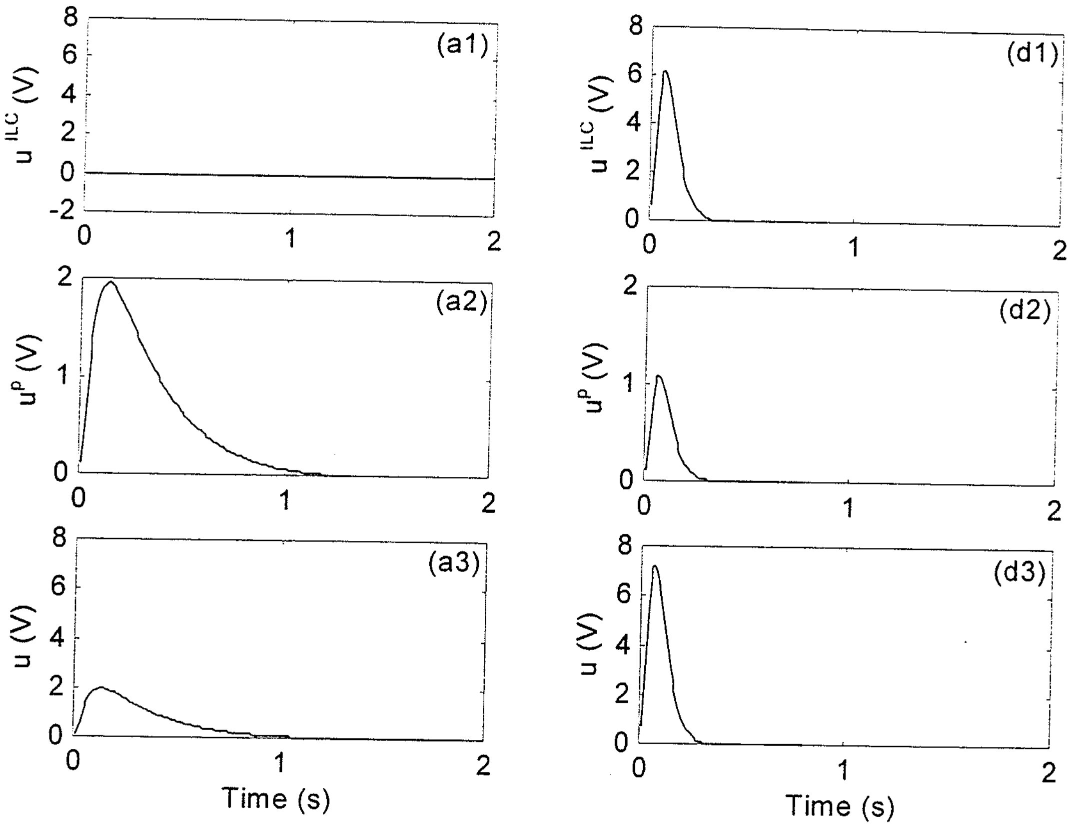

Figure 6.17: Control signal contributions of ILC with current cycle feedback: (a1), (a2), and (a3) at 1st trial; (d1), (d2), and (d3) at 40th trial (experiments).

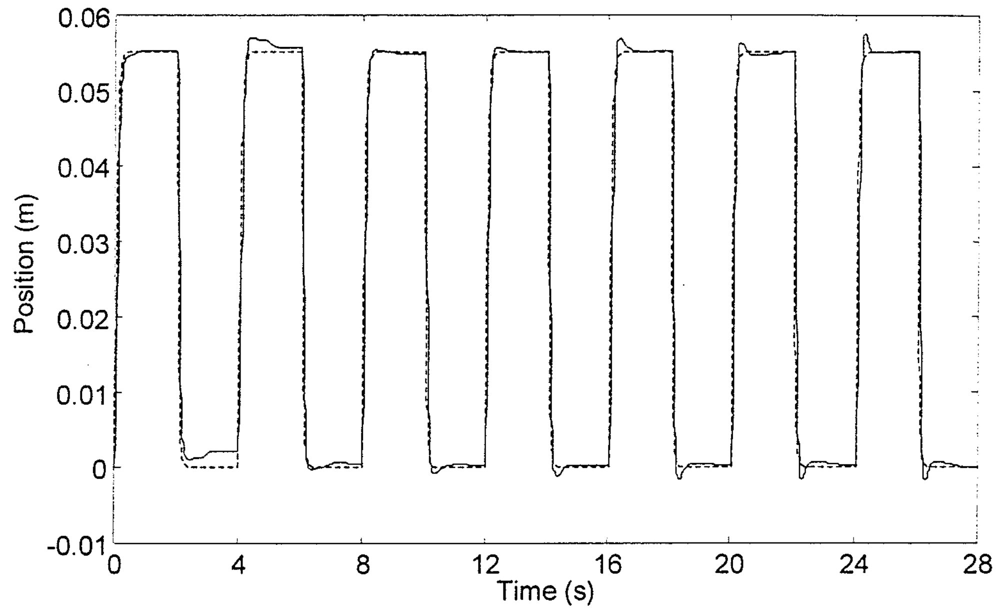

Figure 6.18: System response of ILC with current cycle feedback: (----- desired output, —— actual output) under normal operation (experiments)

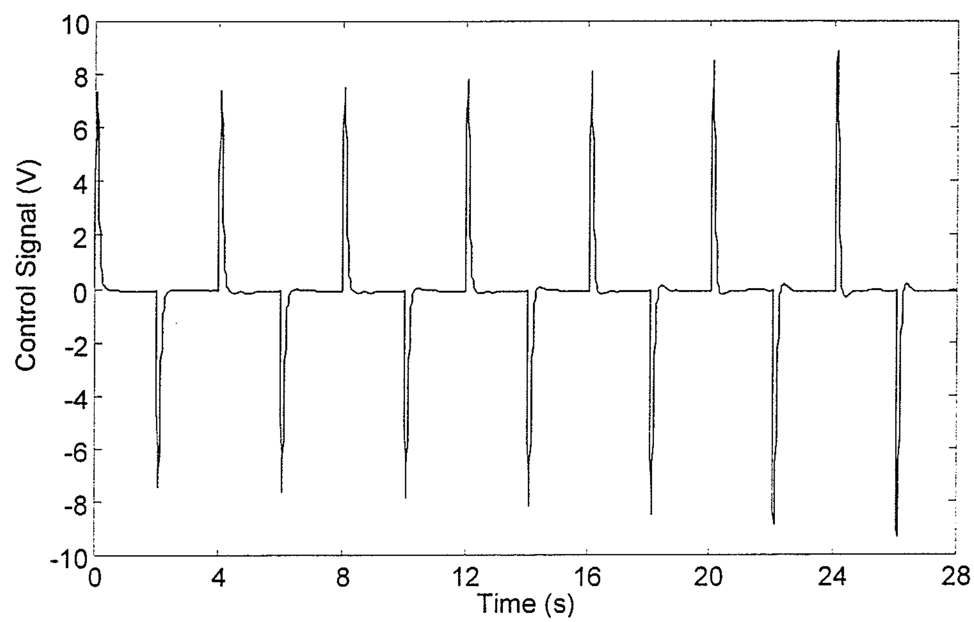

Figure 6.19: Control signal of ILC with current cycle feedback under normal operation (experiments).

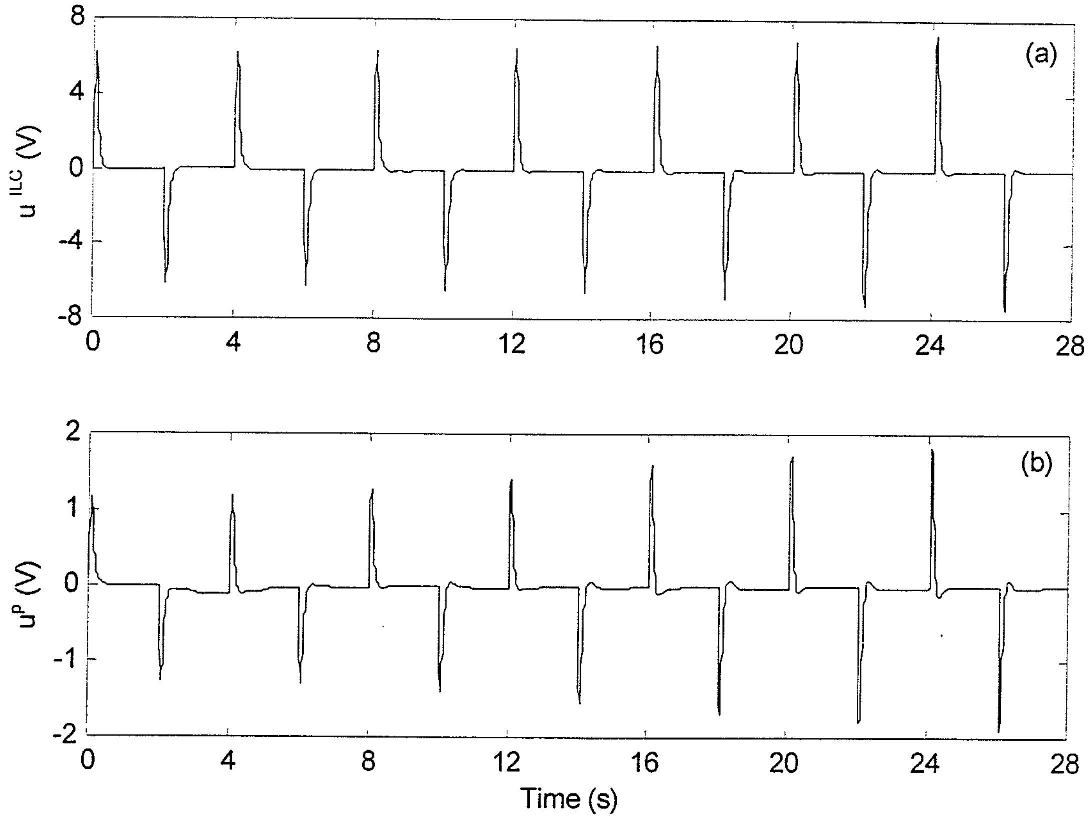

Figure 6.20: Control signal contribution of the ILC with current cycle feedback under normal operation: (a) feedforward term, (b) feedback term (experiments).

Case study 2 (faulty operation): In this experiment, the initial conditions of the system were reset to the same values at the beginning of each trial and an internal leakage was introduced to the system after the 40th trial. The results are shown in Figures 6.21 through 6.24. Figure 6.21a shows the system response of the ILC with current cycle feedback when the fault occurred. Figures 6.21b, c, and d show the system responses at 42nd, 43rd, and 45th trials, respectively. It is seen that within only 4 trials the system was able to overcome the leakage fault and to track the desired trajectory. Figures 6.22a, b, c, and d show the controller responses at the 41^{st}, 42^{nd}, 43^{rd}, and 45^{th} trials, respectively. It is seen that within only 4 trials, the controller was able to correct output response for the desired trajectory and overcome the internal leakage fault.

Figures 6.23a1, a2, and a3 show the controller responses when an internal leakage occurred in the system. Figures 6.23d1, d2, and d3 show the control signals behavior after 4 trials from applying the leakage. When these results are compared, it is clear that after 4 trials from applying the leakage the feedforward signal is very close to the total control signal and the feedback signal is nearly zero. Figures 6.24a, b, c, and d show the internal leakage flow rates at the 41^{st}, 42^{nd}, 43^{rd}, and 45^{th} trials, respectively.

In the next experiment, a step signal of a period of 4 seconds was performed without resetting the initial conditions of the system to the same values at the beginning of each trial. An internal leakage was introduced to the system after 4 seconds. The results are shown in Figures 6.25 through 6.28. Figure 6.25 shows the system response of the ILC with current cycle feedback with the occurrence of the internal leakage. It is shown that the controller is able to reduce the position error due to the leakage and track the desired trajectory.

Figure 6.26 shows the total control signal of the ILC with current cycle feedback; Figures 6.27a and 6.27b show the feedforward term and the feedback term of the control signal respectively. When these results are compared, it is clear that within 6 trials from applying the leakage the feedforward signal is so close to the total control signal and the feedback is nearly zero. Figure 6.28 shows the internal leakage flow rate.

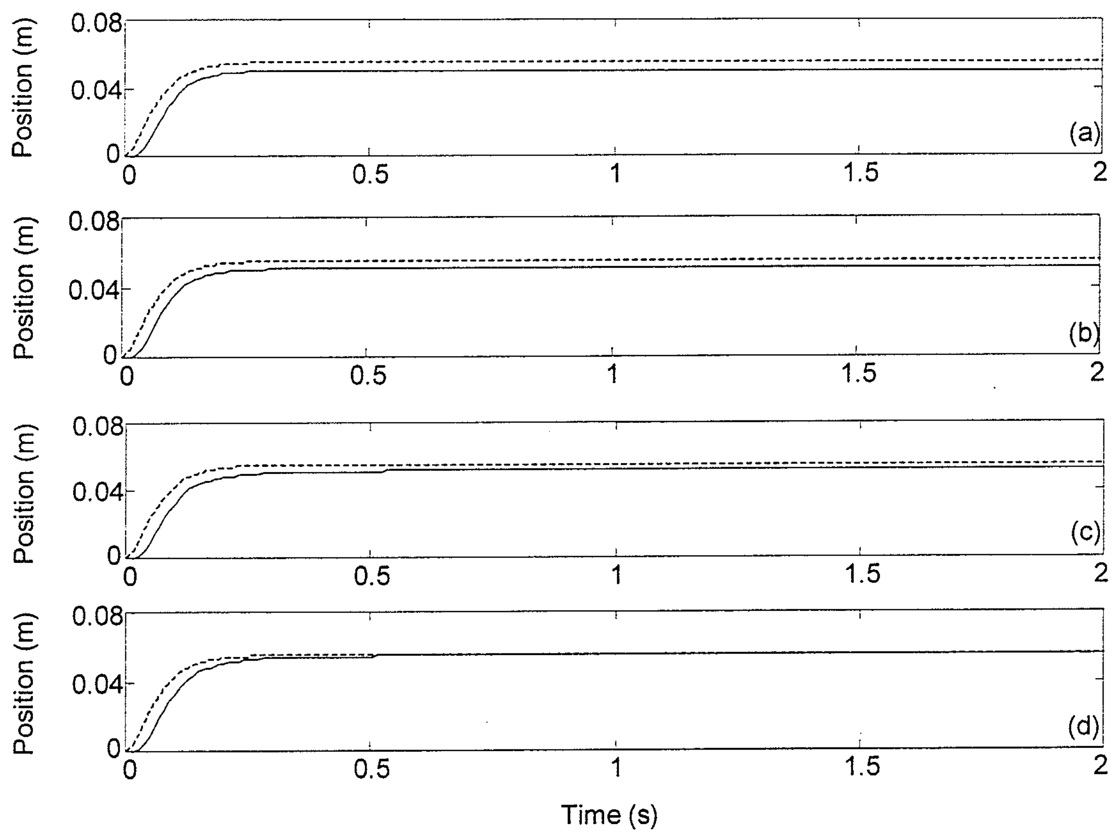

Figure 6.21: System response of the ILC with current cycle feedback under faulty operation: (---- desired position, — actual position): (a) at 41st trial; (b) 42nd trial; (c) 43rd trial; (d) 45th trial (experiments).

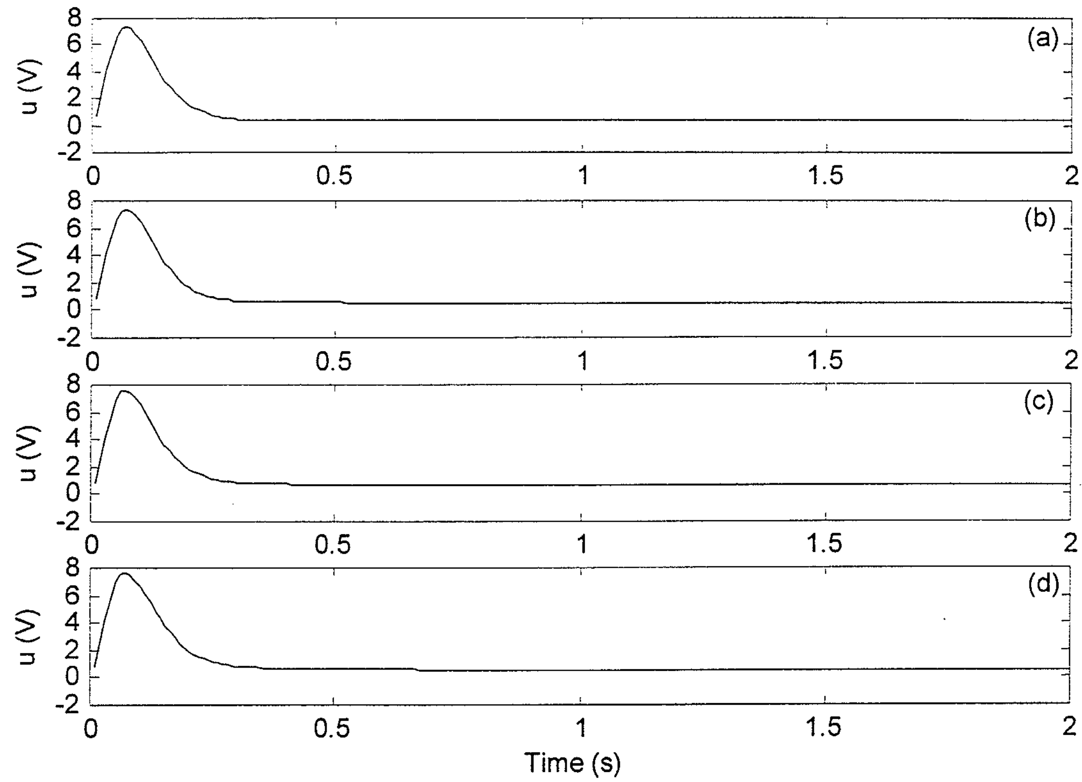

Figure 6.22: Control signals of the ILC with current cycle feedback: (a) at 41st trial; (b) 42nd trial; (c) 43rd trial; (d) 45th trial (experiments).

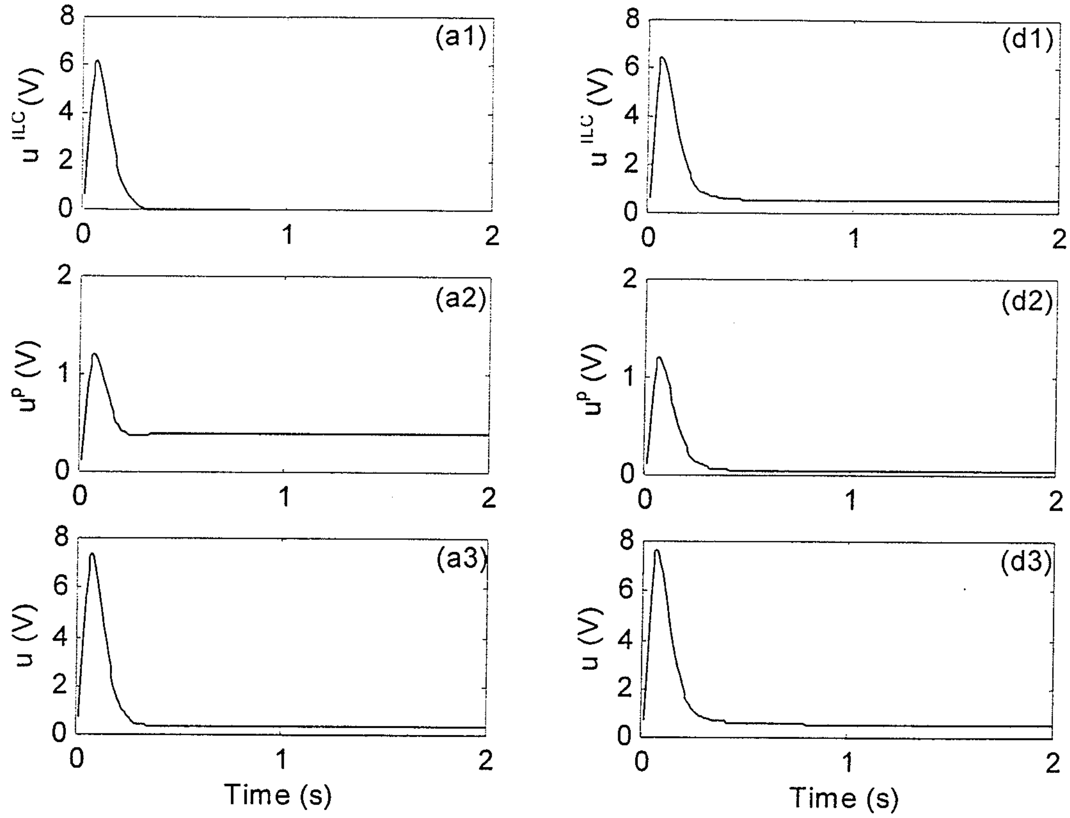

Figure 6.23: Control signal contributions of the ILC with current cycle feedback (a1), (a2), and (a3) at the 41st trial, (d1), (d2), and (d3) at the 45th trial (Experiments).

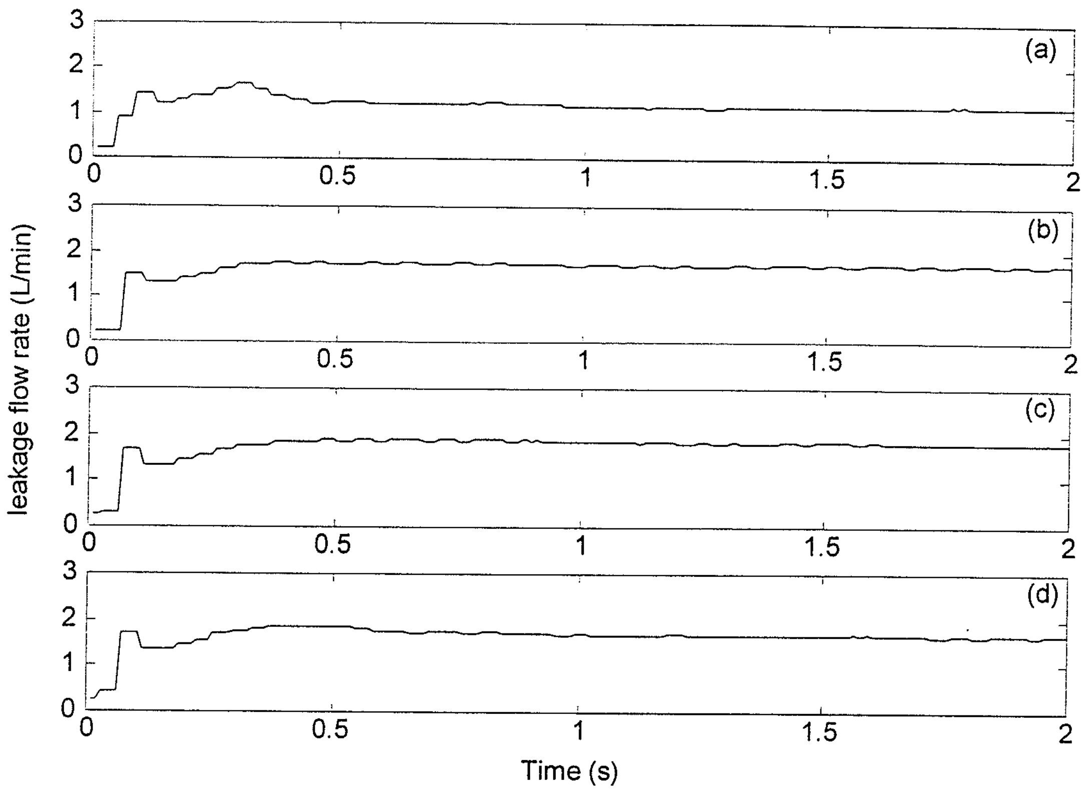

Figure 6.24: Internal leakage flow rates: (a) at 41st trial; (b) 42nd trial; (c) 43rd trial; (d) 45th trial (experiments).

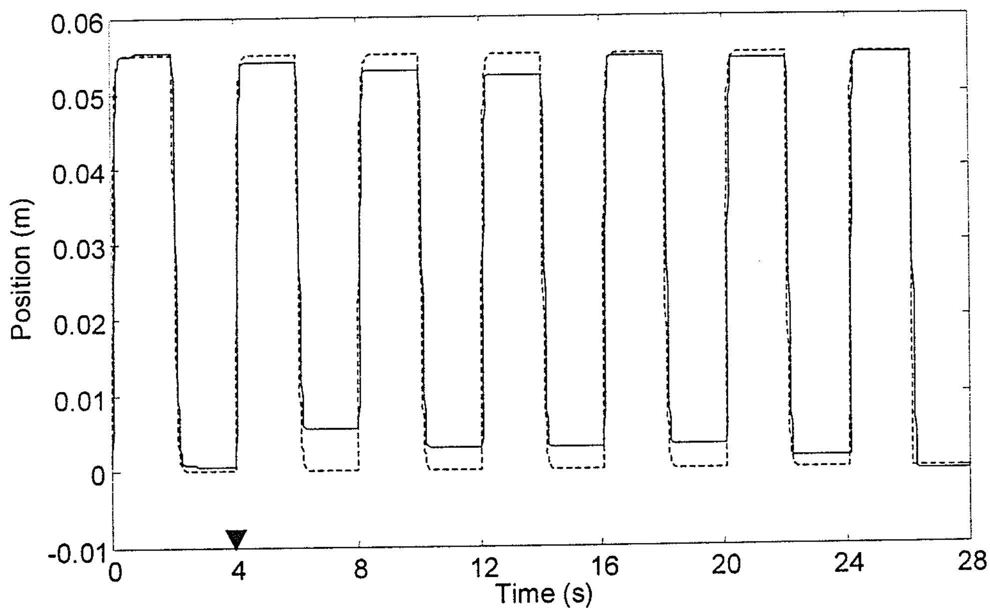

Figure 6.25: System response of the ILC with current cycle feedback under faulty operation (----- desired output, —— actual output) (experiments).

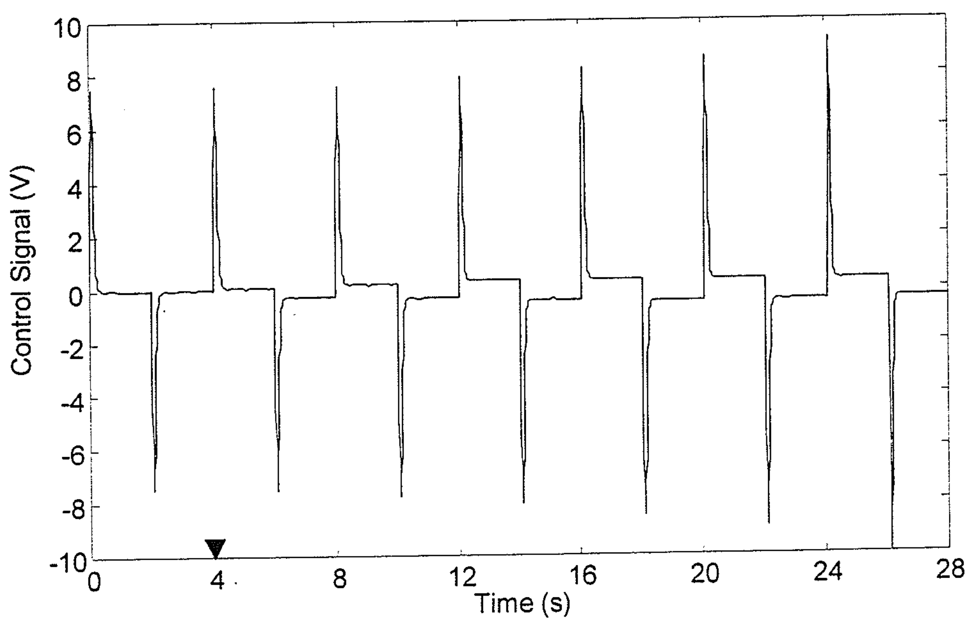

Figure 6.26: Control signal of ILC with current cycle feedback under faulty operation (experiments).

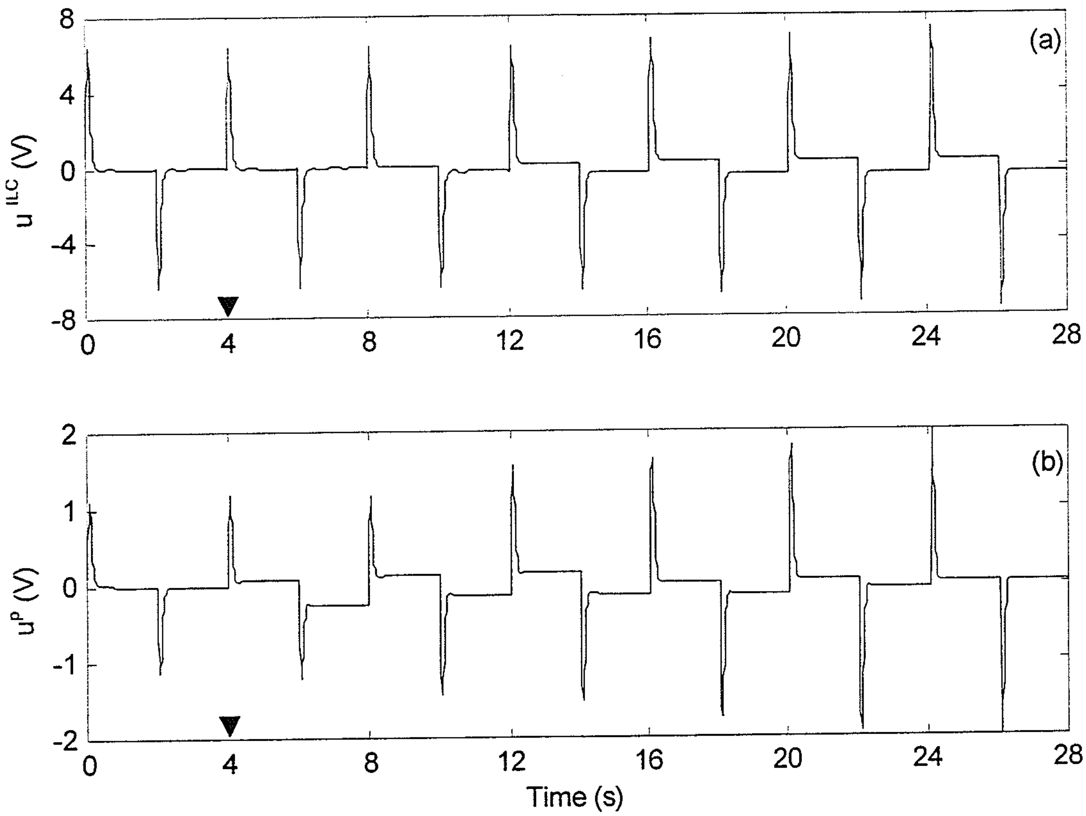

Figure 6.27: Control signal contribution of the ILC with current cycle feedback under faulty operation: (a) feedforward term; (b) feedback term (experiments).

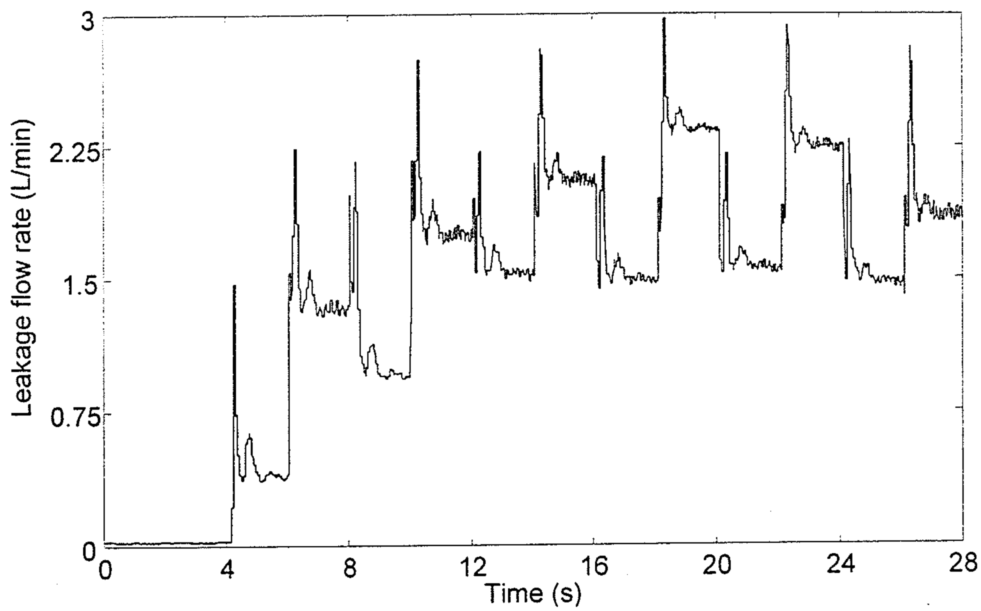

Figure 6.28: Internal leakage flow rate (experiments)

6.4 Summary and Discussions

The gains found in the simulation studies were first used for the initial experiments. Final values of the gains were then obtained by trial and error during the experiments. The final values of the controller gains are listed in Table 6.1. Comparing the gains used in the simulations and the experiments, it is seen that for the ILC with proportional error feedback scheme only T_u had to be reduced by 5% in the experiments. Similarly, for the ILC with current cycle feedback scheme λ in the experiments was approximately 9% less than the one used in the simulations. During the experiments, the initial training was done by moving the actuator only in one direction (extension). When applying the leakage fault, the actuator was allowed to move continuously in both directions and no resetting to the initial conditions were performed. This is in-line with real implementation of the ILC schemes. Further experiments were performed for increased leakage faults approximately 4L/min. The effect of the control signal saturation on the convergence and the characteristics of the responses were found to be similar to the one observed through the simulations.

Chapter 7

Conclusions

In this thesis, three selections of ILC approaches were made. These three schemes were tested on the electrohydraulic actuator. The ILC schemes stretched from a very simple structure i.e., the basic ILC, to the ILC with proportional error feedback and to the ILC approach with current cycle feedback.

Most ILC algorithms require the same initial conditions at the beginning of each trial. In this thesis, tests were performed on each ILC algorithm. In the first test, the three ILC algorithms were applied to follow a repetitive task under normal and faulty operations with resetting the initial conditions to the same values at the beginning of each trial (this is very common within the context of the ILC). In the second test, the three ILC algorithms were applied to follow a repetitive task under normal and faulty conditions without the need of resetting the initial conditions to the same values at the beginning of each trial; and that is more practical and desirable from the implementation view point.

The simulation results showed that under the condition of resetting the initial conditions of the system to the same values at the beginning of each trial, all three control algorithms had good responses under the normal operation, but with different speed of convergence. Both the ILC with proportional error feedback and the ILC with current cycle feedback were two times faster than the basic ILC to track the desired trajectory, while with the faulty operation, the ILC with current cycle feedback recovered from the internal leakage fault two times faster than the basic ILC and 1.33 times faster than the ILC with proportional error feedback. In the second test, a step signal was repetitively performed without resetting the initial conditions of the system to the same values at the beginning of each trial. The results showed that both ILC with proportional error feedback and the ILC with current cycle feedback gave similar results under normal and faulty operations, while the system with the basic ILC was unstable.

The experimental results showed that under the condition of resetting the initial conditions of the system to the same values at the beginning of each trial, both the ILC with proportional error feedback and the ILC with current cycle feedback tracked the desired trajectory with equal number of trials. However with the faulty operation, the ILC with current cycle feedback recovered from the internal leakage fault two times faster than the ILC with proportional error feedback. When the initial conditions of the system was not reset to the same values at the beginning of each trial, the results showed that both controllers tracked the desired trajectory with very small error under normal operation. However under the faulty operation the ILC with current cycle feedback was able to decrease the error caused by the internal leakage faster than the ILC with proportional error feedback.

This study provided a groundwork for using an ILC-base fault tolerant control scheme for hydraulic actuators. It was shown that all of the conventional ILC algorithms could be classified as fault tolerant controllers under the condition of resetting the initial conditions to the same values at the beginning of each trial. The modified ILC approaches which use the information from both the current and the previous trials (such as the ILC with proportional error feedback or the ILC with current cycle feedback) can be classified as a fault tolerant ILC, without the need for resetting the initial conditions to the same values at the beginning of each trial. The ILC with current cycle feedback found to be the best according to this study. The method has a simple design and the best performance.

This thesis has investigated the robust ILC of an electrohydraulic positioning system with a faulty actuator piston seal. Future work in this area should examine the robustness of ILC to various levels of leakage and examine the behavior the ILC scheme with environmental interaction. In this work the controller gains are constant; therefore, using variable gain give a greater degree of freedom and that is a good field for a future work.

Chapter 8

References

Amann, N., Owens, D. H., and Rogers, E., "Iterative Learning Control for Discrete Time Systems using Optimal Feedback and Feedforward actions". *International Journal of Control*, vol. 65,no. 2,pp. 277-293, September 1996.

Arimoto, S., Kawamura, S., and Miyazaki, F., "Bettering operation of a dynamic system by learning: a new control for servomechanism or mechatronic system". *Proceeding 23rd IEEE Conference. On Decision and Control*, pp. 1064-1069, Las Vegas, Nevada, 1984.

Chen, Y., Xu, J-X, and Lee, T. H., "An Iterative Learning Controller Using Current Iteration Tracking Error Information and Initial State Learning". *Proceeding of the 35th Conference on Decision and Control*, pp. 3064-3069, Japan, December 1996.

Chen, Y., Gong, Z., and Wen, C., "Analysis of a High-Order Iterative Learning Control Algorithm for Uncertain Nonlinear Systems with State Delays". *Automatica*, vol. 34, no. 3, pp. 345-353, 1998.

Choi, Joon-Young, Uh, J., and Lee, J. S., 'Iterative Learning Control of Robot Manipulator with I-Type Parameter Estimator". *Proceeding of the American Control Conference*, pp. 646-651, Arlington, VA, June 25-27, 2001.

Gunnarsson, S., and Norrlöf, M., "On the design of ILC algorithm using optimization". *Automatica,* vol 37,pp. 2011-2016, 2001.

Karpenco, M., "Fault Tolerant Control design for an Electrohydraulic Actuator with application to positioning of Aircraft Flight Control Surfaces". *Msc thesis, Department of Mechanical and industrial engineering. The University of Manitoba.* April 23, 2002.

Merrite, H.E., *Hydraulic Control Systems*, Wiley, New York, 1967

Moog Inc., *D765 Series servovalve with electronic feedback and integrated electronics*, catalog CDL6563, revision E, from no 500-300 601, Moog Inc., New York.

Moore, K., and Bahl, V., "An Iterative Learning Control technique for Mobile Robot Oath-Tracking Control". *Part of the SPIE Conference on Mobile Robots XIV*, vol. 3838, pp. 240-251, Boston, Massachusetts, September 1999.

Moore, K., "Iterative learning control - an expository overview. Applied and computational Controls, Signal Processing and Circuits", 1998.

Norrlöf, M., "Comparative study of first and second order ILC – frequency domain analysis and experiments". *Proceeding of the 39th IEEE Conference on Decision and Control.*, pp. 3415-3420, Sydney, Australia, December 2000.

Norrlöf, M., "Iterative Learning Control: Analysis, Design, and Experiments". *Ph.D. thesis, Linkoping University*, Linkoping, Sweden, 2000.

Sison, L.G., and Chong, E.K.P., "No-Reset Iterative Learning Control". *Proceedings of the 35th Conference on Decision & Control*, pp. 3763-3764, Japan, December 1996.

Sison, L.G., and Chong, E.K.P., "Design of Repetitive learning Controllers". *Proceedings of the 36th Conference on Decision & Control,* pp. 3763-3764, San Diego, California USA, December 1997

Scholten, P., "Iterative Learning Control: A Design for a Linear Motor Motion System". *Msc Thesis University of Twente. Faculty of Electrical Engineering*, August 2000.

Thompson, D.F., Pruyn, J.S., and Shhukla, A., "Feedback design for Robust Tracking and Robust Stiffness in Flight Control Actuators Using a modified QET Technique". *International Journal of control*, vol. 72, no. 16, pp. 1480-1497, 1999b.

Tsao, Tsu-Chin, and Tomizuka, M., "Robust Adaptive and repetitive Digital Tracking Control and Application to Hydraulic Servo for Noncircular Machining". *Journal of Dynamic System, Measurement, and Control*, vol 116, pp. 24-32, March 1994

Uchiyama, M., "Formation of High Speed Motion Pattern of Mechanical Arm by Trial". *Transactions of the Society of Instrumentation and Control Engineers*, vol. 19, no. 5, pp. 706-712, May 1978.

Xu, Jian-Xin., "Direct Learning of Control Efforts for Trajectories with Different Magnitude Scales". *Automatica*, vol. 33, no. 12, pp. 2191-2195, 1997.

Xu, Jian-Xin., Wang, Xiao-Wei, and Lee Tong Heng., "Analysis of Continuous Iterative Learning Control Systems Using Current Cycle Feedback". *Proceedings of 1995 American Control Conference ACC'95*, vol. 6, pp. 4221-4225, Seattle, WA, June 1995.

Zheng, D., Heather, H., and Alleyene, A., "Nonlinear Adaptive learning for electrohydraulic Control System". *Proceedings of the 1998 ASME FPST*, pp.CA, Nov. 1998.

Appendix

The experiments Shown in Figures 6.5 to 6.6 and Figures 6.18 to 6.19 were repeated again for longer number of trials. The results are given in Figures A1 to A4.

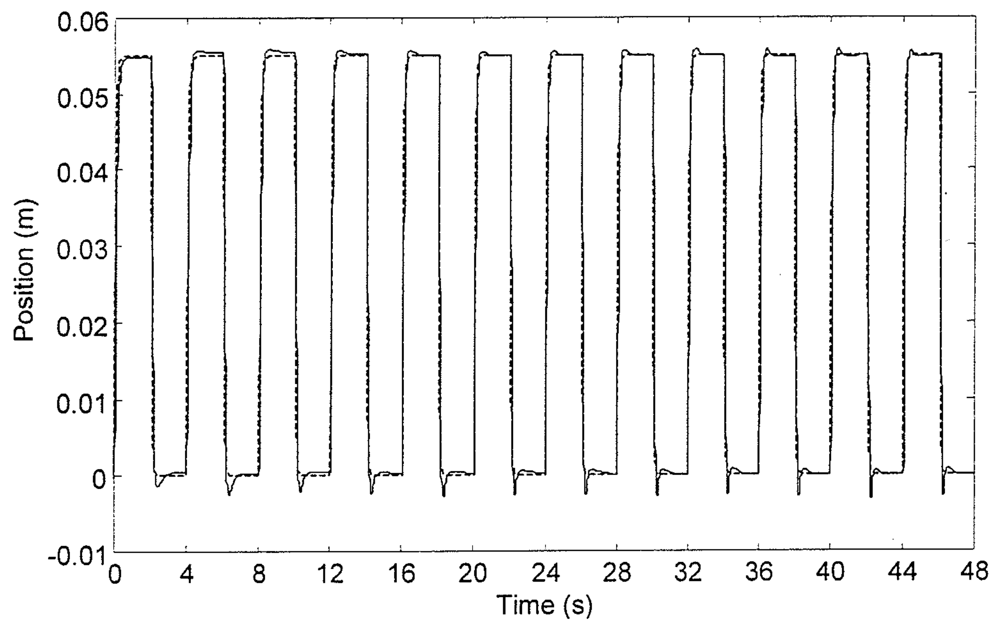

Figure A1: System response of the ILC with proportional error feedback (-----desired, —— actual) under normal operation (experiments).

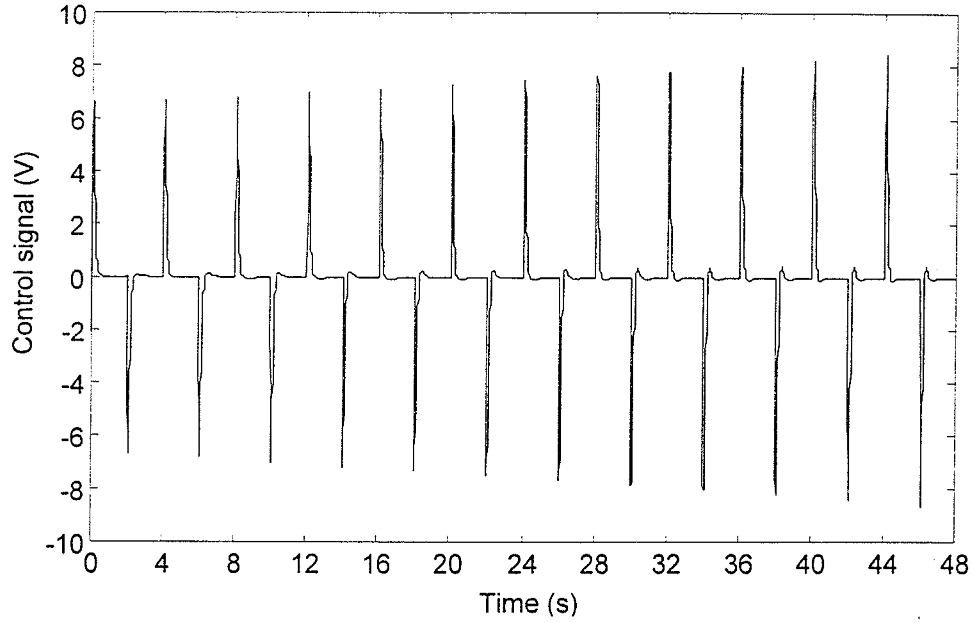

Figure A2: Control signal of the ILC with proportional error feedback under normal operation (experiments).

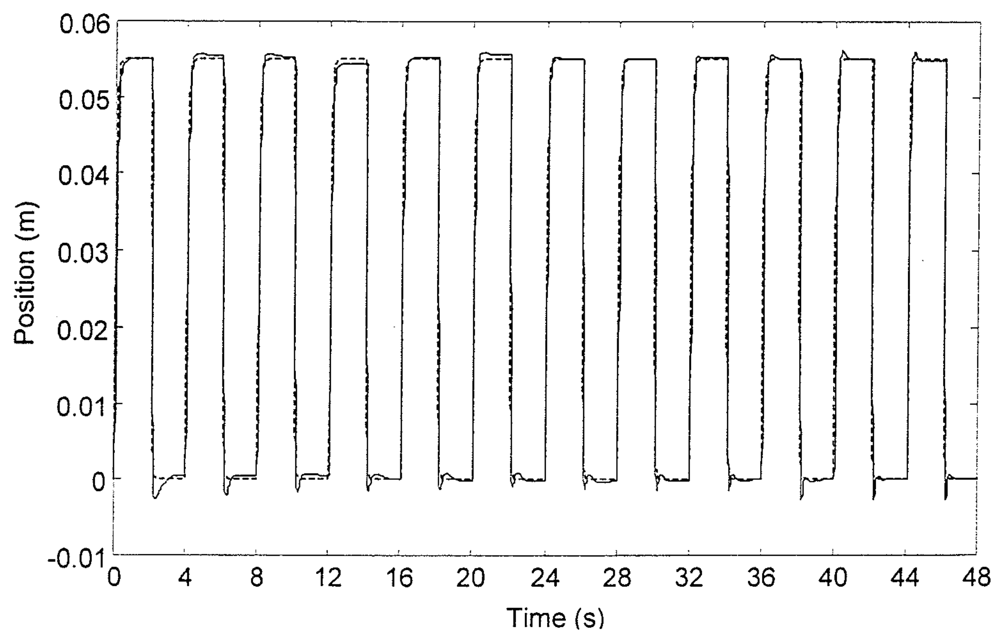

Figure A3: System response of the ILC with current cycle feedback (----- desired, —— actual) under normal operation (experiments).

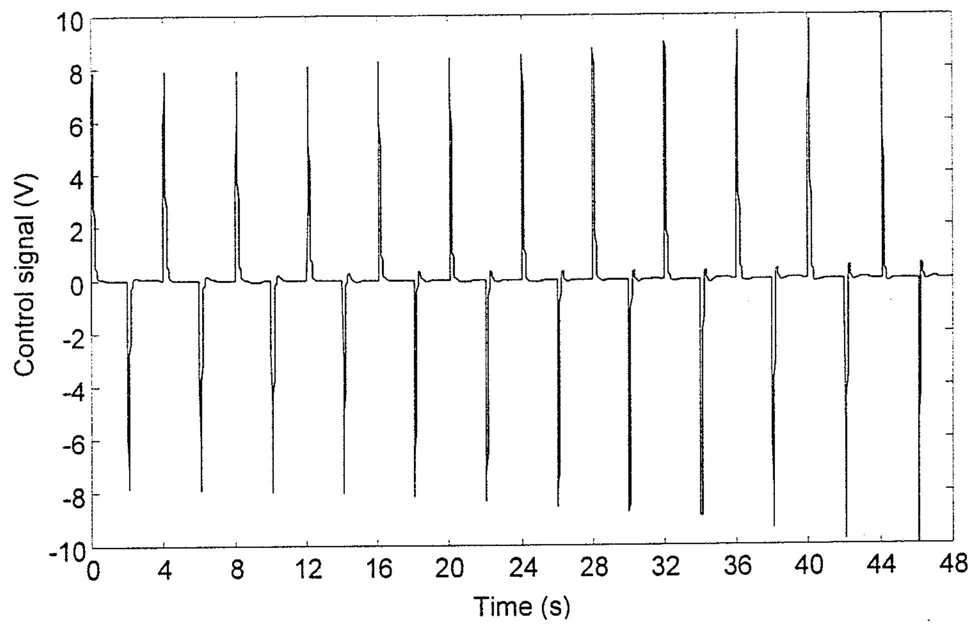

Figure A4: Control signal of the ILC with current cycle feedback under normal operation (experiments).